SHIBAURA INSTITUTE OF TECHNOLOGY

Economic planning and operation in electric power system using meta-heuristics based on Cuckoo Search Algorithm

by

Nguyen Phuc Khai

A thesis submitted in partial fulfillment for the
degree of Doctor of Philosophy

in the
Regional environment systems

September 2017

"The important thing is to not stop questioning. Curiosity has its own reason for existing."

Albert Einstein

Abstract

The main purpose of this thesis is to propose an improved Cuckoo Search Algorithm and evaluate it on various economic problems of the electric power system in order to investigate its effectiveness. Cuckoo Search Algorithm is a meta-heuristic developed by Yang and Deb since 2009. This method is based on the Lévy distribution to generate new solutions and illustrate the process of Cuckoo's reproduction strategy to carry better solutions over the next generation. In this study, the proposed method gives a chance for Cuckoo eggs to modify itself following better solutions to enhance the performance. A learning factor p_l is employed to control the modification stage of Cuckoo eggs and prevent the search engine fall into local optimum points. Thus, the proposed is named Self-Learning Cuckoo Search Algorithm.

In order to investigate the efficiency, Self-Learning Cuckoo Search Algorithm is evaluated on four common economic problems on the power system. The first application is the Multi-Area Economic Dispatch. The objective of this problem is to minimize the total fuel cost when combining power systems of many areas together while satisfying the power balance in each area. This problem consists of many non-convex fuel cost functions, such as multi-fuel cost function, the functions considering valve-point effects or prohibited operating zone. Numerical results of three case studies show that the proposed method is better than the conventional Cuckoo search algorithm.

The second obtained problem is the Optimal Power Flow, which is the major tool to operate and analyze the power system. This problem determines power and voltage of generators to minimize the total fuel cost while handling a huge of equal and unequal operational constraints. Self-Learning Cuckoo Search Algorithm is evaluated up to the IEEE 300-bus system to investigate its efficiency on large-scale problems. Numerical results show that the proposed method is successful in solving the large-scale problem while the conventional is unsuccessful.

Thirdly, Self-Learning Cuckoo Search Algorithm is evaluated on the Optimal Reactive Power Dispatch. This problem is a special type of the Optimal Power Flow when its objective function is to minimize the total power loss. According to numerical results of 30-, 57- and 118-bus systems, the proposed method keeps giving better solutions than the conventional.

The final problem is the optimal sizing and placement of shunt-VAR compensators. This problem has multiple objectives and combines integer and real numbers together. In this study, Self-Learning Cuckoo Search Algorithm is compared with the Teaching-Learning based Optimization, Particle Swarm Optimization, Improved Harmony Search and the conventional Cuckoo Search Algorithm.

According to numerical results of obtained problems, the proposed Self-Learning Cuckoo Search Algorithm is better than the conventional in giving the optimal solutions, especially on large-scale systems. Thus, the proposed method is favorable to apply for practical operation.

Acknowledgements

I would like to use this opportunity to thank my advisor, my fellow and diploma students, my many friends and my family for their time, ideas and encouragement.

First of all, I would like to thank my advisor, Prof Goro Fujita. You gave me professional assistance, careful reading, valuable feedbacks and, especially, the opportunity of writing this thesis. You helped me not only on professional research but also on my life. I am deeply grateful and proud to become a student of yours.

I also would like to thank to Assoc. Prof. Vo Ngoc Dieu at Ho Chi Minh University of Technology in Viet Nam and Prof. Fukuyama at Meiji University, for your useful comments and pointing me in right directions.

Special thank to Shibaura Institute of Technology for your financial support through the Hybrid Twin Program. Your support gives my whole mind to study.

Warmly thank to other fellow doctoral students in my lab for your significant contribution and your supports when I write this thesis. I am also thankful to other master and diplomat students in my laboratory for your always being helpful.

Last I would like thank to my family and numerous friends who always encouraged me to finish my research.

NGUYEN PHUC KHAI

Contents

List of Figures

List of Tables

Abbreviations

ABC	**A**rtificial **B**ee **C**olony
CSA	**C**uckoo **S**earch **A**lgorithm
DE	**D**ifferential **E**volutionary
EP	**E**volutionary **P**rogramming
GSA	**G**ravitional **S**earch **A**lgorithm
IHS	**I**mporved **H**armony **S**earch
MFO	**M**oth-**F**lame **O**ptimization
OPF	**O**ptimal **P**ower **F**low
ORPD	**O**ptimal **R**eactive **P**ower **D**ispatch
MAED	**M**ulti-**A**rea **E**conomic **D**ispatch
PSO	**P**article **S**warm **O**ptimization
SLCSA	**S**elf-**L**earning**C**uckoo **S**earch **A**lgorithm
SOHPSO-TVAC	**S**elf-**O**rganizing **H**ierarchical **P**article **S**warm **O**ptimization with **T**ime-**V**arying **A**cceleration **C**oefficients
SVC	**S**hunt - **V**AR **C**ompensator
TLBO	**T**eaching-**L**earning **B**ased **O**ptimization

Chapter 1

Introduction

1.1 Research Background:

1.1.1 Economic operation:

Economic operation is very important for a power system to return a profit on the capital invested. Operational economics are involved in both of power generation and delivery. Thus, economic operation in power system can be divided into two main objectives. The first objective is to minimize the total cost of power production called *economic dispatch* and the other dealing with *minimum-loss* delivery of the generated power to the loads.

Economic dispatch determines the power output of each plant or each generating unit within the plant which will minimize the overall cost of fuel needed to serve the system load. Thus, economic dispatch focuses upon coordinating the production costs at all power plants operating on the system. Problems of economic dispatch usually include various non-convex functions, such as: valve-point-effect or multi-fuel functions, and require a robust method to give the optimal solutions.

Minimum-loss objective focuses on reducing the power loss as much as possible by controlling all components of the power transmission system, such as: taps of transformers, shunt VAR compensators, voltage of generators, etc. Problems of minimum-loss objective have to handle all constraints of these components and keep them working in safe

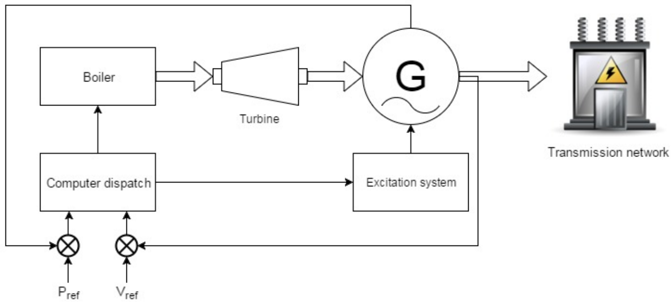

FIGURE 1.1: Simplified block diagram of a thermal generating unit

condition. Some common constraints of components are capacities of transmission lines and transformers, limits of voltage at load buses. The operators employ the *power flow analysis* in order to calculate voltages at all buses and current flows through the transmission system. The power flow analysis discussed in the part 1.1.4. Then, they provide an optimal setting solution for all components.

On other hand, the minimization of total fuel costs and minimization of power loss can be solved at the same time by the *optimal power flow* (OPF) program. Different from economic dispatch problems, the OPF includes controlling all components of power system, for e.g: voltage of generators, transformers, shunt VAR compensators, to reduce the loss and, of course, also minimizing the total fuel cost. When the OPF only focuses to minimize the power loss, the problem is called *optimal power reactive dispatch* (OPRD).

1.1.2 Process of economic operation in the control of a generating unit

In the electric power system, all system operators always try to operate generators in stable and economic. However, it is not easy to control high-power generating units in power plants. The figure 1.1 shows a common block diagram for a thermal generator. The control system of a generator basically includes a control center and governor to calculate and set output power P_{set} of the generator. On another hand, the excitation system supplies the excited current to control the terminal voltage of the generator basing on the reference voltage V_{ref}.

In actual operation, the system operators have three stages to commit a generator as Fig. 1.2. The main purpose of this process is to keep the balance between generating and

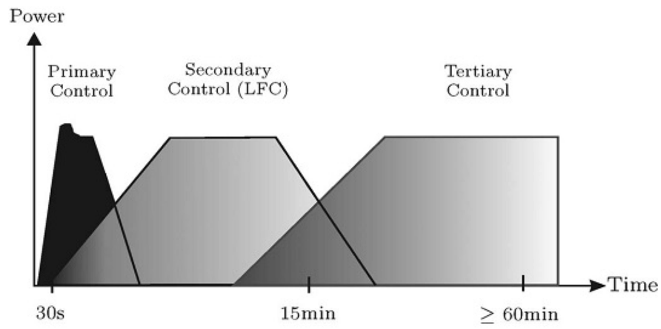

FIGURE 1.2: Approximate time scale controlling a generator according to the standard of the Central Europe system

demand powers. Furthermore, the process also tries to operate the system in economic. In the primary control stage, the controller occurs automatic within a few seconds after the disturbance. The objective of this stage is to maintain the balance between generation and demand immediately. The change of power can be decentralized to generators basing on their setting speed governors. In the secondary control, the system operators usually relieve the state of the primary control and modify output powers of generators in order to bring the system frequency back its nominal value while satisfying the power balance. This stage can be took a few minutes. In the last stage, the system operators continues distributing the power to generators and considering the most economic solution. This stage is usually activated each 15 minutes. Economic operation effects on the tertiary control of a generating unit and contributes to provide economic solutions to various problems of power system. An economic solution for a generating unit basically consists of the output power P_{set} and the reference voltage V_{ref}.

The figure 1.3 illustrates changes of the frequency in the primary and secondary control stages. Before the disturbance occurred, the frequency has been working over 50Hz. After that, the frequency dropped down 49.96Hz within 10 seconds, due to the primary control. Then, the system operators bring the frequency back to 49.97Hz after 30s by the secondary control. Finally, the system is stable at 49.97Hz.

1.1.3 Input-Output characteristic of thermal unit

In operation and planning the electric power system, the relationship between real output power and operating cost has been described via the fuel cost function. The fuel cost

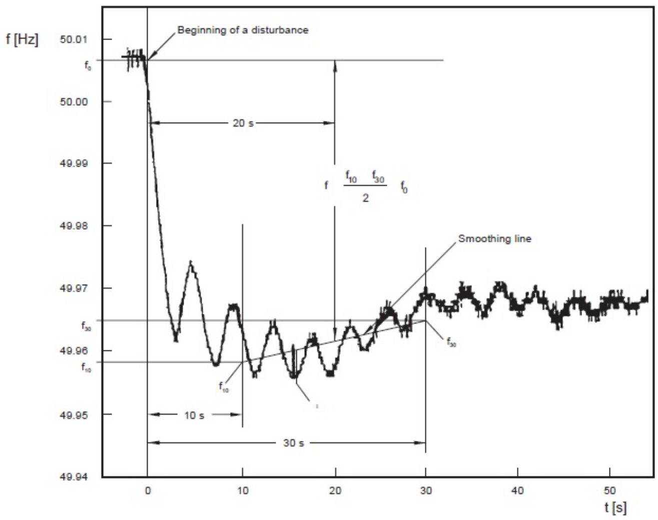

FIGURE 1.3: Example of the primary and secondary controls

function plays a key role to determine the economic target of a project or operating plan. Popularly there are three types of fuel cost functions have been researched. The simplest type is the quadratic function, while other types consider practical operating conditions of power plants.

1.1.3.1 Quadratic fuel cost function:

In simplified economic dispatch problems, a quadratic polynomial of generated power has usually been employed. Equation (1.1) describes this fuel cost function.

$$F(P) = a + b.P + c.P^2 \tag{1.1}$$

where P is the output power of generating unit; a, b and c are cost coefficients of the generator.

1.1.3.2 Fuel cost function with valve-point loading effect:

For large steam turbine generators, the input-output characteristics are not always as smooth as Fig. 1.4. Large steam turbine generators will have a number of steam admission valves that are opened in sequence to obtain ever-increasing output of the unit. Figure

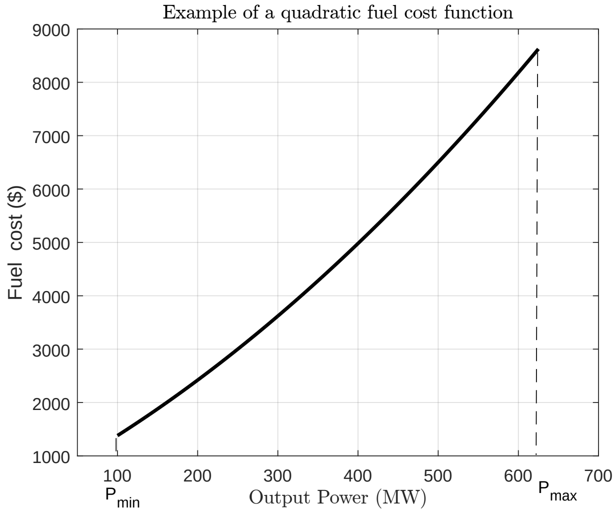

FIGURE 1.4: Example of a quadratic fuel cost function with $a = 0.008, b = 8, c = 500$

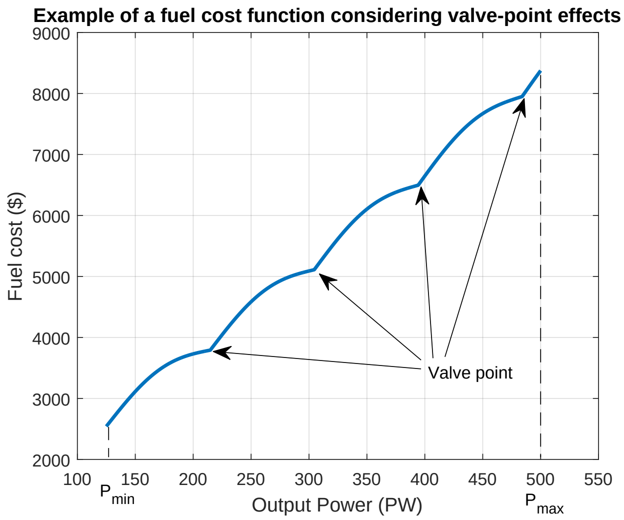

FIGURE 1.5: Example of a fuel cost function considering valve-point effects

1.5 shows an input-output characteristic for a unit with four valves. Mathematically, a sinusoidal element is added to the quadratic fuel cost function as (1.2). This type of input-output characteristic is non-convex; hence, optimization techniques that require convex characteristics may not be used with impunity.

$$F(P) = a + b.P + c.P^2 + |e.\sin(f.(P_{\min} - P))| \tag{1.2}$$

where e and f are coefficients considering valve point loading effect, P_{min} is the lower-bound power of the generating unit.

1.1.3.3 Fuel cost function with multiple fuels:

Another type of power plant was the common-header plant, which contained a number of different boilers connected to a common steam line (called a common header). Since 1960s, these common-header plants are replaced by modern and more efficient ones. However, a few plants in urban areas are still working to supply both of electricity and heating steam. Figure 1.6 is an illustration of a rather complex common-header plant. A common-header plant will have a number of different input-output characteristics that result from different combinations of boilers and turbines connected to the header.

The fuel cost function of a common-header plant combines many fuel cost functions. Each fuel cost function is represented with a quadratic one. Equation (1.3) reflects the effect of fuel type changes. Figure 1.7 shows the fuel cost function of a common-header plant with three various fuels.

$$F(P) = \begin{cases} a_1 + b_1.P + c_1.P^2 + \left|e_1.\sin\left(f_1.\left(P_{\min} - P\right)\right)\right|, \text{if} P_{\min} \leq P < P_1 \\ a_2 + b_2.P + c_2.P^2 + \left|e_2.\sin\left(f_2.\left(P_1 - P\right)\right)\right|, \text{if} P_1 \leq P < P_2 \\ \dots \\ a_n + b_n.P + c_n.P^2 + \left|e_n.\sin\left(f_n.\left(P_{n-1} - P\right)\right)\right|, \text{if} P_{n-1} \leq P \leq P_{\max} \end{cases} \quad (1.3)$$

Where n is the number of fuel costs and P_{max} is the maximum power of the generating unit.

1.1.4 Power flow analysis

Power flow or load flow is the name given to a network solution in steady-state condition of the power system. Power flow calculates and provides the solution of network due to the description of network, generating power of generators and power loads. The description of network includes *bus data* and *line data*. Bus data list values of P, Q and V at each bus, while line data show information of transmission lines and transformers. The solution obtains the magnitude, phase angle of the voltage, real and reactive power at each bus, and power flowing in each transmission line. Thus, power flow plays a key role in planning,

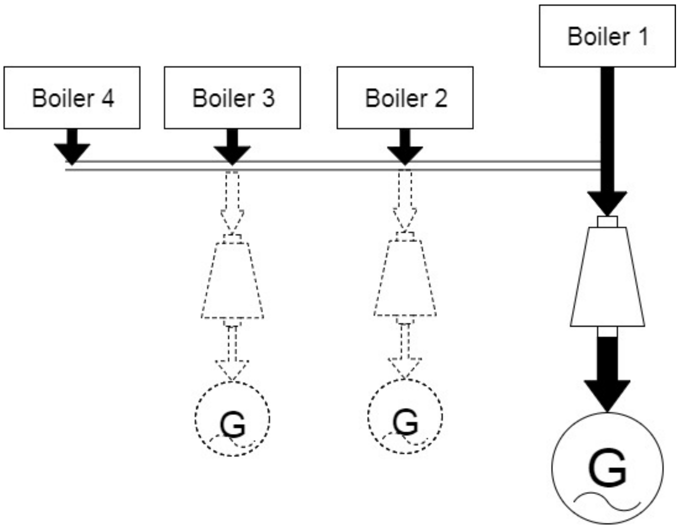

FIGURE 1.6: Diagram of a common-header plant using multiple fuel cost function

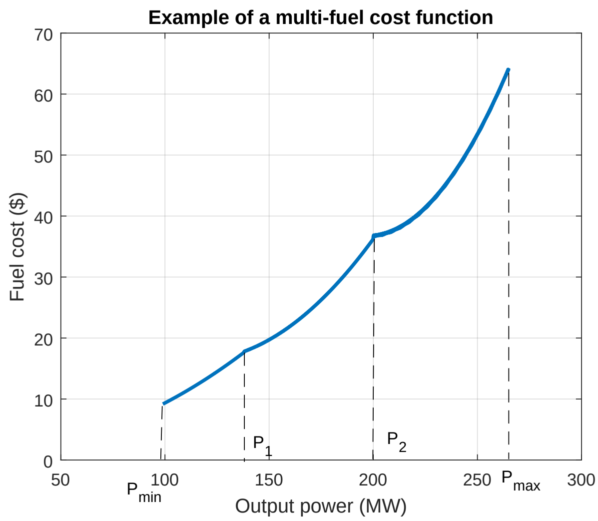

FIGURE 1.7: Example of a multi-fuel cost function

designing, analyzing and operating the power system.

Example 1.1. *A small power system has the one-line diagram as Fig. 1.8. The system includes two generators at buses 1 and 4 while loads are located at all four buses. The line data given in Tab. 1.1 shows the normal-π equivalents of four transmission lines in per-unit values with base power is 100MVA and base voltage is 230kV. The bus data in Tab. 1.2 gives the values of powers and voltages at each bus before the calculation of power flow. The generator at bus 1 is the slack bus or reference bus, thus the voltage magnitude and angle are constant. The generator at bus 4 is a voltage-controlled generator, thus its active power P_4^G and voltage magnitude $|V_4|$ are also constant. The solution of power flow will give values of powers of generators, voltages at load buses and current through*

TABLE 1.1: Line data of Example 1.1

From bus	To bus	R (p.u.)	X (p.u.)	Shunt $Y/2$ (p.u.)
1	2	0.01008	0.05040	0.05125
1	3	0.00744	0.03720	0.03875
2	4	0.00744	0.03720	0.03875
3	4	0.01272	0.0636	0.06375

TABLE 1.2: Bus data of Example 1.1

Bus	P_i^G(MW)	Q_i^G(MVar)	P_i^D(MW)	Q_i^D(MVar)	V_i(p.u.)	**Remarks**
1	-	-	50	30.99	$1.00\angle 0^0$	Slack bus
2	0	0	170	105.35	-	Load bus
3	0	0	200	123.94	-	Load bus
4	318	-	80	49.58	$1.02\angle -$	Voltage controlled

transmission lines.

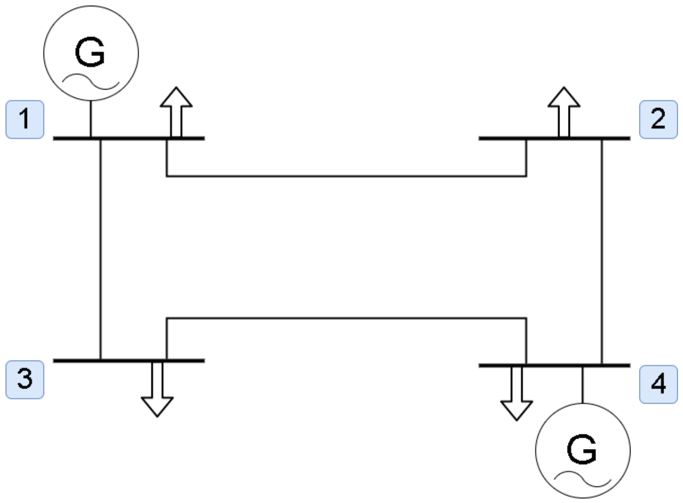

FIGURE 1.8: One-line diagram of the example system with bus numbers

In general, the relationship between current and voltage in a N_b-bus system is described as followings:

$$\begin{bmatrix} Y_{11} & Y_{12} & \dots & Y_{1N_b} \\ Y_{21} & Y_{22} & \dots & Y_{2N_b} \\ \dots & \dots & \dots & \dots \\ Y_{N_b1} & Y_{N_b2} & \dots & Y_{N_bN_b} \end{bmatrix} \begin{bmatrix} \dot{V}_1 \\ \dot{V}_2 \\ \dots \\ \dot{V}_{N_b} \end{bmatrix} = \begin{bmatrix} \dot{I}_1 \\ \dot{I}_2 \\ \dots \\ \dot{I}_{N_b} \end{bmatrix} \tag{1.4}$$

where Y_{ij} is the element of the admittance matrix, $\dot{V}_i$ and $\dot{I}_i$ are voltage and injected current at the i^{th} bus.

The injected current can be rewritten by generating powers, load demands and bus voltage as:

$$\dot{I}_i = \frac{\hat{S}_i}{\hat{V}_i} = \frac{\hat{S}_i^G - \hat{S}_i^D}{\hat{V}_i} = \frac{\left(P_i^G - P_i^D\right) - j\left(Q_i^G - Q_i^D\right)}{\hat{V}_i} \tag{1.5}$$

where:

- S_i: the complex power injection
- P_i^G Q_i^G: generating real and reactive powers, respectively
- P_i^D, Q_i^D: real and reactive of load powers, respectively

Substituting equation (1.4) into equation (1.5), the general form of power flow equation as:

$$\frac{\left(P_i^G - P_i^D\right) - j\left(Q_i^G - Q_i^D\right)}{\hat{V}_i} = \sum_{k=1}^{N_b} Y_{ik}\dot{V}_i \tag{1.6}$$

or

$$\left(P_i^G - P_i^D\right) + j\left(Q_i^G - Q_i^D\right) = \dot{V}_i \sum_{k=1}^{N_b} \hat{Y}_{ik}\hat{V}_i \tag{1.7}$$

The polar form of equation (1.7) is:

$$P_i^G - P_i^D = V_i \sum_{i=1}^{N_b} \left[V_j \left[G_{ij}\cos\left(\delta_i - \delta_j\right) + B_{ij}\sin\left(\delta_i - \delta_j\right)\right]\right] \tag{1.8}$$

$$Q_i^G - Q_i^D = V_i \sum_{i=1}^{N_b} \left[V_j \left[G_{ij}\sin\left(\delta_i - \delta_j\right) - B_{ij}\sin\left(\delta_i - \delta_j\right)\right]\right] \tag{1.9}$$

where

- G_{ij}, B_{ij}: real and imaginary components of elements of the admittance matrix, respectively

- V_i, δ_i: magnitude and angle of voltage, respectively

There are many algebraic methods solving the power flow. Some common methods have been listed in [3], such as: Newton-Raphson, Gauss-Seidel and Fast Decoupled. In this study, all power flow problems are solved by Newton-Raphson method.

For the small system given in Example 1.1, the power flow solution gives powers and voltages at all buses and powers through transmission lines in Tab. 1.3 and 1.4 with 4.81MW loss, respectively:

TABLE 1.3: Power-flow solution of Example 1.1

Bus	P_i^G(MW)	Q_i^G(MVar)	P_i^D(MW)	Q_i^D(MVar)	V_i(p.u.)
1	186.81	114.5	50	30.99	$1.00\angle 0^0$
2	0	0	170	105.35	$0.982\angle -0.976^0$
3	0	0	200	123.94	$1.00\angle -1.872^0$
4	318.00	182.43	80	49.58	$1.02\angle 1.523$
Total	504.81	295.93	500.00	309.86	

TABLE 1.4: Line flow of Example 1.1

From bus	To bus	(MW)	(MVar)
1	2	38.69	22.30
2	1	-38.46	-31.24
1	3	98.12	61.21
3	1	-97.09	-63.57
2	4	-131.54	-74.11
4	2	133.25	74.92
3	4	-102.91	-60.37
4	3	104.75	56.93

1.1.5 Conventional optimization techniques

Conventional methods, which use derivative or require convex characteristics as Lagrange method, have some disadvantages to solve non-convex problems. Figure ?? shows an example of the lack of derivative for solving problems considering multi-fuel cost functions. Since the multi-fuel cost function is non-smooth and non-derivative at $P = 200$MW, if we employ the Lagrange method, the search engine will be stuck at X_1 and can not give the best solution.

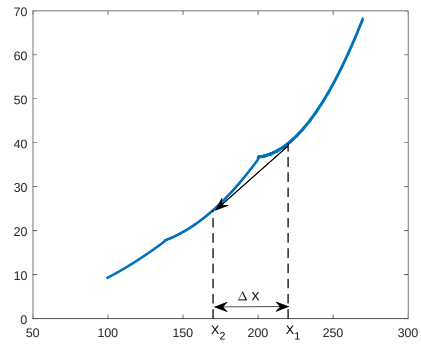

FIGURE 1.9: Disadvantages of conventional methods

1.2 Motivation of this thesis

Since the industrial revolution, the demand consumption of energy in human societies has been increasing rapidly. As an important form of energy, electricity impacts on our modern life and make us more comfortable and safer. In the daytime, factories with a huge of induction motors operate every day to make the economy developed. In the nighttime, electric lights make cities safer and other facilities, such as air-conditioner, fridge,. . . , provide a pleasant and enjoyable life. In actual fact, the more societies developed, the more electricity the human need. For an example, in the North America, the demand has been doubling every ten years. As a result of the development of societies, the number of generators has been increasing and the power system has been interconnecting. Finding the way to operate the system in economic is always the big challenge for operators.

On another hand, the development of computers gives new approaches to solving problems in engineering, and particularly electrical engineering. Meta-heuristics or evolutionary computation methods become more popular and widely applied for various fields of engineering. Among the modern optimization methods, Cuckoo search algorithm is an effective and powerful method to solve engineering problems.

This thesis proposes an improved version of the Cuckoo search algorithm, namely Self-Learning Cuckoo search algorithm (SLCSA), and applies it to popular problems of the power system to operate it economically. This study is firstly useful to the control center to compute the optimal reference values of controlled variables in the tertiary control. Due to the success on solving the Multi-Area Economic Dispatch and the Optimal Power Flow problems, the proposed method is a powerful tool to support the central transmission operators to give the most economic solution to operate the system. In addition, the proposed SLCSA is effective on the Optimal Reactive Power Dispatch problem. Thus, it also helps the local operating center reduce the power loss in their own network. Finally, the consultant companies may get benefit from this study to propose solutions to reconfigure the grid, such as identifying the sizing and place to install shunt-VAR commentators.

1.3 Research issues

In this thesis, the following objectives are pursued:

- The first objective is to understand the Cuckoo search algorithm (CSA) and propose an improved Self-Learning Cuckoo Search Algorithm (SLCSA). Basing on the idea and explanation of Yang and Deb, we study on the Cuckoo search algorithm and then, we propose an improvement to enhance the performance of Cuckoo eggs in the search space. Both of versions of Cuckoo search algorithm have been applied for a simple mathematical function to understand the effectiveness of the proposed method (see chapter 3).

- The second objective is to evaluate and understand the effectiveness of proposed SLCSA on the Multi-Area Economic Dispatch problem (MAED). The objective of the problem is to identify the optimal operating power of generators when many power systems interconnect. The problem is a type of non-convex ones, which includes many non-derivable functions, such as multi-fuel function or the fuel function considering valve-point effect (see Chapter 4).

- The third objective is to evaluate and understand the effectiveness of proposed SLCSA on the Optimal Power Flow problem (OPF). The problem is an important and popular tool for operating and planning the power system. The solution of this problem has to satisfy amount of unequal constraints with a huge of discrete and continuous controlled variables (see Chapter 5).

- The forth objective is to evaluate and understand the effectiveness of proposed SLCSA on the Optimal Reactive Power Dispatch problem (ORPD). This problem is a special version of the OPF problem, and its objective is to minimize the loss power. This problem is too difficult to distinguish the effectiveness because the change of optimal solutions is very small. It is also the big challenge to any compared methods (see Chapter 6).

- The final objective is to evaluate and understand the effectiveness of proposed SLCSA on proposing the optimal sizing and placement of shunt VAR compensators in the system. The problem consists of discrete variables with large changing steps. Due to the changing steps, the search engine can be fallen into the local optimum (see Chapter 7).

1.4 Structure of this thesis:

This thesis is organized in eight chapters. The detail of each chapter is below:

- Chapter 2: Literature review: This chapter places the definition of heuristics, meta-heuristics and briefly introduces some well-known and recent meta-heuristics.
- Chapter 3: Self-learning Cuckoo search algorithm: This chapter explains ideas of Yang and Deb to develop the Cuckoo search algorithm. Later, the proposed Self-Learning Cuckoo search algorithm is described and applied for the Ackleys mathematical function.
- Chapter 4: Multi-Area Economic dispatch problem
- Chapter 5: Optimal power flow problem
- Chapter 6: Optimal reactive power dispatch problem
- Chapter 7: Optimal sizing and placement of shunt-VAR compensators
- Chapter 8: Conclusion and futureworks

Chapter 2

Literature Review

This chapter presents a comprehensive study on meta-heuristics and their applications on electrical engineering. The first part places definitions and classification of heuristics and meta-heuristics. Other parts briefly introduce some popular optimization methods, e.g. Particle Swarm Optimization, Differential Evolution, Harmony Search, and some modern methods like Teaching learning-based optimization and Moth-Flames Optimization. The introduction provides the main idea and basic equations of the methods and discusses about their frequent utilization.

2.1 Heuristics and meta-heuristics:

2.1.1 Heuristics:

Heuristics are optimization techniques that employ practical methods to propose an approximately optimal solution. The word "heuristic" is derived from the verb "heuriskein" in Greek language and it means "to find" or "to discover". The fundamental idea of most heurictics is "trial and error"; thus, heuristics are very easy to apply for most of problems. They usually generate random solutions in the search space and evaluate them to figure out the optimal solution. Hence, the solution proposed by heuristics can be not the best one, but it is "good enough" or acceptable to apply for engineering problems. G. Polya suggested some commonly used heuristics as follows in [4]:

- Understanding a problem
- Try to use experience from related problems to plan an attack
- Carry out the attack
- Ask yourself whether you really believe the answer you have gots

2.1.2 Meta-heuristics:

The word "meta" in Greek language means "beyond" or "upper level"; thus, we can think that meta-heuristics are upper level heuristics. According to F. Glover in ref. [5], a meta-heuristic has a master strategy that guides and modifies other heuristic to produce solutions those that are normally generated in a quest for local optimality. In other words, the meta-heuristic include a strategy to lead stochastic components of the heuristic to discover the global solution and prevent the local optimal points.

Since the development of computation sciences, meta-heuristics are also skyrocket and diverse. Many researchers try to introduce various strategies and apply them for engineering problems. In general, meta-heuristics can be divided into two main approaches: single solution-based and population-based methods [6]. Simulated annealing and Tabu search are well-known single solution-based algorithms. These methods try to encourage one solution and avoid it fall into local optima. The new solution generated by these methods can be different from the neighborhood of the current solution. On the contrary, population-based meta-heuristics explore the search space through a set of solutions.

Resent years, the population-based methods develop much more than single solution-based ones, and most of the algorithms are basing on behaviors of human or animals in nature. Thus, these methods can be named nature-inspired methods. Basing on essential ideas, the population-based meta-heuristics can be classified such as: evolutionary strategy, swarm intelligence, . . . Evolutionary strategy prefers to using techniques concerned with natural evolution like selection, mutation, crossover, recombination,. . . Genetic algorithm, Differential evolution and Evolutionary programming are popular examples of these strategies. On another hand, swarm intelligence methods focuses on performances of species in their population. For instance, the Particle Swarm Optimization is based on the behaviors of birds in migrating flights [7]; the Ant Colony Optimization is developed from the action of ants when finding the shortest path from their nest to food [8].

Finally, another interesting approach of meta-heuristics is hybrid methods, which combine the two or more stochastic techniques to enhance the performance of the search engine. For example, F. Glover et al. proposed a combination of Genetic Algorithm and Tabu Search [9], while Y. Kao and E. Zahara suggested a hybrid version of Genetic Algorithm and Particle Swarm Optimization for multimodal functions [10]. Another popular hybrid of PSO and Differential Evolution [11], namely DEPSO, is also successful in solving optimal problems of electrical engineering. Hybrid algorithms make meta-heuristics much more diverse and efficient.

2.2 Particle Swarm Optimization

Particle Swarm Optimization is one of the most popular meta-heuristics since invented by Kennedy and Eberhart in 1995 [7], because of its simplicity and ability to find widely optimal solutions. The main idea of this method is based on the behaviors of birds in their annual migrating or finding food flights. In a flock, the bird basing on its own experience and the best location determines its optimal position to minimize the energy consumption. Each swarm in PSO has a position x_i, representing a solution, and a velocity v_i. For each iteration, the velocity is randomly updated from its best position $pbest_i$ and the best current location $gbest$. In the original PSO, the velocity v_i and position x_i of a particle are changed according to following equations:

$$v_{i,G+1} = v_{i,G} + c_1.(pbest_i - x_{i,G}) + c_2.(gbest - x_{i,G}) \quad (2.1)$$

$$x_{i,G+1} = x_{i,G} + v_{i,G+1} \quad (2.2)$$

where c_1 and c_2 are coefficients of cognitive and social components.

Later works, there are many types of PSO proposed in literature. Some researches invent new strategies to improve its efficiency and speed. For example, Clerc and Kennedy proposed a constriction factor with the fixed value of two coefficients $c_1 = c_2 = 2.05$ [12]. In this approach, PSO becomes a non-parameter algorithm. Another well-known version of PSO, namely Self-Organizing Hierarchical Particle Swarm Optimizer with Time-Varying Acceleration Coefficients, was introduced by A.Ratnaweera et al.[13]. By changing two coefficients c_1 and c_2, the authors proposed the strategy that particles fly widely in search space at the beginning and converge toward the global optimal at the end of search. They also proved that the previous velocity component can be neglected when updating the new velocity in the eq. (2.1).

2.3 Differential Evolution

Differential Evolution is an evolutionary strategy-based algorithm developed by P. Storn and K. Price since 1996 [14]. This method employs the mutation and crossover processes of evolution. In the mutation stage, a mutant vector $v_{i,G+1}$ is generated from the current solution $x_{i,G}$ as follows:

$$v_{i,G+1} = x_{r_1,G} + F.\left(x_{r_2,G} - x_{r_3,G}\right) \tag{2.3}$$

where r_1, r_2 and r_3 are random indexes of population, and F is the mutation factor

In the crossover stage, the trial solution $u_{i,G+1}$ is randomly created from the mutant vector $v_{i,G+1}$ and the current solution $x_{i,G}$ as below. The figure 2.1 illustrates the process of generating a 7-dimension trial solution:

$$u_{i,G+1} = \begin{cases} v_{i,G+1}, \text{if} rand() \leq CR, \\ x_{i,G}, \text{otherwise} \end{cases} \tag{2.4}$$

2.4 Harmony Search Algorithm

Harmony search algorithm is an optimization method based on natural musical performance processes [15]. Engineers seek for a global solution determined by an objective

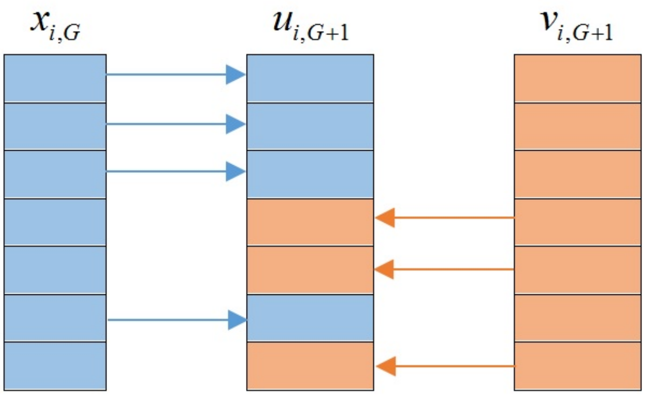

FIGURE 2.1: Illustration of crossover stage of Differential Evolution algorithm

function, just as the musicians seek a pleasing harmony determined by aesthetic. In music improvisation, pitches of each player in a possible range make a harmony vector. If the harmony vector shows a good solution, it is stored in memory. The harmony memory (HM) stores all feasible harmonies, and the harmony memory size determines the number of stored harmonies. A new harmony is generated from the HM by selecting the components of different vectors randomly. If the New Harmony is better than the existing worst harmony in the HM, the HM would include the new harmony and replace the worst one. This process is repeated until the fantastic harmony is found. To improve the performance, M. Mahdavi et al proposed a new strategy for the Harmony search algorithm [16]. The pitch-adjusting rate (PAR) and the bandwidth (bw) are updated with generation number instead of setting as constant in the original version as followings.

$$bw_i = bw_{\max}.\exp\left(\frac{\ln\left(\frac{bw_{\min}}{bw_{\max}}\right)}{MAXITER}.iter\right) \tag{2.5}$$

$$PAR_i = PAR_{\min} + \frac{PAR_{\max} - PAR_{\min}}{MAXITER}iter \tag{2.6}$$

Where $bw_{\max}$, $bw_{\min}$ are the maximum and minimum bandwidth; $PARmax$, $PARmin$ are the maximum and minimum pitch adjust rate. The steps in the procedure of IHS are as follows:

- Step 1: Initialize the algorithm parameters
- Step 2: Harmony memory initialization

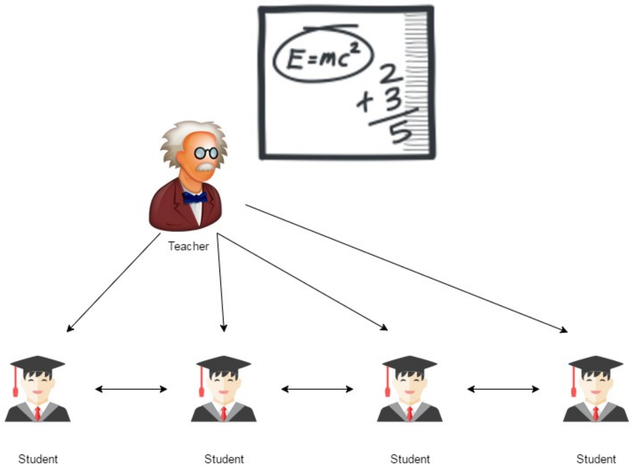

Figure 2.2: Illustration of potential idea of the Teaching-learning based optimization

- Step 3: Generate new harmonies by three rules: memory considerations, pitch adjustments and randomization. New harmonies can be conducted from Harmony memory or randomly generated. Then, they have a probability rate PAR_i to adjust by adding the bandwidth bw_i. The process to generate new harmony is shown in the fig.
- Step 4: Update HM and replace the worst harmony if necessary.
- Step 5: Repeat Steps 3 and 4 until the terminating criterion is satisfied.

2.5 Teaching-learning-based optimization

In 2011, R.V. Rao et el developed the Teaching-learning- based optimization, a kind of population-based method [17]. This method simulates communications between the teacher and learners in a class. A good teacher can transfer his knowledge to learners better than another average-level teacher can. It leads his learners get better marks. On the hand, learners in a class can exchange their knowledge together to improve themselves. Basing on these basic ideas, R.V. Rao et el proposed the method with two stages in its process of working. The first stage is namely Teacher phase and the other is Learner phase. The figure 2.2 illustrates the potential idea of the TLBO.

In teacher phase, the recent best solution plays role as a good teacher to move the mean value Mi toward the higher level. A factor, named teaching factor, TF decides the changes of mean value. The teaching factor can be 1 or 2 and is decided randomly. Follow equations show the probable value of the teaching factor, the change of mean value and updated values for solutions:

$$T_F = round\,(1 + rand()) \tag{2.7}$$

$$D\_mean = rand().\,[M_{best} - T_F.M_i] \tag{2.8}$$

$$X_{new,i} = X_{old,i} + D\_mean \tag{2.9}$$

where:

- $rand()$ is a probability function, returns a random number in the range [0, 1]
- M_{best} is the current best solution
- M_i is the mean value of populations
- $X_{old,i}$, $X_{new,i}$ are the existing and updated solutions, respectively.

In learner phase, a learner selects randomly another one in his class to exchange knowledge. He may learn something new from his friend if the friend is better than he is. Otherwise, he will help his friend improve knowledge of his friend. The advantage of the teaching-learning-based optimization is that it is a parameter-less algorithm. Hence, it is very easy to apply for solving complex problems.

2.6 Moth-Flame Optimization

Basing on the convergence of moths towards the light, Seyedali Mirjalili proposed the Moth-flame optimization (MFO) [1]. Moths are fancy insects and familiar with butterflies. Moths have a special navigation method at night. They use the moon light to direct their fly by maintaining a constant angle with respect to the moon. Since the moon is far away from the earth, this mechanism help moths fly in a straight path. However, moths are usually confused because of artificial light sources. The human-made circle lights attract

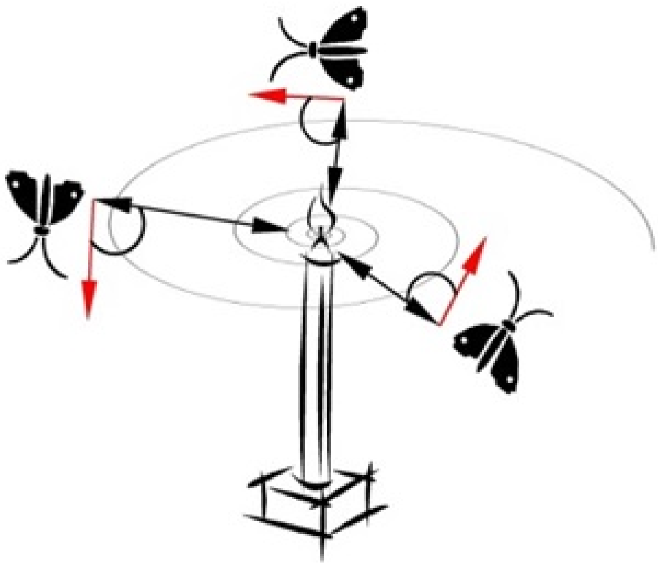

FIGURE 2.3: Spiral-flying path around a close light [1]

moths and let them into a deadly way [18, 19]. When moths see a circle light, they keep maintaining a fixed angle with the light. Unfortunately, the light compared with the moon is extremely close, thus moths fly path becomes a spiral path. Fig. 2.3 shows a conceptual model of this behavior.

In MFO, each moth represents a solution and variables of the problem are the position of the moth. Flames, which are artificial light sources, store the best positions of the moths. The new position of a moth is updated with respect to a flame via the spiral function as following equation. Figure 2.4 illustrates the positions of the flame, the moth and the logarithmic spiral function.

$$M_i = S(M_i, F_j) = F_j + D_i \cdot e^{bt} \cdot \cos(2\pi t) \tag{2.10}$$

$$D_i = |F_j - M_i| \tag{2.11}$$

where:

- M_i indicates the position of the i^{th} moth.
- F_j indicates the position of the j^{th} flame.
- b is a constant for defining the shape of logarithmic spiral.
- t is a random number in the range [-1;1].

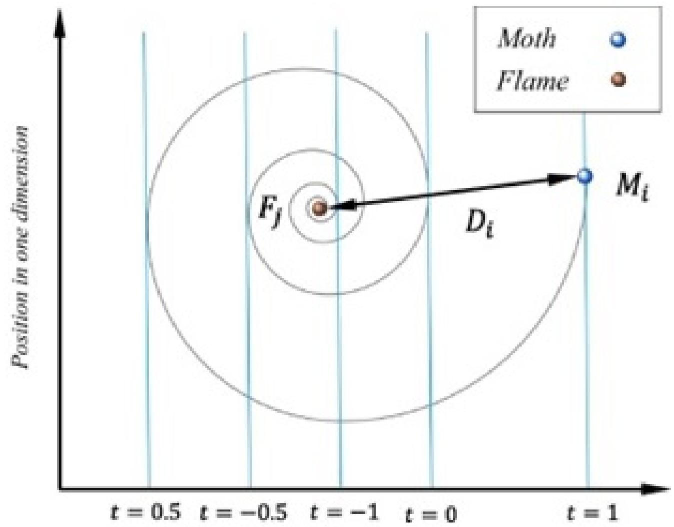

FIGURE 2.4: Logarithmic spiral, space around a flame, and the position with respect to t [1]

- D_i indicates the distance between the M_i moth and F_j flame.

In order to enhance performance of moths on searching the global optimum, the author proposed a limited number of flames that moths are attracted to. This number is decreased over the course of iterations to cause moths to focus on global solution at the end of the process. The following formula defines this number:

$$flame\_no = round\left(N - it \cdot \frac{N-1}{T}\right) \tag{2.12}$$

where it is the current number of iteration, N is the maximum number of flames and T is the maximum number of iterations.

2.7 Discussion

2.7.1 Apply a meta-heuristic for solving a problem

According to the brief introduction of above meta-heuristics, the major equation of most meta-heuristics to generate a new solution is simple as following, where ΔX is generated randomly basing on the strategy of meta-heuristics. ΔX can consider the previous best solutions as PSO, or be a mixture of solutions as DE, or be generated by the comparison of current solution and the best solution as TLBO and MFO.

$$X_{new,i} = X_{old,i} + \Delta X \tag{2.13}$$

The overall process to apply a meta-heuristic for solving a problem is commonly as followings:

1. **Step 1:** Determine independent and dependent variables. Independent variables are generated randomly as (2.13), and dependent variables are calculated from independent ones.
2. **Step 2:** Determine the fitness function. The fitness function must include the objective and handle all constraints of dependent variables.
3. **Step 3:** Generate solutions of independent variables according to algorithm of the meta-heuristic.
4. **Step 4:** Evaluate the fitness function due to independent and dependent variables. Store the best value of fitness function and the best solution.
5. **Step 5:** If the process reaches the stopping criterion, stop the iteration. If not, return Step 3.
6. **Step 6:** The optimal solution given from the optimization calculation has to check again whether it violates constraints or not.

2.7.2 Effectiveness of meta-heuristics

Above optimization methods can be divided into three groups according to the way they make random solutions. The first group including PSO and CSA generates the new state by employing various distribution functions and comparing with the current best solution. On another hand, DE and HSA represents the second group. In this group, a part of new solutions are randomly conducted from the current memory, and the others are newly generated in the search space. Finally, TLBO and MFO can be in the third group that generate new states by considering the distance between current solutions and the best one.

In another approach, comparing the number of controlled parameters, PSO, DE and HMS consist of too many coefficients or probability rate. For example, in the original PSO, the authors proposed three fluctuating coefficients ω, c_1 and c_2, and each set of these coefficients can give various results. DE and HSA also have probability rate to conduct solutions for the memory and other parameters to generate new state. Furthermore, CSA is a parameter-less meta-heuristic. In the brief introduction, Yang and Deb proposed two controlled parameters K_{scale} and p_a. Later works, they nominated the effective range for these parameters in [20]. On the contrary, TLBO and MFO are non-parameter methods. The number of controlled parameters is also necessary to pay attention when applying meta-heuristics for solving problems, because it can take time to choose the best set of parameters.

In order to compare the effectiveness on solving problems, we can follow the competition of meta-heuristics at the annual congress on evolutionary computation. Furthermore, we can get problems of the competition to evaluate by ourselves as [21]. In addition, some researchers also announce their comparing results on their fields such as [22, 23].

Chapter 3

Self-Learning Cuckoo search algorithm

The cuckoo search algorithm (CSA) is an optimization technique developed by Yang and Deb in 2009. In comparison with other meta-heuristic search algorithms, the CSA is a new and efficient population-based heuristic evolutionary algorithm for solving optimization problems with the advantages of simple implement and few control parameters. This algorithm is based on the obligate brood parasitic behavior of some cuckoo species combined with the Lévy flight behavior of some birds and fruit flies. In this chapter, we explain the main idea and procedure of the CSA. This chapter includes three sessions. The first session describes the basic idea to develop the conventional CSA. The method is basing on the parasitic behavior of Cuckoo birds and the Lévy flight, which is based on the Lévy distribution. The second session is the proposed Self-Learning Cuckoo Search Algorithm. The evaluations of both algorithms on common tested benchmarks place in the third session. Moreover, the final session is a brief review of the applications of Cuckoo search algorithm on engineering problems.

FIGURE 3.1: Cuckoo bird in nature

3.1 Cuckoo search Algorithm

3.1.1 Cuckoos breeding behavior

In nature, Cuckoo birds are interesting ones with their beautiful sound and aggressive reproduction strategy. The figure 3.1 shows a beautiful Cuckoo bird in nature. Basing on study of Payne et al [24], most of Cuckoo species are lazy parents. They engage the obligate brood parasitism by laying their eggs into the neighbors' nests. Parasitic Cuckoos are used to choosing the nest where the host bird has just laid its own eggs. Some host birds can directly conflict with the intruding Cuckoos. If the host bird discovers that the eggs are not its own ones, it will either remove the eggs or simply abandon its nest and built up another one elsewhere. In order to reduce the probability of their abandoned eggs, female parasitic Cuckoos have to learn the color and pattern of a few chosen host birds' egg. They try their best to generate their eggs as similar to the host birds eggs as possible. The figure 3.2 shows a neighbors nest with a Cuckoo egg. The pattern of Cuckoo egg is close to the neighbor's egg, but its size is slightly bigger.

According to the study of Payne et al., Cuckoos are extremely aggressive species [24]. The mature Cuckoos do not only engage to parasitic reproduction, but the Cuckoo chicks also harm to the host birds eggs. In general, once the Cuckoo eggs hatch earlier the host birds eggs, the Cuckoo chick will evict the host birds eggs by propelling them out of nest to increase provided food by the host bird. Furthermore, the Cuckoo chick can mimic

FIGURE 3.2: Neighbors nest with a Cuckoo egg

sounds of the host bird to gain access to more feeding opportunity.

3.1.2 Lévy flight

We wonder how animals search for foods. In general, the foraging path of an animal is effectively a random walk because their next step is based on their current position and the transition probability of the next location. The transition probability can be modeled mathematically. Various studies [25, 26] have proved that the flight behavior of many animals and insects is the typical characteristic of Lévy flights.

The Lévy flight provides a random walk while the random step length is drawn from the Lévy distribution. The Lévy distribution is a continuous probability distribution for non-negative random variable. With any random variable x in the range $(\mu; \infty), \mu > 0$, the probability density function of Lévy distribution is below:

$$f(x; \mu, c) = \sqrt{\frac{c}{2\pi}} \frac{e^{-\frac{c}{2(x-\mu)}}}{(x-\mu)^{3/2}} \tag{3.1}$$

where μ is the location parameter and c is the scale parameter.

When $\mu = 0$, the equation (3.1) becomes follows and its cumulative with various values of c is shown in Fig. 3.3:

$$f(x; c) = \sqrt{\frac{c}{2\pi}} \frac{e^{-\frac{c}{2x}}}{x^{3/2}} \tag{3.2}$$

According to the description of conventional Cuckoo search algorithm, the value c is set at 1.5.

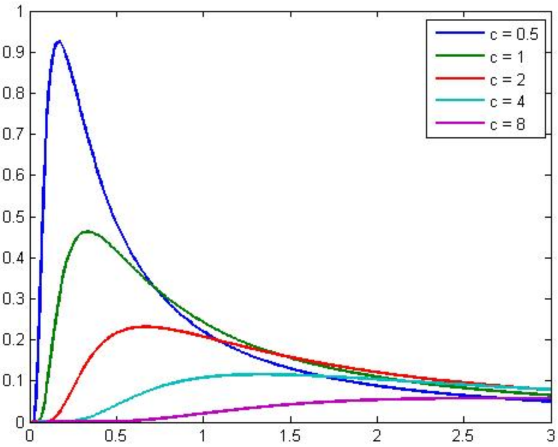

FIGURE 3.3: Cumulative of the Lévy distribution

3.1.3 Conventional Cuckoo search algorithm

Since 2009, Yang and Deb proposed a new population-based algorithm by combining the Lévy flight with the obligate brood parasitic behavior of Cuckoo [27, 28]. The algorithm is simply described within following three rules:

1. Each cuckoo lays one egg at a time, and dumps it in a randomly chosen nest.
2. The best nests with high quality of eggs (solutions) will carry over to the next generations.
3. The number of available host nests is fixed, and a host can discover an alien egg with a probability $p_a \in [0, 1]$. In this case, the host bird can either throw the egg away or abandon the nest to build a completely new nest in a new location.

For simplicity, at the last rule, if the host bird discovers an alien egg, it will replace the current nest by a new one. It means that new solutions are randomly generated to replace the current solutions. The general system equation generates a new solution and adds Cuckoo eggs to the previous one by the Lévy flight. The detail formula is given as below:

$$X_i^{t+1} = X_i^t + rand() \cdot stepsize \tag{3.3}$$

where $rand()$ is the random function, which returns a random value in the range $[0;1]$. $stepsize$ is the step size of the Lévy flight.

The step length shows the similarity between a Cuckoos egg and a hosts egg. This generation is tricky in implementation and a good algorithm is Mantegnas one [29]. Following equations formulate the Mantegnas algorithm to generate the step length for Lévy flight:

$$stepsize = K_{scale} \cdot step \cdot (X_{best} - X_i) \tag{3.4}$$

$$step = \frac{u}{v^{\frac{1}{\beta}}}; \tag{3.5}$$

$$u = rand().\sigma; v = rand() \tag{3.6}$$

$$\sigma = \left(\frac{\Gamma(1+\beta).\sin\left(\frac{\pi.\beta}{2}\right)}{\Gamma\left(\frac{1+\beta}{2}\right).\beta.2^{\frac{\beta-1}{2}}} \right)^{\frac{1}{\beta}}; \beta = \frac{3}{2} \tag{3.7}$$

Here the factor K_{scale} is the step size scaling factor, which is related to the scales of the problem of interest. According to the review made by Yang and Deb [20], if the factor K_{scale} is lower than 0.1, the search engine should be more effective and avoid flying so far. Thus, for all case studies in this research, we set $K_{scale} = 0.05$.

After laying the Cuckoo eggs into the nests, the authors employed a probability rate p_a to discover alien eggs. In case the host bird discover the Cuckoo eggs, she will abandon her nest and replace it by a new one. The new nest will be generated randomly from populations. Following equations describe the way of replacing the nests:

$$X_i^{t+1} = X_i^t + K.\Delta X_i^{dis} \tag{3.8}$$

$$K = \begin{cases} 1, rand() < p_a \\ 0, \text{otherwise} \end{cases} \tag{3.9}$$

$$\Delta X_i^{dis} = rand()\left[randperm(X_i) - randperm(X_i)\right] \tag{3.10}$$

where $randperm(X_i)$ is the random perturbation for positions of nests.

3.2 Proposed Self-learning Cuckoo Search Algorithm

The Self-learning Cuckoo search algorithm proposes an improvement to enhance the performance of Cuckoo eggs. We propose a simply way to help the Cuckoo eggs modify themselves and avoid being abandoned by the host bird. The Cuckoo eggs learn from other better solutions and modify to follow them. Following equations describe the proposed idea:

$$X_i^{t+1} = X_i^t + rand().\Delta X_i^{improve} \tag{3.11}$$

$$\Delta X_i^{improve} = \begin{cases} X_i - X_j, \text{if} f\left(X_i\right) < f\left(X_j\right) \\ X_j - X_i, \text{otherwise} \end{cases} \tag{3.12}$$

Where $f(x)$ is the fitness function.

The proposed process gives a gradient to let Cuckoo eggs follow the better eggs and helps the search engine converge faster. We employ a learning factor p_l to control the convergence of search engine. If the learning factor p_l is near to 1, the proposed method will converge faster but it may fall into local solutions. If the learning factor p_l is zero, the proposed method will become the conventional Cuckoo search algorithm. In this research, the effectiveness of the factor p_l has been investigated. The figure 3.4 shows the general pseudo-code of the proposed SLCSA.

With the pseudo-code of SLCSA, I have to design setting parameters of SLCSA, the fitness function and the stopping criterion to apply for optimization problems. The parameters of SLCSA include the probability rate p_a, the learning factor p_l and the number of particles NP. The number of particles NP is based on my experience. IF NP is too large, the search engine can find the optimal solution better, however the calculation time will be too much. If NP is too small, the search engine can not reach the optimal solution. The fitness function has to include the objective of each problem and satisfy all constraints of the problem.

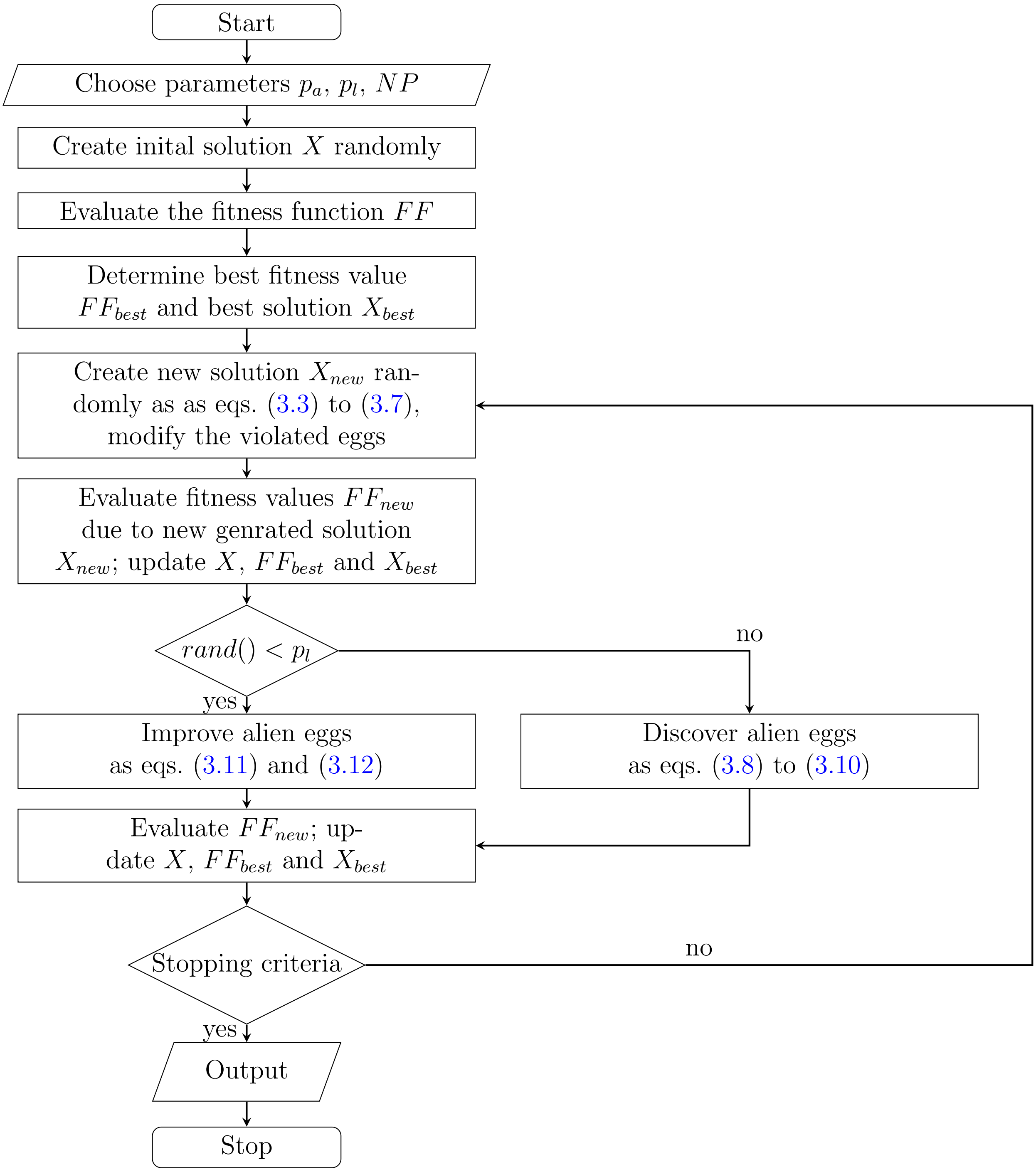

FIGURE 3.4: Flow chart of Self-Learning Cuckoo search Algorithm

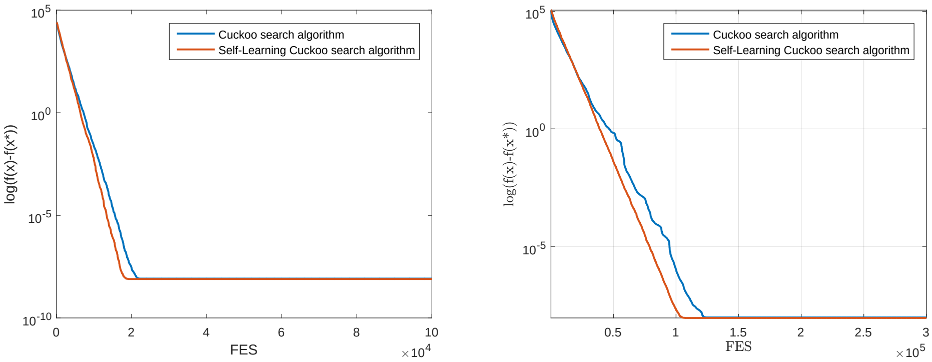

(a) 10 dimentions

(b) 30 dimensions

FIGURE 3.5: Convergence characteristics of the Shifted Sphere function

3.3 Evaluation on tested benchmarks

In order to investigate the efficiency of the proposed modification, SLCSA and CSA are evaluated on two common benchmarks: the Shifted Sphere function and the Shifted Schwefel's problem 1.2. The probability p_a changes from 0.1 to 0.9 with step 0.1, while the learning factor p_l changes from 0 to 1 with step 0.1. Note that when $p_l = 0$, the proposed SLCSA becomes the conventional CSA.

The tested benchmarks are collected from the Special Session on real-parameter optimization of the 2005 IEEE Congress on Evolutionary Computation [30]. Each benchmark is run on 10 and 30 dimensions with the termination error is 10^{-8}; the number of populations for each benchmark is 20 and 40, respectively.

For the Shifted Sphere function, both algorithms give the optimal solutions before reaching the Maximum iterations. Comparing the convergence characteristics in Fig. 3.5, the proposed Self-Learning Cuckoo Seach Algorithm is faster than the conventional in 10- and 30-dimension problems. When the number of dimensions is increasing, the proposed method converges more earlier.

For the Shifted Schwefel's problem 1.2 with 10 dimensions, both algorithms give the optimal solutions. However, the conventional CSA is only successful when the p_a factor is lower than 0.5 as Fig. 3.6(a). On another hand, the SLCSA gives the optimal solution on most couples of p_a and p_l factors, except that $p_a = 0.9$ and $p_l = 0.1$.

On the 30-dimension problem, both algorithms do not finish the searching process. The

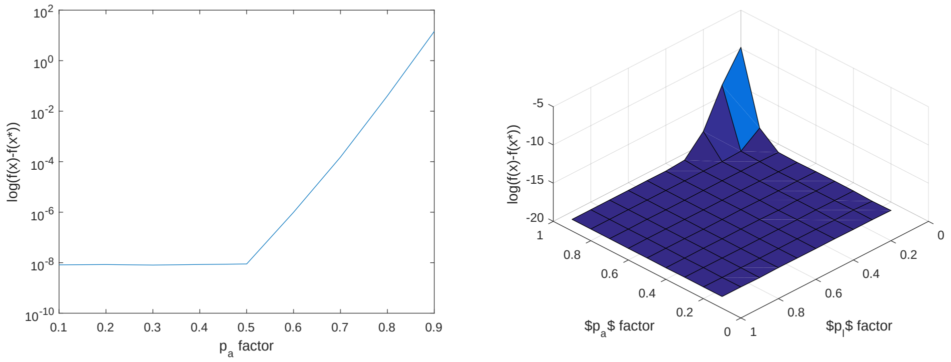

(a) Cuckoo search algorithm (b) Self Learning Cuckoo search Algorithm

FIGURE 3.6: Mean fitness values of the Schwefel's problem with 10 dimensions

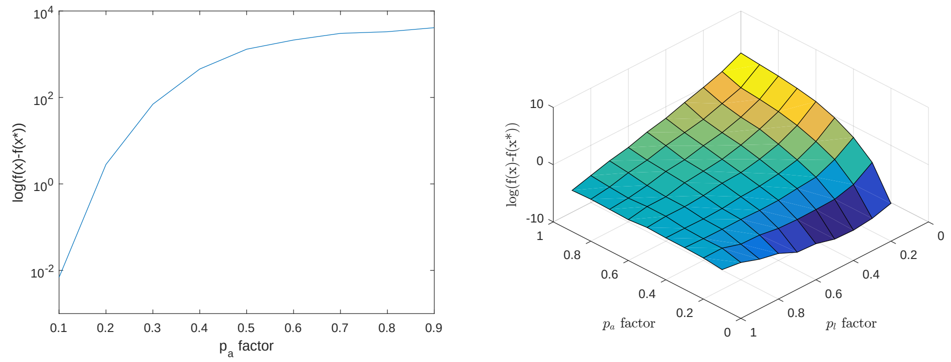

(a) Cuckoo search algorithm (b) Self Learning Cuckoo search Algorithm

FIGURE 3.7: Mean fitness values of the Schwefel's problem with 30 dimensions

conventional CSA give the best solution when the factor $p_a = 0.1$, and again, the proposed SLCSA gives better solutions in most of cases, except that the factor $p_l = 0.1$ in Fig. 3.7. Comparing the convergence characteristics, the SLCSA is extremely faster than the conventional CSA as Fig. 3.8.

3.4 Applications on engineering problems

At the first works to develop this method, Yang and Deb shown that the Cuckoo search algorithm is better than Particle Swarm Optimization and Genetic Algorithm in finding optimal solutions for 10 tested functions [27]. After that, they applied Cuckoo Search Algorithm for Spring design optimization and Welded beam design to proof that their method is favorable for engineering design problems [28]. Furthermore, the Cuckoo search

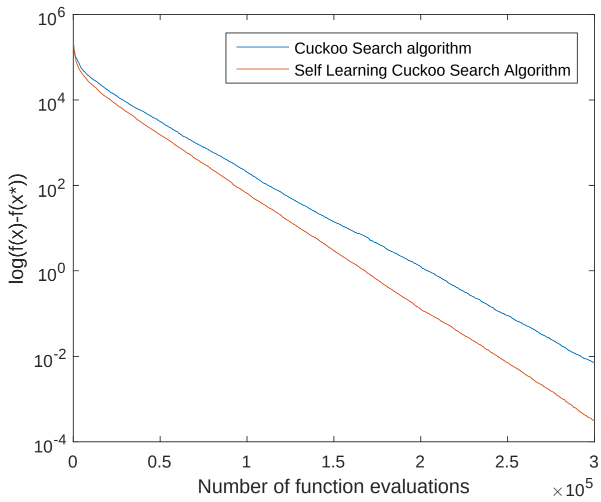

FIGURE 3.8: Convergence characteristics of SLCSA and CSA for the Schwefel's problem with 30 dimensions

algorithm became more popular in solving engineering problems. In literature, CSA is good at solving design optimization, forecasting ...

For design optimization, Q. Wang et al. employed CSA for the design of water distribution system considering multiple objectives [31]. Pani P. R. et al. used CSA to design planar ebg structures for power/ground noise suppression [32]. Lim W.C.E. et al. optimized the process of drilling PCB holes via CSA [33]. Gandomi A. H. et al. employed the CSA to solve 12 structural problems [34]. The CSA is also used to give the optimal parameters for milling operations[35].

Cuckoo search algorithm is also popular in various fields of information and communication technology. Khodier M. employed CSA to optimize antenna arrays [36]. Dhivya M. et al. uses CSA to improve energy efficient cluster information in wireless sensor network [37]. Chifu V. R. et al. compared CSA and ABC to optimize web services composition [38]. An enhanced CSA is used to filter spam mails [39].

In fields of forecasting, Cuckoo search algorithm is used to recognize human voices [40] and face [41]. Chaowanawatee K. and Heednacram A. combines CSA with neural networks to forecast flood in Thailand [42]. Kavousi-Fard A. and Kavousi-Fard F. proposed CSA to forecast short-term load in electricity market [43].

In the power system, many applications has employed the CSA. For instance, V. N. Dieu et al. applied the CSA for the non-convex economic dispatch [44], or Ahmed, J., and

Salam, Z. used the CSA to give the solution for a maximum power point tracking of photo-voltaic systems[45]. Rangasamy S. and Manickam P. employed a version of CSA to analyze the stability of power system [46].

Furthermore, P. Civicioglu and E. Besdok made a deep survey to compare the effects of the conventional Cuckoo search algorithm with other three evolutionary methods [47]. After obtaining 50 mathematical functions, they conducted that differential evolution and the Cuckoo search are quite better than PSO and artificial bee colony algorithm. Many researchers have tried to improve the performance of the Cuckoo search algorithm. For instance, H. Zheng and Y Zhou replaced the Lévy flight by Gauss distribution [48]. In addition, A. Ouaarab et al. proposed a fraction for smart Cuckoo eggs to improve the standard Cuckoo search algorithm for discrete problems [49]. On summary, there are many improvements of the original Cuckoo search algorithm, but no method is clearly more effective than the conventional one.

Chapter 4

Multi-Area Economic dispatch problem

This chapter proposes a Self-Learning Cuckoo search algorithm to solve Multi-area economic dispatch problem (MAED). The objective of this problem is to minimize a total generation cost while satisfying generator operational constraints and tie- line constraints. The proposed method has been compared with the conventional Cuckoo search algorithm and Teaching-learning-based optimization to obtain its effectiveness. Numerical results show that the proposed method gives better solutions than two compared methods with high performance. This chapter includes six sections. The first section gives a literature review about the MAED problem. Section 2 describes the objective functions and operation constraints of Multi-area economic dispatch problem. The proposed Self-Learning Cuckoo search algorithm has been discussed in Section 3. Section 4 is the implementation of the proposed method for MAED problem. Section 5 shows numerical results and discussion. Finally, conclusions and future works have been made.

4.1 Introduction

4.1.1 Economic dispatch

Economic dispatch is an essential task in operation and planning of electric power system.The primary of this problem is to determine output power of generators at minimum cost while satisfying capacities of generators. This problem can be used to schedule committed generating units in the power system. The improvement of proposed schedules helps to save fuel cost or reduce pollutant emission.

A system consists of N thermal-generating units connected to a single bus-bar serving an electrical load P_{load} as Fig. 4.1. The input to each unit, shown as F_i, represents the fuel cost of the unit. The output of each unit P_i is the electrical power generated by that particular unit. The total cost rate of this system FC is the sum of the costs of each individual units. The essential constraint, named balanced-power constraint, on the operation of this system is that the sum of the output powers must equal the load demand. The problem is to minimize FC subject to the constraint that the sum of the powers generated must equal the receive load.

Example 4.1. *Looking back Example 1.1, two generators supply to loads at four buses with 500MW total demand. In Example 1.1, capacities and fuel costs of generating units are not mentioned. If two generators have fuel cost functions and limits of generating active powers as follows, how to determine the economic operating point of generators neglecting power loss of transmission system.*

$$F_1\left(P_1\right) = 785.96 + 6.63P_1 + 0.00298.P_1^2 + \left|300.\sin\left(0.035.\left(P_{1,\min} - P_1\right)\right)\right| \tag{4.1}$$

$$F_4\left(P_4\right) = 654.69 + 12.8P_2 + 0.00569.P_4^2 + \left|200.\sin\left(0.042.\left(P_{4,\min} - P_4\right)\right)\right| \tag{4.2}$$

and $254MW \leq P_1 \leq 550MW$*;* $94MW \leq P_4 \leq 375MW$

Mathematically speaking, the problem is formulated as:

$$\min FC(P_1, P_4) \tag{4.3}$$

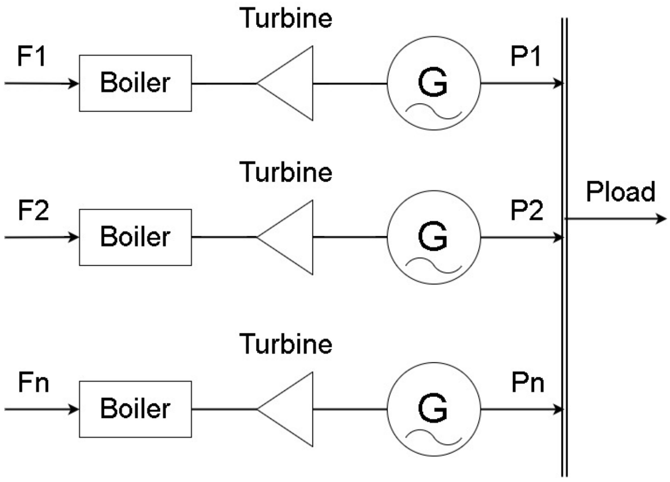

FIGURE 4.1: Illustration of N thermal-generating units serving a load

where:

$$FC(P_1, P_4) = F_1(P_1) + F_4(P_4) \tag{4.4}$$

subject to:

$$P_1 + P_4 = 500MW \tag{4.5}$$

$$254MW \leq P_1 \leq 550MW$$

$$94MW \leq P_4 \leq 375MW$$

The formulation is very common in mathematical optimization, the well-known method Lagrange multipliers can be a strategy to find the minimal point of the problem. However, due to the sinusoidal elements of fuel cost functions, the Lagrange method is incapable of solving this problem.

The following strategy is applied the proposed SLCSA for solving the problem. The strategy is also available for any meta-heuristics. At first, like the Lagrange method, the equal constraint (4.5) is combined to the total fuel cost (4.4) via a penalty factor K as follows, where K is as much as possible. In this case, I propose $K = 10,000$.

$$|P_1 + P_4 - 500| < 10^{-2} \tag{4.6}$$

When the fitness function FF is minimized, the balanced-power constraint will be satisfied and the optimal value of FF will be equal to the minimum total fuel cost. The balanced-

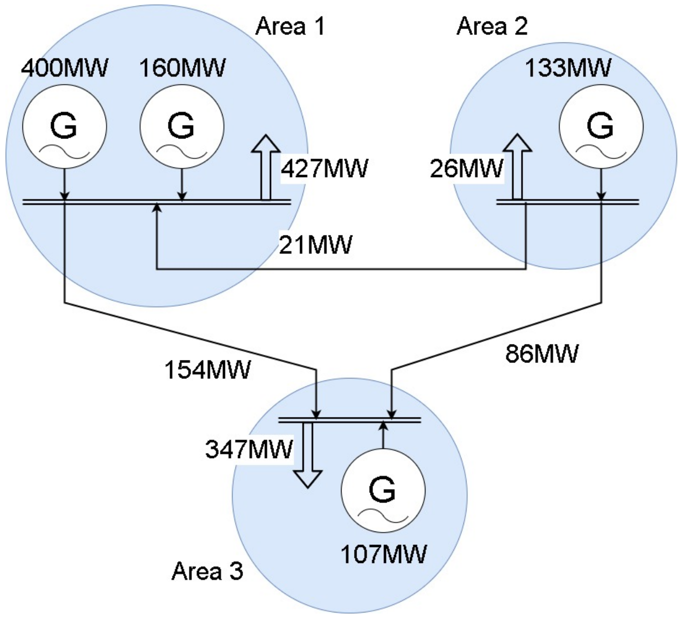

FIGURE 4.2: Example of a Multi-area economic dispatch problem

power constraint is the stopping criterion of the problem as follows:

$$FF(P_1, P_4) = F_1(P_1) + F_4(P_4) + K(P_1 + P_4 - 500)^2 \tag{4.7}$$

The minimal solution of this problem calculated by SLCSA is 6231.16468 \$ when $P_1 = 401.106064MW, P_4 = 98.850937$, the average calculation time is 0.069312 seconds. The detailed code of this application is placed at Appendix F.

4.1.2 Multi-area economic dispatch:

Multi-area economic dispatch (MAED) is an expansion of the economic dispatch. In this problem, operators have to determine generating power of each generator and transmission power between areas. Figure 4.2 illustrates an example of a MAED problem. Four generators are located in three various areas. In each area, operators have to maintain the balanced-power constraint. This problem can propose optimal solutions to operate connected power systems of neighbor countries.

4.2 Problem formulation

4.2.1 Objective function:

The objective of the Multi-area economic dispatch problem is to minimize the total fuel cost of generators in all areas while satisfying all operating constraints. The constraints of MAED include the balanced-power constraint in each area, limitations of generating units, limitations of tie-line capacity and the prohibited operating zone of generating units. The objective function of MAED is written as:

$$\min F, F = \sum_{i=1}^{N} \sum_{j=1}^{M_i} F_{ij}\left(P_{ij}\right) \tag{4.8}$$

Where:

- N is the number of areas
- M_i is the number of generators in the i^{th} area
- $F_{ij}(P_{ij})$ is the fuel cost function of the j^{th} generator in the i^{th} area.

4.2.2 Operating constraints:

4.2.2.1 Real balanced-power constraint:

In each area, output power of generators must satisfy the power demand and power loss of that area and the transmission power from that area to others. Equation (4.9) describes this constraint in the ith area. The power loss of the ith area is expressed by using the B-coefficients as (4.10).

$$\sum_{j=1}^{M_i} P_{ij} = PD_i + PL_i + \sum_{\substack{k=1 \\ k \neq i}}^{N} T_{ik} \tag{4.9}$$

$$PL_i = \sum_{k=1}^{M_i} \sum_{l=1}^{M_i} P_{ik}.B_{i,kl}.P_{il} + \sum_{k=1}^{M_i} P_{ik}.B_{0i,k} + B_{00i} \tag{4.10}$$

Where:

- PD_i is the power demand of the i_{th} area.
- PL_i is the power loss of the i_{th} area.
- T_{ik} is the transmission power from the i_{th} area to the k_{th} area.
- B_i, B_{0i} and B_{00i} are coefficients of power loss in the i_{th} area.

4.2.2.2 Limitation of output power:

Each generator has upper and lower bound limits of generating capacity. The formula of this constraint is following:

$$P_{ij,\min} \leq P_{ij} \leq P_{ij,\max} \tag{4.11}$$

Where P_{min} and P_{max} are lower and upper limited powers of the generator.

4.2.2.3 Limitation of transmission lines:

Each transmission line has upper limit that should not exceed because of security condition. We note that the sign of transmission power represents the direction of transmission power from the i_{th} area to the k_{th} area. This constraint is written as:

$$|T_{ik}| \leq T_{ik,\max} \tag{4.12}$$

4.2.2.4 Prohibited operating zone constraint:

In actual operation, some generators have prohibited operating zones. This constraint has been created because of vibration in a shaft bearing caused by steam valves or faults of equipments such as boiler, feed pump, etc. It is too difficult to identify its actual performance. Thus, the operators avoid operating generators in these areas. Hence, the fuel cost function is discontinued at the prohibited operating zone. Equation (4.13) describes this constraint as following:

$$\begin{aligned} &P_{ij,\min} \leq P_{ij} \leq P_{ij,L1} \\ &P_{ij,U1} \leq P_{ij} \leq P_{ij,L2}; \dots \\ &P_{ij,Un} \leq P_{ij} \leq P_{ij,\max} \end{aligned} \tag{4.13}$$

4.3 Previous works on Multi-area economic dispatch problem

In literature, many researchers proposed various evolutionary computing techniques to solve the MAED problem. P. S. Manoharan et al. made an investigation to determine effectiveness of four evolutionary algorithms [50]. Their results shown that Covariance-Matrix-Adapted Evolution Strategy is better than Real-coded Genetic algorithm, Particle Swarm Optimization and Differential Evolution. On another approach, L. Wang and C. Sigh proposed an improved Multi-objective Particle Swarm Optimization to solve a Multi-area environment/economic dispatch [51]. In addition, M. Basu proposed the Teaching-learning-based Optimization (TLBO) for solving MAED problems [52]. According to three tested systems, the author shown that the TLBO is more efficiency than Differential Algorithm, Evolutionary Programming and Real-coded Genetic algorithm. All of above population-based methods are successful to determine optimal solutions for MAED problems. However, each method can solve some problems effectively. Thus, the requirement to develop a new optimization technique and apply it for various problems increasingly continues.

4.4 Implementation for Multi-area economic dispatch problem

4.4.1 Determining output power of slack generator in each area

Each area has a slack generator as a reference bus to analyze the power flow. Basing on above constraints, we can conduct the output power of the slack generator in each area.

This step is very useful to reduce the number of unknowns, thus it can help to reduce the computational time. From the balanced-power constraint in (4.9), output power of the M_i^{th} generator is calculated from $M_i - 1$ generators as following:

$$P_{iM_i} = PD_i + PL_i + \sum_{\substack{k=1 \\ k \neq i}}^{N} T_{ik} - \sum_{j=1}^{M_i-1} P_{ij} \tag{4.14}$$

We replace the power loss PL_i by the (4.10) in (4.14).

$$P_{iM_i} = PD_i + \sum_{\substack{k=1 \\ k \neq i}}^{N} T_{ik} - \sum_{j=1}^{M_i-1} P_{ij} + \left(\sum_{k=1}^{M_i} \sum_{l=1}^{M_i} P_{ik}.B_{i,kl}.P_{il} + \sum_{k=1}^{M_i} P_{ik}.B_{0i,k} + B_{00i} \right) \tag{4.15}$$

After expanding and rearranging (4.15), we have a quadratic equation in which output power of the M_i^{th} generator is an unknown.

$$\begin{aligned} & B_{i,M_iM_i} P_{iM_i}^2 + \left(2 \sum_{k=1}^{M_i-1} B_{i,M_ik} P_{ik} + B_{0i,M_i} - 1 \right) P_{iM_i} + \\ & + \left(\begin{array}{l} PD_i + \sum\limits_{\substack{k=1 \\ k \neq i}}^{N} T_{ik} + \sum\limits_{k=1}^{M_i-1} \sum\limits_{l=1}^{M_i-1} P_{ik} B_{i,kl} P_{il} + \\ + \sum\limits_{k=1}^{M_i-1} B_{0i,k} P_{ik} - \sum\limits_{k=1}^{M_i-1} P_{ik} + B_{00i} \end{array} \right) = 0 \end{aligned} \tag{4.16}$$

4.4.2 Solution vector:

According to the objective of this problem, real power of generators in all areas and transmission powers are unknowns. However, we can decrease the number of calculated generators because M_i slack generators in areas can be solved from (4.16). If we call N_{gen} is the sum of generators in all area, the number of unknowns represent output power are equal to $(N_{gen} - M_i)$. On another hand, the number of transmission powers is a 2-combination of a set N, $C_{N,2}$. Finally, Equation (4.17) describes the solution vector for this problem. Furthermore, Equation (4.18) and (4.19) express the calculation of N_{gen} and the 2-combination of a set N, respectively.

$$X = \begin{bmatrix} \left(P_{11}, P_{12}, ..., P_{1(M_1-1)}\right), \left(P_{21}, P_{22}, ..., P_{2(M_2-1)}\right), ..., \\ \left(P_{N1}, P_{N2}, ..., P_{N(M_N-1)}\right), \\ \left(T_{12}, T_{13}, ..., T_{1N}\right), \left(T_{23}, T_{24}, ..., T_{2N}\right), ..., \left(T_{(N-1)N}\right) \end{bmatrix}' \tag{4.17}$$

$$N_{gen} = \sum_{i=1}^{N} M_i \tag{4.18}$$

$$C_{N,2} = \frac{N!}{2!\,(N-2)!} \tag{4.19}$$

4.4.3 Fitness function:

The fitness function considers the objective function and constraints of depended unknowns. In this problem, output powers of M_i slack generators are depended unknowns. The values of M_i slack generators conducted from (4.16) have to lay in their upper and lower limits. In order to handle this constraint, we define a limit function as (4.20) and the formula to identify violated values is in (4.21).

$$V^{\lim}(x) = \begin{cases} x_{\max}, \text{if} x > x_{\max} \\ x_{\min}, \text{if} x < x_{\min} \\ x, \text{otherwise} \end{cases} \tag{4.20}$$

$$Violated\_Mi = \sum_{i=1}^{N} \left(P_{iM_i} - V^{\lim}(P_{iM_i})\right)^2 \tag{4.21}$$

For the constraint of prohibited operating zone, we define a POZ function. Its value returns zero if the output power out of prohibited operating zone. On contrary, it returns the value of output power. The POZ function is written as:

$$POZ\left(P_{ij}\right) = \begin{cases} P_{ij}, \text{if} P_{ij,L} < P_{ij} < P_{ij,U} \\ 0, \text{otherwise} \end{cases} \tag{4.22}$$

Finally, the fitness function FF of this function is following, where K is the penalty factor:

$$FF = \sum_{i=1}^{N} \sum_{j=1}^{M_i} F_{ij} \left(P_{ij} \right) + K.Violated\_Mi + K.POZ \tag{4.23}$$

4.4.4 Overall procedure of the proposed method for MAED:

The overall procedure for the implementation of the Self-Learning Cuckoo search algorithm to solve the MAED is following and the flow chart is given in Fig. 4.3.

- Step 1: Choose controlling parameters for the Self-Learning Cuckoo search algorithm. They include the probability of discovering Cuckoo eggs p_a, the learning factor p_l, the number of nests NP and the number of iterations It_{max}.
- Step 2: Create randomly initial nests X, and solve the quadratic equation (4.16) to find M_i output powers of slave generators. Evaluate value of the fitness function FF in (4.23).
- Step 3: Determine the best value of the fitness function FF_{best} and the best nest X_{best}. Set the iteration counter $it = 1$.
- Step 4: Create Cuckoo eggs via Lévy flight and the new nests X_{new}, modify the eggs that violate the limitations.
- Step 5: Solve the quadratic equation (4.16) to find M_i output powers of slave generators. Evaluate the fitness function for new nests; we have new values of the fitness function FF_{new}
- Step 6: Compare the new values FF_{new} to the current ones FF to pick up the better nests. Update the X, the best value of fitness function FF_{best} and the best nest X_{best}.
- Step 7: Randomly decide either discovering alien eggs or improving alien eggs. Modify the eggs that violate the limitations.
- Step 8: Once again, solve the quadratic equation (4.16) and evaluate the fitness function FF_{new} for new nests X_{new}

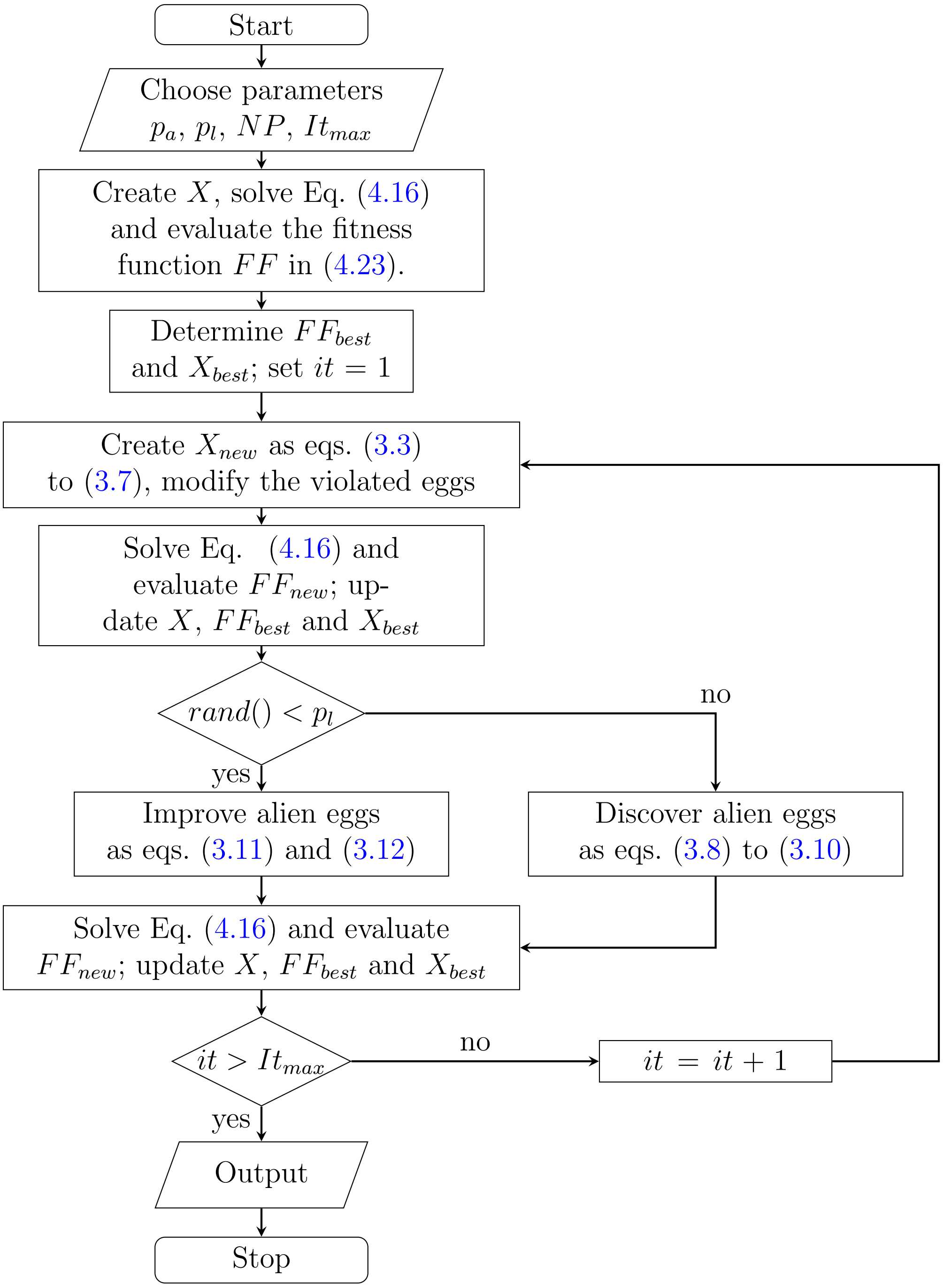

FIGURE 4.3: Flow chart of the implementation for MAED

- Step 9: Compare the new values FF_{new} to the current ones FF to pick up the better nests. Update the X, the best value of fitness function FF_{best} and the best nest X_{best}.

- Step 10: Check if the iteration counter it is lower than the maximum iteration $Iter_{max}$, increase it and return step 5. Otherwise, stop.

4.5 Numerical results

The proposed Self-Learning Cuckoo search algorithm has been evaluated on four case studies of the MAED problem. In order to investigate the effectiveness of the proposed method, we also applied the conventional Cuckoo search algorithm and the Teaching-learning-based optimization (TLBO) to compare numerical results. All algorithm has been programmed in Matlab 2015a and run in a personal computer (Pentium Core 2 Duo 2.4 Ghz and 4 GB RAM).

TABLE 4.1: Number of controlled vectors for each case study

	Number of controlled generators	Number of transmission power	Total controlled variables
Case 1	4	1	7
Case 2	7	3	10
Case 3	36	6	42
Case 4	135	8	143

4.5.1 Case study 1:

The first benchmark is a two-area system supplies for total 1263 MW load demand. The first area handles 60% of load demand with three generators, while the another area delivers to 40% of load demand with other three generators as Fig. 4.4. The transmission capacity between two areas is 100MW. In this case, the prohibited-operating-zone constraint has been considered and the fuel cost functions are quadratic ones. All data of fuel cost functions, prohibited-operating-zone constraint, B-coefficients and other limits are in Appendix A.

For this test system, the population size and the maximum iteration of three selected methods are 100 and 100, respectively. Controlling parameters of the Self-Learning Cuckoo search algorithm consists of the probability rate of discovering alien eggs $p_a = 0.5$ and the learning factor $p_l = 0.7$. In the conventional Cuckoo search algorithm, the probability rate of discovering alien eggs p_a is 0.8.

Table 4.2 shows the Monte Carlo results of three compared algorithms. Optimal solu-

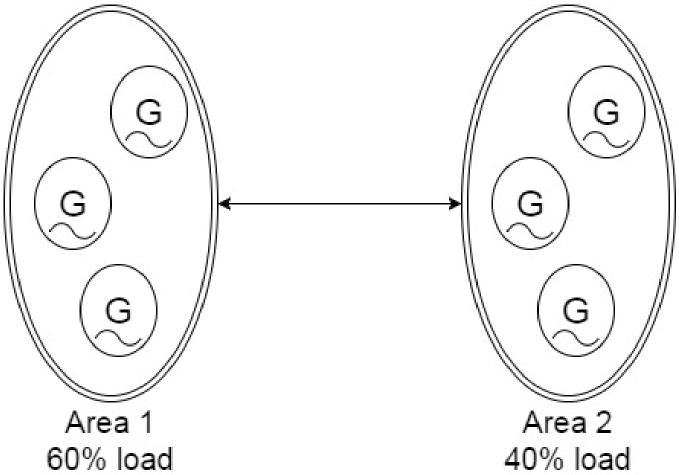

FIGURE 4.4: Illustration of the problem of case study 1

TABLE 4.2: Numerical results of three methods in 2-area system

Fitness function	SLCSA	CSA	TLBO
Minimum	12,246.34	12,246.44	12,246.34
Average	12,247.01	12,252.42	12,246.45
Maximum	12,250.29	12,267.89	12,257.59
Standard deviation	0.7741	3.5274	1.1193

tions of three methods seem to be the same. However, the proposed method is higher performance than conventional CSA and TLBO.

4.5.2 Case study 2:

In this tested case, a three-area system with ten generators supplies for 2,700MW load demand. The first area consists of four generators and assumes 50% of total load demand. The second area includes three generators and delivers to 25% of total load demand. Other three generators are in the third area and handle last 25% of total load demand. Figure 4.5 illustrates the problem of this case study. Three areas connect together by transmission lines with limited capacity is 100 MW. The fuel cost function is the multiple fuel sources combining valve point loading effect. The data of generators and B-coefficients are in Ref [53].

In order to solve this benchmark, we employ 100 particles and run in 200 iterations. The probability rate pa of conventional Cuckoo search algorithm is 0.3, while selected

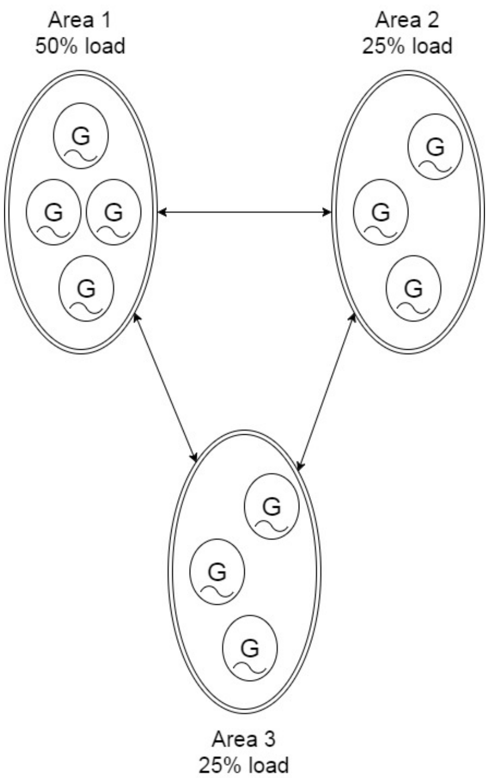

FIGURE 4.5: Illustration of the problem of case study 2

TABLE 4.3: Numerical results in the 3-area system

Fitness function	Worst	Best	Average	Standard deviation	CPU time [s]
SLCSA	655.1246	654.6799	654.9886	0.0670	25.49
CSA	656.1529	655.3398	655.6919	0.2353	25.40
PSO [50]	689.1066	689.9965	690.0995	0.0362	2.69
CMAES [50]	686.9850	686.9850	686.9850	0	3.07
RCGA [54]	-	657.3325	-	-	133.84
EP [54]	-	655.1716	-	-	108.06

TABLE 4.4: Optimal solution proposed by SLCSA

$P_{1,1}$(MW)	223.7185	$P_{3,1}$(MW)	236.1453
$P_{1,2}$(MW)	213.1915	$P_{3,2}$(MW)	329.2540
$P_{1,3}$(MW)	490.0142	$P_{3,3}$(MW)	250.3776
$P_{1,4}$(MW)	240.5801	$P_{T1,2}$(MW)	-99.9221
$P_{2,1}$(MW)	250.9924	$P_{T1,3}$(MW)	-99.8414
$P_{2,2}$(MW)	235.2053	$P_{T2,3}$(MW)	-32.2726
$P_{2,3}$(MW)	266.2348	-	-

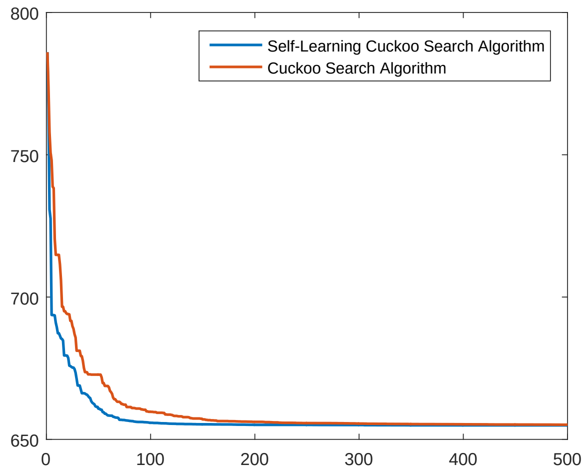

FIGURE 4.6: Comparison of convergence characteristics of three methods in case study 2

parameters for Self-Learning Cuckoo search algorithm are following:$p_a = 0.4$, $p_l = 0.5$.

According numerical results in Tab. 4.3, the Self-Learning Cuckoo search algorithm is better than conventional CSA. Figure 4.6 shows convergence characteristics of two methods. The SLCSA converges faster than the conventional and reach the global solution earlier. Comparing with other methods in literature, the conventional CSA is slightly worse than the Evolutionary Programing, while the proposed SLCSA gives the best solution. The optimal result oF SLCSA is shown in Tab. 4.4.

4.5.3 Case study 3:

This benchmark simulates a bulk power system with 40 generators divided into four areas. Each area has ten generators and supplies to a percentage of total load demand as Figure 5. Fuel functions with valve-point-loading effect of 40 generators are conducted from Ref [55]. In this case, the power loss in each area is neglected.

The population size and the maximum iteration of three compared methods are 200 and 800, respectively. Controlling parameters of the Self-Learning Cuckoo search algorithm consists of the probability rate of discovering alien eggs $p_a = 0.5$ and the learning factor $p_l = 0.7$. In the conventional Cuckoo search algorithm, the probability rate of discovering alien eggs p_a is 0.8.

TABLE 4.5: Numerical results of three methods in 4-area system

Fitness function value	SLCSA	CSA	TLBO	ABC [54]
Minimum [$]	**122,255**	125,719	122,427	124009.4
Average [$]	**122,786**	127,360	123,527	-
Maximum [$]	123,783	128,403	124,867	-
Standard deviation	307	565	596	-
CPU time [s]	128.29	126.16	128.47	126.93

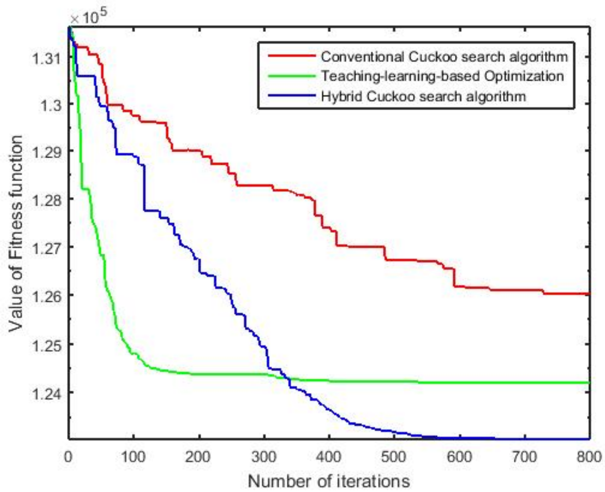

FIGURE 4.7: Comparison of convergence characteristics of three methods in case study 3

Table 4.7 shows results of three algorithms. The Self-Learning Cuckoo search is clearly more effective than other methods in finding the global solution. Convergence characteristics from Figure 3 show that the proposed method converges slower than TLBO; however, finally it gives better solution. In addition, the standard deviation of the proposed method is lowest among compared methods.

4.5.4 Case study 4:

The power system has 140 generators divided into 5 areas and supplies total 49,342 MW load demand. The numbers of generators in each area are 29, 28, 28, 35 and 20, respectively. The capacity of all transmission lines is 500MW. The illustration of the system is given in Fig. 4.8. All coefficients of fuel cost functions are taken from [56]. 12 of 140 generators have valve-point-loading effects on fuel cost functions, others are quadratic functions. The power loss in each area is neglected.

TABLE 4.6: Numerical results of three methods in 5-area system

Fitness function value	SLCSA	CSA	DCPSO [2]
Minimum [$]	**1,720,134**	1,720,295	1,721,134

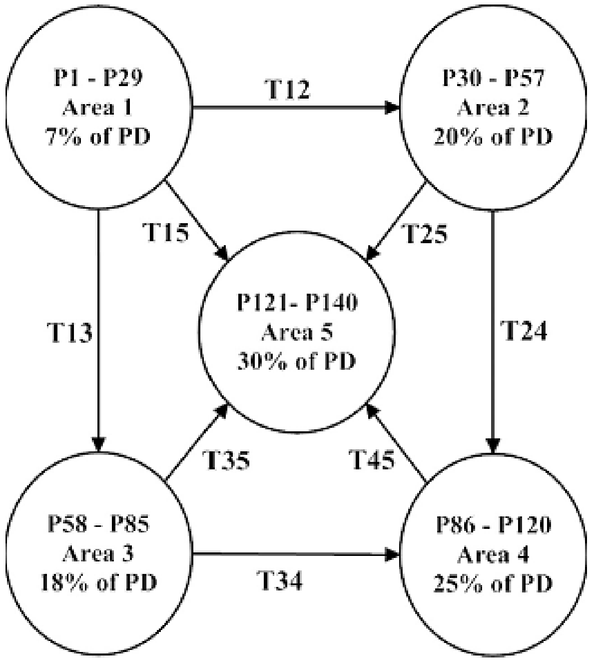

FIGURE 4.8: Illustration of the problem of case study 2 [2]

The population size and number of maximum iterations are 200 and 5000, respectively. According to the minimum total cost in Tab. 4.6, the result shows that SLCSA is better than Dynamically Controlled Particle Swarm Optimization (DCPSO) [2] on search the global solution. However, the computational time is much more slower. Table **??** shows the optimal solution for case study 2.

4.6 Conclusions

The proposed Self-Learning Cuckoo search algorithm has been successful in solving the MAED problem. The proposed method employs the learner stage of Teach-learning-based optimization to enhance the performance of Cuckoo eggs. A learning factor ph has been used to prevent Cuckoo eggs fall into local optima when employing the learner stage. According to three benchmarks of the MAED problem, the Self-Learning CSA is much better than the conventional CSA in finding optimal solutions. Comparing with the TLBO, the proposed method gives better solution in the large system with higher performance. MAED is a type of non-smooth, non-convex problems. Thus, the proposed method is favorable to apply for other optimization problems in engineering.

Chapter 5

Optimal power flow problem

This chapter proposes the Self-Learning Cuckoo search algorithm to solve optimal power flow problems in large-scale electric power systems. The proposed method is an improved version of the Cuckoo search algorithm by employing a new strategy to focus Cuckoo eggs on the global optima. Cuckoo eggs have to learn and modify themselves to enhance their performance. The learning strategy of Cuckoo eggs is also controlled by a learning factor to prevent the search engine falling into local optima. The proposed method has been applied for solving optimal power flow problems to investigate its effectiveness. The optimal power flow is an important, complex and non-convex problem in the electric power system. The aim of the problem is to minimize the total fuel cost while satisfying equal and unequal operating constraints of elements in the system. The proposed Self-learning Cuckoo search algorithm is also evaluated on optimal power flow problems on four standard IEEE 30-bus, 57-bus, 118-bus and 300-bus systems. According to numerical results, the proposed method gives better solutions than the conventional Cuckoo search algorithm and other compared algorithms in literature. Furthermore, the Self-learning Cuckoo search algorithm is more effective when the learning factor is around 0.8.

This chapter has been divided into six sections. The literature review about the optimal power flow is given in the first section. The second section gives the formulas of the optimal power flow problem. The proposed SLCSA has been discussed in the third section. The next section is the implementation of the proposed SLCSA including its overall procedure. Numerical results are given in the fifth section, and the final is the conclusion and future works.

5.1 Introduction

The optimal power flow has a long history in its development. It was first discussed by Carpentier in 1962 and took a long time to become a successful algorithm that could be applied in everyday use.

In Chapter 4, I introduced the concept of economic dispatch. In the economic dispatch, the balanced-power constraint must be satisfied, that means the total generation to equal the total load plus losses. As an expansion of the economic dispatch, the Multi-area economic dispatch considers the power flow between areas in a power system. However, a more detailed solution of the power system, which considers voltages at all buses and flows through all transmission lines, is necessary. The economic dispatch calculation in terms of the generation costs as Chapter 4 combines with the set of equations needed for the power flow itself as constraints, which were introduced in Chapter 1. This formulation is called an optimal power flow.

In the dispatch calculation developed in Chapter 4, the only adjustable variables were the generator MW output themselves. In the OPF, there are many more adjustable or "control" variables that be specified. A partial list of such variables would include:

- Generator voltage
- LTC transformer tap position
- Phase shift transformer tap position
- Swiched capacitor settings
- Reactive injection for a static VAR compensator

Thus, the OPF gives us a framework to have many control variables adjusted in the effort to optimize the operation of the transmission system.

5.2 Problem formulation

5.2.1 Objective function

The main objective of the optimal power flow is to minimize total fuel cost of generating units while satisfying operating constraints and limitations of installed elements on the power system. In this study, the fuel cost function of a generator is a quadratic function of generating real power. Generally, the mathematical formula and the fuel cost function of the OPF problem are as below:

$$\min F(x,u); \tag{5.1}$$

$$FC = \sum_{i=1}^{N_g} FC_i\left(P_i^G\right) \tag{5.2}$$

subject to:

$$g(x,u) = 0 \tag{5.3}$$

$$h(x,u) \leq 0 \tag{5.4}$$

where:

- $F(x,u)$, $FC(P_i^G)$: the objective function and fuel cost function, respectively
- x, u: vectors of controllable and dependent variables, respectively
- a, b, c: fuel cost coefficients of generators
- P_i^G: output real powers of generators
- $g(x,u), h(x,u)$: equal and unequal constraints, respectively

5.2.2 Operational constraints

5.2.2.1 Power balance constraint

As the primary constraint of operating the electric system, both of generating real and reactive powers have to satisfy load powers. This constraint is represented by the equal constraint $g(x, u)$ in the general formulas. On another hand, the $h(x, u)$ function in (5.4) represents limitation constraints of elements. The power balance constraint is as below:

$$P_i^G - P_i^D = V_i \sum_{i=1}^{N_b} \left[V_j \left[G_{ij} \cos(\delta_i - \delta_j) + B_{ij} \sin(\delta_i - \delta_j) \right] \right] \tag{5.5}$$

$$Q_i^G - Q_i^D = V_i \sum_{i=1}^{N_b} \left[V_j \left[G_{ij} \sin(\delta_i - \delta_j) - B_{ij} \sin(\delta_i - \delta_j) \right] \right] \tag{5.6}$$

where

- Q_i^G: generating reactive powers
- P_i^D, Q_i^D: real and reactive of load powers, respectively
- G_{ij}, B_{ij}: real and imaginary components of elements of the admittance matrix, respectively
- V_i, δ_i: magnitude and angle of voltage, respectively
- N_b: number of buses

5.2.2.2 Limited constraints of generators

In order to keep generators work in stable, the terminal voltage V_i^G and generating powers of a generator have to be in a range as follows:

$$V_{i,\min}^G \leq V_i^G \leq V_{i,\max}^G \tag{5.7}$$

$$P_{i,\min}^G \leq P_i^G \leq P_{i,\max}^G \tag{5.8}$$

$$Q_{i,\min}^G \leq Q_i^G \leq Q_{i,\max}^G \tag{5.9}$$

5.2.2.3 Shunt-VAR compensators capacity

Each shunt-VAR compensator has a limit to inject/absorb reactive power Q_i^C into the system as follow:

$$Q_{i,\min}^C \leq Q_i^C \leq Q_{i,\max}^C \tag{5.10}$$

5.2.2.4 Limitation of tap changers of transformers

The tap changer of a transformer only works in restricted upper and lower limits as shown below:

$$V_{i,\min}^T \leq V_i^T \leq V_{i,\max}^T \tag{5.11}$$

5.2.2.5 Limitation of load bus voltages

In order to guarantee the quality of system, load-bus voltages must be kept around nominal values.

$$V_{i,\min}^L \leq V_i^L \leq V_{i,\max}^L \tag{5.12}$$

5.2.2.6 Capacity of transmission lines

All transmission lines have to satisfy limited thermal condition represented by an upper bound as follow:

$$|S_{li}| \leq S_{li}^{\max} \tag{5.13}$$

5.3 Previous works on optimal power flow studies

Optimal power flow (OPF) is a conventional and important tool to analyze the electric power system. This problem focuses on controlling the power flow to minimize the total operation costs of the power system. The OPF is really a non-convex problem. because its controlled variables consist of continuous discrete or binary values. Real power and magnitude voltage of generators are usually continuous variables, while switchable shunt capacitors or tap settings of transformers can be discrete or binary values. On another hand, the solution of the OPF has to satisfy many operating constraints to keep the power system working in stable. Some frequent constraints needed to be handled are the balance of real and reactive powers, limitation of equipments, for instance: generators, transformers, transmission lines... In addition, when the power system is much more interconnected, the OPF is also more complicated.

In literature, many proposed methods are applied to solve the OPF problems. Since 1973, O. Alsac and B. Scott employed the gradient method to solve the problem on the 30-bus system[57], they also considered the system in normal case and in contingent case. Later works, Yuryevich J. and Wong K. P. proposed the OPF problems considering various types of fuel cost functions and solved it on the 30-bus system by the Evolutionary Programming[58]. Since the development of computer science, heuristic methods has skyrocketed to employ for the OPF problems and the scale of the problem is also expended. In 2012, Duman S. et al. proposed the Gravitational Search Algorithm to solve the optimal power flow problem on the 57-bus system. On another hand, Bouchekara, H.R.E.H et al. proposed the Teaching-learning based optimization to solve the OPF on the 118-bus system [59]. However, they neglected the controlled VAR compensators on the evaluated case study. As an expansion of the OPF problem, R.H. Liang et al. proposed the Fuzzy based hybrid Particles Swarm optimization to solve the OPF problem combines with the emission of thermal units[60]. All mentioned methods have been successful in solving the OPF problems with various types of objective functions and scales of systems. However, most of case studies have been evaluated on the 118-bus or smaller systems. Hence, the require to develop a powerful computation tool to apply for large-scale systems continues increasingly.

5.4 Implementation of Self-learning Cuckoo Search for OPF

5.4.1 Controllable and dependent variables:

Controllable variables x include generating real power of generators P_i^G, terminal voltages of generators V_i^G, injected reactive powers of shunt VAR compensators Q_i^C and positions of tap changers of transformers V_i^T. On another hand, dependent variables u are output real power of the generator at the slack bus P_1^G, generating reactive powers of generators Q_i^G, magnitude voltages at load buses V_i^L and apparent powers of transmission lines S_i.

$$x = \left[P_2^G ... P_{N_g}^G, V_1^G ... V_{N_g}^G, Q_1^C ... Q_{N_c}^C, V_1^T ... V_{N_t}^T\right] \tag{5.14}$$

$$u = \left[P_1^G, Q_1^G ... Q_{N_g}^G, V_1^L, ..., V_{N_l}^L, S_1, ..., S_{N_{br}}\right] \tag{5.15}$$

where N_g, N_c, N_t, N_l and N_{br} are the number of generators, shunt capacitors, transformers, load buses and branches of the power system, respectively.

5.4.2 Fitness function

According to the objective of OPF problem, the fitness function $F(x, u)$ is a combination of the fuel cost function $FC(P_i^G)$ and operational constraints. The limitations of controllable variables, e.g. (5.7), (5.8), (5.10), (5.11), are self-modified during the optimizing process. The limitations of dependent variables, e.g. (5.12), (5.9), (5.13), are handled by the limited function, $X^{\lim}(x)$ as (5.17) and combined to the fitness function via penalties factors. Penalty factors K_P, K_Q, K_S are set at 1000 and the penalty factor K_V is 10^6. The power balance constraints (5.5), (5.6) are implicitly satisfied by the power flow algorithm. Finally, the fitness function is as followings:

$$F(x,u) = \sum_{i=1}^{N_g} FC_i(P_i^G) + K_P\left(P_{slack}^G - P_{slack}^{\lim}\left(P_{slack}^G\right)\right)^2 + K_Q.\sum_{i=1}^{N_g}\left(Q_i^G - Q_i^{\lim}(Q_i^G)\right)^2 + \\ +K_S.\sum_{i=1}^{N_{br}}(|S_{li}| - S_{li}^{\max})^2 + K_V.\sum_{i=1}^{N_b}\left[V_i^L - V_i^{\lim}\left(V_i^L\right)\right]^2 \tag{5.16}$$

$$X^{\lim}(x) = \begin{cases} x_{\max}, \text{if} x > x_{\max} \\ x, \text{if} x_{\min} \leq x \leq x_{\max} \\ x_{\min}, \text{if} x < x_{\min} \end{cases} \tag{5.17}$$

5.4.3 Overall procedure:

The overall procedure for the implementation of the Self-learning Cuckoo search algorithm to solve the OPF is following.

Step 1: Choose controlling parameters for the Self-learning Cuckoo search algorithm. They include the probability of discovering Cuckoo eggs p_a, the learning factor p_l, the number of nests NP and the number of iterations $Itmax$.

Step 2: Create randomly initial nests X, analyze the power flow for each solution and evaluate value of the fitness function $F(x,u)$ in (5.16).

Step 3: Determine the best value of the fitness function F_{best} and the best nest X_{best}. Set the iteration counter $it = 1$.

Step 4: Create Cuckoo eggs via Lévy flight and the new nests X_{new} as eqs. (3.3) to (3.7), modify the eggs that violate the limitations.

Step 5: Analyze the power flow for each solution and evaluate the fitness function F_{new} for new nests. Update the solutions X, the best value of fitness function F_{best} and the best nest X_{best}.

Step 6: Randomly decide either discovering alien eggs as eqs. (3.8) to (3.10) or improving alien eggs as eqs. (3.11) and (3.12). Modify the eggs that violate the limitations.

Step 7: Once again, analyze the power flow for each solution anf evaluate the fitness function F_{new} for new nests X_{new}. Update the current nests X, the best value of fitness

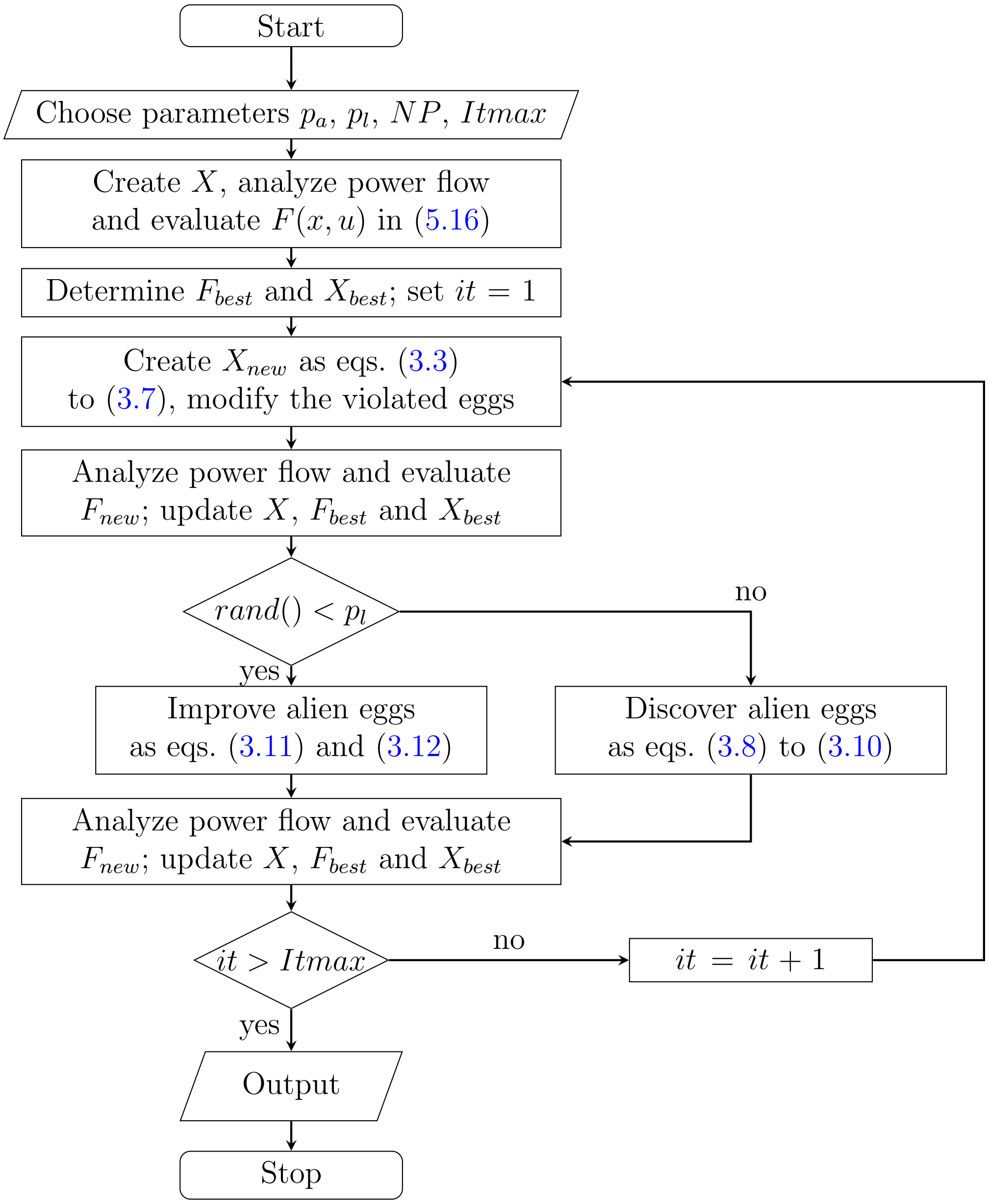

FIGURE 5.1: Flow chart

function F_{best} and the best nest X_{best}.

Step 8: Check if the iteration counter it is lower than the maximum iteration $Itmax$, increase it and return step 4. Otherwise, stop.

Figure 5.1 shows the flow chart of the implementation of SLCSA for OPF problems. According to the flow chart, when the learning factor $p_l = 0$, the SLCSA becomes the original CSA.

5.4.4 Example of Optimal power flow problem

Example 5.1. *Looking back Example 1.1 and Example 4.1, two generators have the fuel cost functions as Eq.* (4.1), (4.2)*, capacities given at Example 4.1 and supply the power system as Fig. 1.8. According to conditions of OPF, controlled variables of this system are voltages* V_1^G *and* V_4^G *of generators, generating power* P_4^G *of the generator at bus 3. The bus data in Tab. 1.2 is rewritten as follows.*

TABLE 5.1: Bus data of Example 5.1

Bus	P_i^G(MW)	Q_i^G(MVar)	P_i^D(MW)	Q_i^D(MVar)	V_i(p.u.)	**Remarks**
1	-	-	50	30.99	$V_1^G\angle 0^0$	Slack bus
2	0	0	170	105.35	-	Load bus
3	0	0	200	123.94	-	Load bus
4	P_4^G	-	80	49.58	$V_4^G\angle -$	Voltage controlled

The problem is to determine values of V_1^G, V_4^G *and* P_4^G *to minimize the total fuel cost and satisfy the condition of voltages at all buses as* $0.9 \leq V_i \leq 1.1$*, other constraints are neglected.*

For this example, the controlled and dependent variables are as followings:

$$x = \left[P_4^G, V_1^G, V_4^G\right]$$

$$u = \left[P_1^G, V_2^L, V_3^L\right]$$

And the fitness function (5.16) is rewritten as:

$$F(x,u) = FC_1({P_1}^G) + FC_4({P_4}^G) + K_P\left(P_1^G - P_1^{\lim}\left(P_1^G\right)\right)^2 + K_V.\sum_{i=2}^{3}\left[{V_i}^L - V_i^{\lim}\left({V_i}^L\right)\right]^2$$

In this problem, the number of constraints are too much, thus the stopping criterion is the limit of iteration. The final solution must be checked whether it violates constraints or not.

The final solution made by SLCSA is $P_4^G = 94.4754MW, V_1^G = 1.0636p.u., V_4^G = 1.0152p.u.$. At that time, dependent variables are $P_1^G = 412.2806MW, V_2^L = 1.0071p.u., V_3^L =$

$1.0087p.u.$. It is clear that the final solution is satisfied all required constraints, and the final total fuel cost is 6147.692\$.

Comparing with the solution before being optimized in Example 1.1, with the generating powers $P_1^G = 186.81MW$ and $P_4^G = 318MW$ the total cost is 7645.4411\$. The result of optimal solution is extremely better than the unoptimized solution.

5.5 Simulation results

The proposed Self-learning Cuckoo search algorithm has been evaluated on the standard IEEE 30-bus, 57-bus, 118-bus and 300-bus systems to solve the optimal power flow problems. In the 30-bus and 57-bus systems, the proposed method are compared with other algorithms in literature; for the 118-bus and 300-bus systems, all compared methods are programmed and run on a personal computer with a 3GHz Core 2Duo processor and 4Gb RAM. Numerical results of each benchmark are obtained through 30 independent trials in order to compared the effectiveness of the proposed Self-learning Cuckoo search algorithm. The power flow of each benchmark is calculated by the Newton-Raphson method via the MATPOWER toolbox [61].

The optimal power flow is a complex and non-convex problem that combines various types of controllable variables. The real powers P_i^G and the terminal voltages V_i^G of generators are continuous values, while the tap changers of transformer V_i^T are discrete numbers with 0.01 p.u. step size. In the 30-bus system, the reactive powers of shunt-VAR compensators Q_i^C are neglected. In the 57-bus system, the variables Q_i^C are obtained as continuous and binary variables. Furthermore, in the 108-bus and 300-bus systems, they are continuous values.The total number of controlled variables is summarized in Tab. 5.2.

In order to investigate the effectiveness of the enhanced learning factor p_l, we have evaluated three case studies with various values of the learning factor p_l and the probability p_a. We uses the learning factor p_l = 0, 0.1, 0.2, 0.3, 0.4, 0.5, 0.6, 0.7, 0.8, 0.9, 1.0 and the probability p_a = 0.1, 0.2, 0.3, 0.4, 0.5, 0.6, 0.7, 0.8, 0.9. According to the proposed the overall procedure, when $p_l = 0$, the proposed SLCSA becomes the conventional CSA. Setting parameters of the SLCSA for each case study are in Tab. 5.3.

TABLE 5.2: Number of controlled variables

Case study	Generators		Transformer		Shunt compe-nsator	Total of variables
	Output power	Terminal voltage	Tap changer	Fixed tap		
1	5	6	4	0	0	15
2a	6	7	17	0	3	33
2b	6	7	15	2	3	31
3	53	54	9	0	14	130
4	68	69	62	45	14	213

TABLE 5.3: Setting parameters of the SLCSA for evaluated benchmarks

Case study	Factor p_a	Factor p_l	Number of nests NP	Number of iteration $Itmax$
1	0.6	0.5	30	300
2a	0.1	0.8	50	500
2b	0.2	0.8	50	500
3	0.3	0.7	50	1000
4	0.2	0.8	150	1000

5.5.1 Case study 1: IEEE 30-bus system

In literature, two various 30-bus systems have been evaluated to investigate the effectiveness of optimization algorithms; the first system has been proposed by O. Alsac and B. Stott since 1974 [57], while the another has been proposed by K.Y. Lee et al. since 1985 [62]. In this study, we employ the system of O. Alsac and B. Stoot, which is also described in the MATPOWER toolbox [61]. The 30-bus system has six generators, four transformers with tap changers and two installed capacitors at the 10^{th} and 24^{th} buses. The line data and bus data are taken from [61], while operational constraints and fuel cost coefficients are given in [57].

In this benchmark, the proposed SLCSA and the original CSA have been evaluated and compared with other methods in literature, such as: Improved Evolution Programming (IEP), Modified Differential Evolution (MDE), Evolution Programming (EP) and the Gradient method. The numerical results in Tab. 5.4 show that the proposed SLCSA is better than the conventional CSA and other methods in literature. On another hand, the

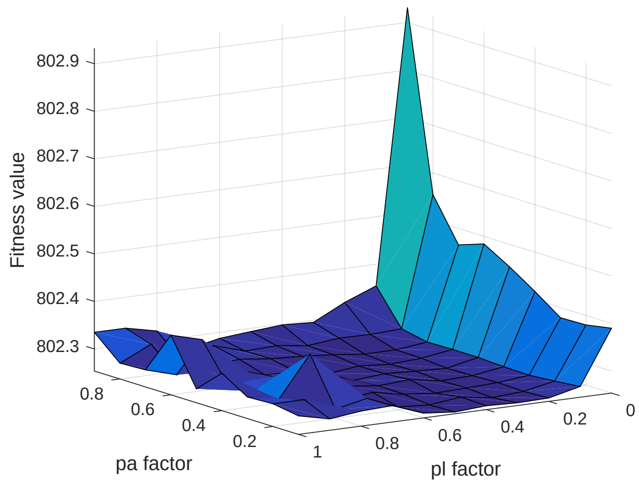

FIGURE 5.2: Mean values of the fitness function with various parameters of the SLCSA for Case study 1

conventional CSA is slightly worse than the Modified Differential Evolution.

Comparing the mean values of the fitness function with various parameters in Fig. 5.2, the conventional CSA gives better solutions when the probability rate of discovering alien eggs p_a is lower 0.3. When the search engine employs the learning factor p_l to enhance the performance of Cuckoo eggs, the optimal solutions have been improved. However, when the factor p_l is over 0.8, the Cuckoo eggs can be excited too much and the effectiveness is also lower.

TABLE 5.4: Comparison of numerical results proposed by the proposed SLCSA and other methods for IEEE 30-bus system

Methods	**Gradient** [57]	**EP** [58]	**MDE** [63]	**IEP** [64]	**CSA**	**SLCSA**
Best [$]	802.40	802.62	802.376	802.465	802.2822	802.2463
Mean [$]	-	-	802.382	802.521	802.3877	802.2542
Worst [$]	-	-	802.404	802.581	802.5033	802.2692
Std. dev.	-	-	-	0.039	0.0473	0.0055
Time [s]	14.3	51.4	23.25	99.013		60.30

5.5.2 Case study 2: IEEE 57-bus system

The standard IEEE 57-bus system consists of seven generators, 17 transformers and three shunt capacitors. Among the transformers, two parallel transformers in the line (24,25) are

TABLE 5.5: Optimal solutions for the IEEE 30-bus system

Variables	**Values**	**Variables**	**Values**	**Variables**	**Values**
P_1^G(MW)	176.1959	V_1^G(p.u.)	1.05	V_{6-9}^T(p.u.)	1.01
P_2^G(MW)	48.8224	V_2^G(p.u.)	1.0379	V_{6-10}^T(p.u.)	0.94
P_5^G(MW)	21.5154	V_5^G(p.u.)	1.0108	V_{4-12}^T(p.u.)	1.00
P_8^G(MW)	22.0839	V_8^G(p.u.)	1.0185	V_{28-27}^T(p.u.)	0.94
P_{11}^G(MW)	12.2204	V_{11}^G(p.u.)	1.0866		
P_{13}^G(MW)	12.0000	V_{13}^G(p.u.)	1.0850		

fixed taps and others have tap changers. We divide this case study into two benchmarks. The first benchmark observes all 17 transformers have tap changers and all injected powers of capacitors are continuous values. On another hand, the second benchmark neglects two fixed-tap transformers and observes the capacitors are binary numbers. The bus data, line data, fuel cost coefficients and operational constraints are taken from MATPOWER Toolbox [61]. The capacities of transmission lines are given in the IEEE testbeds[65].

5.5.2.1 Continuous variables of capacitors

The maximum reactive power of three capacitors is 30 MVar, and the minimum is zero. The numerical results have been compared with other algorithms in literature such as: Improved Teaching-learning based optimization (ITLBO), Artificial Bee Colony algorithm (ABC) and Gravitational Search Algorithm (GSA).

According to Tab. 5.6, the conventional Cuckoo search algorithm is worse than other compared methods. When employing the new strategy, the proposed Self-learning Cuckoo search algorithm improves the search engine and gives the best solution. The best solution of the proposed method is slightly better than the ITLBO. However, the numerical result proposed by ITLBO violates the limitation of load voltage as Fig. 5.5.

The convergence characteristics of the proposed SLCSA and the conventional CSA is given in Fig. 5.3. The proposed SLCSA converges faster than the conventional one in this benchmark.

TABLE 5.6: Comparison of numerical results proposed by the proposed SLCSA and other methods for IEEE 57-bus system with continuous values of capacitors

Methods	GSA [66]	ABC [67]	ITLBO [68]	CSA	SLCSA
Best [$]	41695.8717	41693.9589	41679.5451	41970.6977	41679.4518
Mean [$]	-	41778.6732	-	42418.1983	41718.7217
Worst [$]	-	41867.8528	-	43199.3974	42257.6270
Std. dev.	-	-	-	308.9496	83.1242
Time [s]	-	226.23	-	217.43	218.35

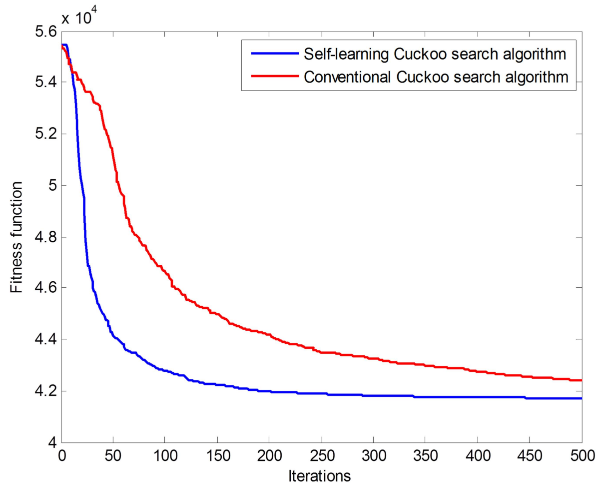

FIGURE 5.3: Convergence characteristics of the proposed SLCSA and CSA in Case study 2a

5.5.2.2 Binary capacitors

In the original system, three installed capacitors are at buses 18, 25 and 53 with amounts of injected reactive powers are 20 MVar, 11.8 MVar and 12.6 MVar, respectively. In this tested case, all capacitors are switchable, thus the injected reactive powers are observed as binary values.

The proposed SLCSA has been evaluated and compared with the conventional CSA and the Teaching-learning-based optimization (TLBO). The original code of the TLBO is given from [69]. Numerical results in Tab. 5.7 show that the proposed SLCSA is better than both of conventional CSA and TLBO. The TLBO is better than the conventional CSA on searching the global solution; however, it can be easy to fall into the local optimum, because its worst solution and its standard deviation are higher than others.

Comparing the mean values of the fitness function with various parameters of the SLCSA

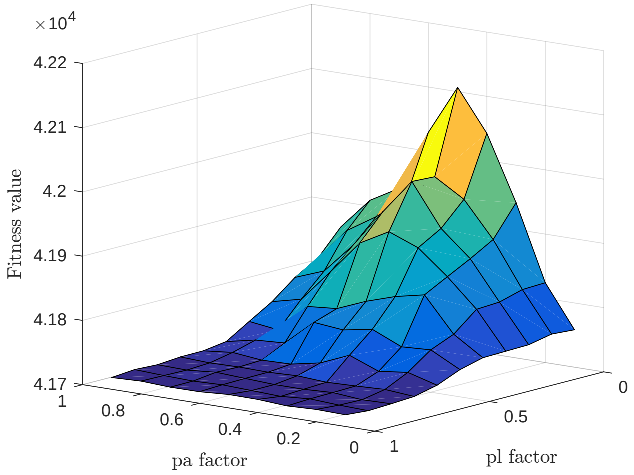

FIGURE 5.4: Mean values of the fitness function with various parameters of the SLCSA for Case study 2b

as Fig. 5.4, the conventional CSA gives the best solution at $p_a = 0.1$ and the worst solution at $p_a = 0.5$. When the learning factor p_l is over 0.5, the proposed SLCSA gives better global solutions.

Figures 5.5, 5.6, 5.7 show the checks of operating constraints. Both of the proposed SLCSA and the conventional CSA handle all of operating constraints.

TABLE 5.7: Comparison of numerical results proposed by the proposed SLCSA and other methods for IEEE 57-bus system with binary values of capacitors

Methods	Best [$]	Mean [$]	Worst [$]	Std. dev.
SLCSA	41,700.2374	41,715.9781	41,731.9547	8.0560
CSA	41,729.8052	41,760.7893	41,807.9366	18.2100
TLBO	41,702.6038	41,760.0653	41,857.4162	27.5996

5.5.3 Case study 3: IEEE 118-bus system

The IEEE 118-bus system includes 54 generators, 9 transformers with load tap changers and 14 installed shunt VAR compensators. Two of compensators are reactors and the others are capacitors. The upper bounds of reactors and the lower bounds of capacitors are zero, while the lower bounds of reactors and the upper bounds of capacitors are taken from MATPOWER Toolbox [61]. The data of the IEEE 118-bus system are given in MATPOWER Toolbox. However, the MATPOWER Toolbox neglects the minimum

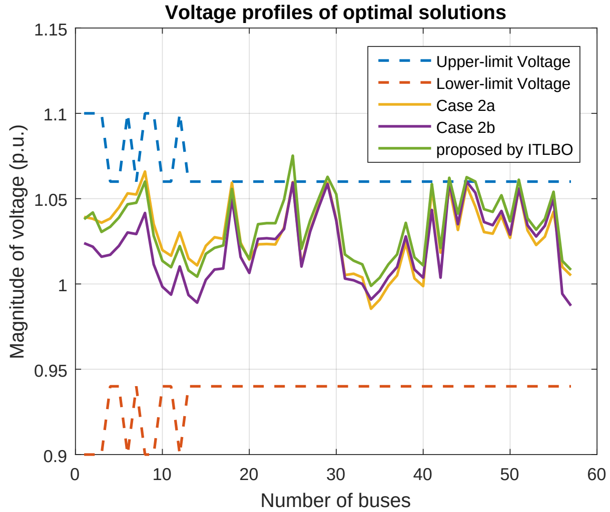

FIGURE 5.5: Voltage profiles of the optimal solution in Case study 2

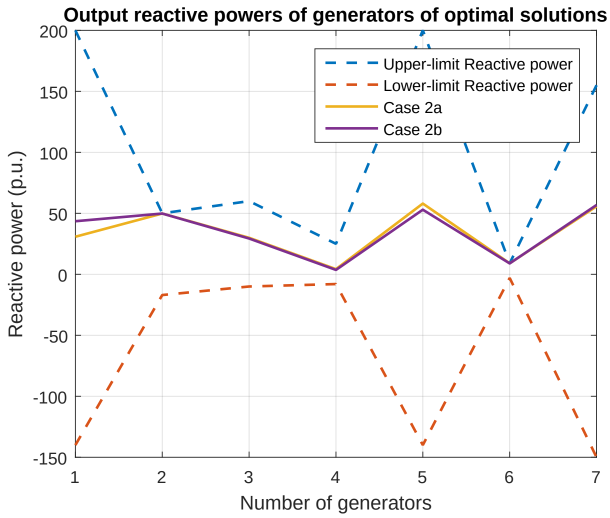

FIGURE 5.6: Generating reactive powers of generators in Case study 2

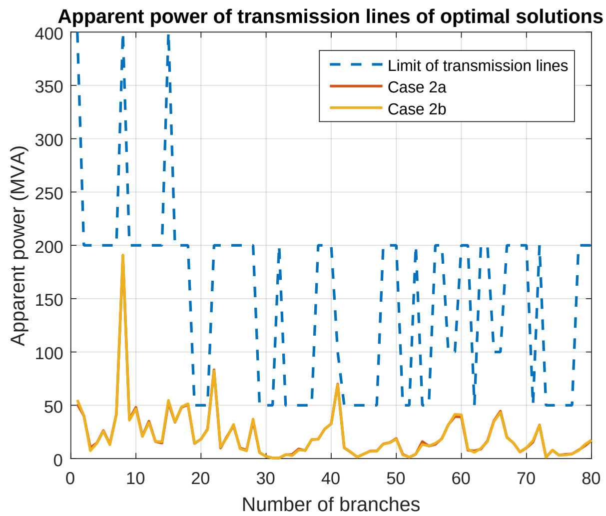

FIGURE 5.7: Apparent power through transmission lines of the optimal solution in Case study 2

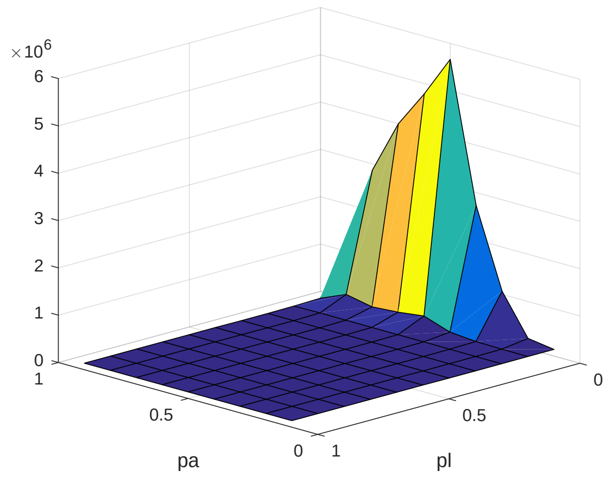

FIGURE 5.8: Mean values of the fitness function with various parameters of the SLCSA for the IEEE 118-bus system

generating powers of generators and the capacities of transmission lines. Thus, these limitations have been taken from the IEEE testbeds[65].

The proposed SLCSA has been evaluated on various parameters of the probability p_a and the learning factor p_l to investigate its effectiveness. The numerical results in Fig. 5.8 shows thats the conventional CSA only solves the problem successfully when the the probability rate of discovering alien eggs $p_a = 0.1$ or 0.2. When using the learning factor p_l, the search engines has clearly been enhanced. The proposed SLCSA is successful in solving this problem with any setting parameters. However, the SLCSA gives better solutions when the learning factor p_l is over 0.3, and the best performance of the SLCSA is at $p_l = 0.7$.

The proposed SLCSA has been compared with the conventional CSA and the Teaching-learning based optimization. Table 5.9 shows that the proposed method gives better solution and higher performance than both of other methods. On another hand, the TLBO also is better than the conventional CSA on searching global optima.

Table 5.9 gives the optimal solution of the proposed SLCSA, and its fitness value is 135,263.1056. The examinations of generating reactive power constraints, voltage profile and apparent powers through transmission lines are given in Fig. 5.9, 5.10 and 5.11. The proposed SLCSA satisfies all of the operating constraints.

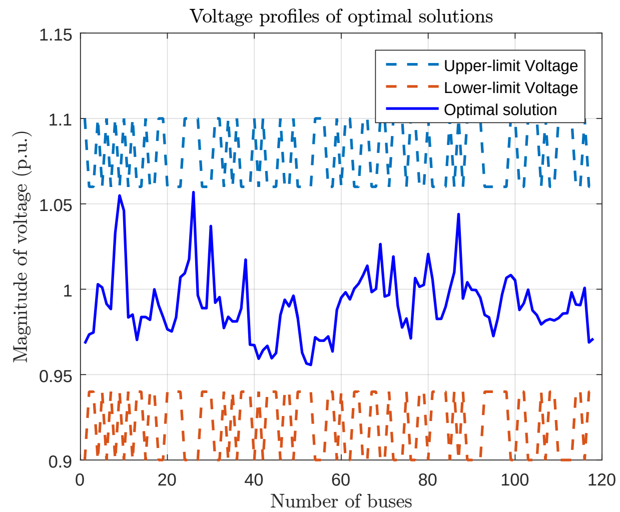

FIGURE 5.9: Voltage profiles of the optimal solution on the IEEE 118-bus system

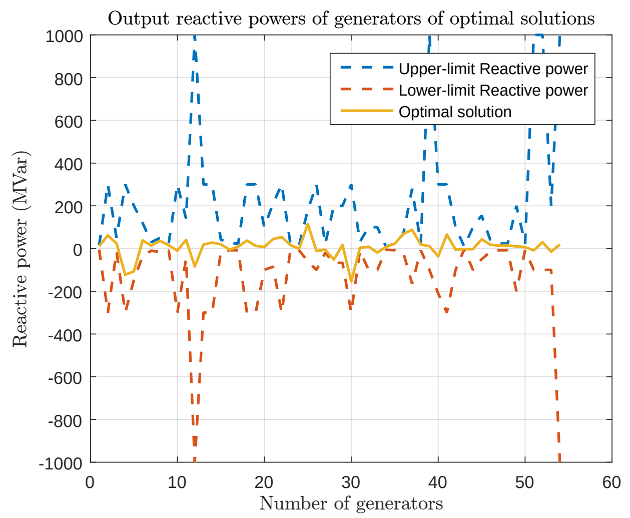

FIGURE 5.10: Generating reactive powers of generators on the IEEE 118-bus system

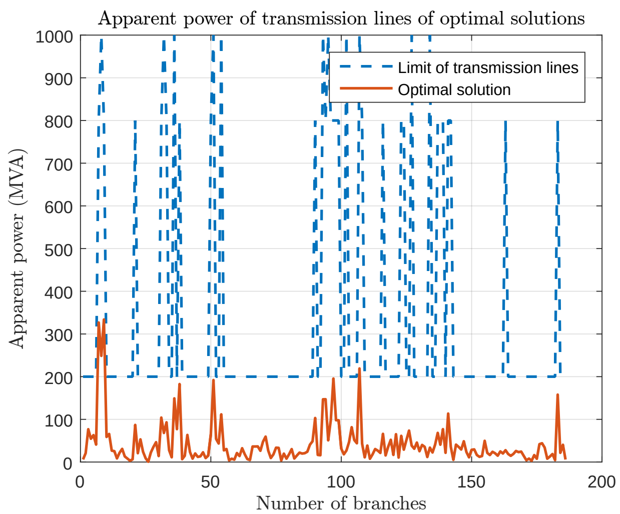

FIGURE 5.11: Apparent power through transmission lines of the optimal solution on the IEEE 118-bus system

Table 5.8: Comparison of numerical results proposed by the proposed SLCSA and other methods for IEEE 118-bus system

Methods	Best [$]	Mean [$]	Worst [$]	Std. dev.
SLCSA	135,263.1056	135,449.5703	135,767.8986	154.5740
CSA	139,916.2029	141,152.2116	142,555.0816	836.1418
TLBO	135,366.9980	135,637.0321	136,156.2073	225.0883

Table 5.9: Optimal solution for the IEEE 118-bus system

Variables	Solution	Variables	Solution	Variables	Solution
P_1^G(MW)	30.1201	P_{42}^G(MW)	30.0074	P_{80}^G (MW)	339.6862
P_4^G(MW)	30.1452	P_{46}^G(MW)	35.7522	P_{85}^G (MW)	30.1017
P_6^G(MW)	30.0545	P_{49}^G(MW)	164.9373	P_{87}^G (MW)	31.2035
P_8^G(MW)	30.0579	P_{54}^G(MW)	44.8718	P_{89}^G (MW)	373.1172
P_{10}^G(MW)	316.5211	P_{55}^G(MW)	30.1564	P_{90}^G (MW)	30.0941
P_{12}^G(MW)	69.8247	P_{56}^G(MW)	30.0951	P_{91}^G (MW)	30.3344
P_{15}^G(MW)	30.0465	P_{59}^G(MW)	129.1517	P_{92}^G (MW)	30.0816
P_{18}^G(MW)	30.0813	P_{61}^G(MW)	117.9601	P_{99}^G (MW)	30.0825
P_{19}^G(MW)	30.0452	P_{62}^G(MW)	30.2423	P_{100}^G (MW)	182.5417
P_{24}^G(MW)	30.0179	P_{65}^G(MW)	287.2499	P_{103}^G (MW)	42.0585
P_{25}^G(MW)	156.6095	P_{66}^G(MW)	288.7371	P_{104}^G (MW)	30.1290
P_{26}^G(MW)	219.8338	P_{69}^G(MW)	374.5763	P_{105}^G (MW)	30.0465
P_{27}^G(MW)	34.5419	P_{70}^G(MW)	30.0482	P_{107}^G (MW)	30.1663
P_{31}^G(MW)	32.1141	P_{72}^G(MW)	30.1292	P_{110}^G (MW)	30.0863
P_{32}^G(MW)	30.1818	P_{73}^G(MW)	30.0301	P_{111}^G (MW)	40.9797
P_{34}^G(MW)	30.3510	P_{74}^G(MW)	30.0000	P_{112}^G (MW)	30.0341
P_{36}^G(MW)	30.1710	P_{76}^G(MW)	30.0609	P_{113}^G (MW)	30.8869
P_{40}^G(MW)	30.1355	P_{77}^G(MW)	30.1667	P_{116}^G (MW)	30.0091
V_1^G(p.u.)	0.9682	V_{42}^G(p.u.)	0.9643	V_{80}^G (p.u.)	1.0206
V_4^G(p.u.)	1.0029	V_{46}^G(p.u.)	0.9848	V_{85}^G (p.u.)	1.0002
V_6^G(p.u.)	0.9914	V_{49}^G(p.u.)	0.9962	V_{87}^G (p.u.)	1.0440
V_8^G(p.u.)	1.0330	V_{54}^G(p.u.)	0.9718	V_{89}^G (p.u.)	1.0041

continued . . .

Table 5.9 Continued: Optimal solution for the IEEE 118-bus system

Variables	Solution	Variables	Solution	Variables	Solution
V_{10}^G(p.u.)	1.0460	V_{55}^G(p.u.)	0.9699	V_{90}^G (p.u.)	0.9997
V_{12}^G(p.u.)	0.9852	V_{56}^G(p.u.)	0.9699	V_{91}^G (p.u.)	0.9995
V_{15}^G(p.u.)	0.9837	V_{59}^G(p.u.)	0.9880	V_{92}^G (p.u.)	0.9950
V_{18}^G(p.u.)	0.9905	V_{61}^G(p.u.)	0.9982	V_{99}^G (p.u.)	1.0083
V_{19}^G(p.u.)	0.9838	V_{62}^G(p.u.)	0.9941	V_{100}^G (p.u.)	1.0053
V_{24}^G(p.u.)	1.0093	V_{65}^G(p.u.)	1.0081	V_{103}^G (p.u.)	0.9997
V_{25}^G(p.u.)	1.0176	V_{66}^G(p.u.)	1.0138	V_{104}^G (p.u.)	0.9876
V_{26}^G(p.u.)	1.0569	V_{69}^G(p.u.)	1.0264	V_{105}^G (p.u.)	0.9849
V_{27}^G(p.u.)	0.9965	V_{70}^G(p.u.)	0.9957	V_{107}^G (p.u.)	0.9816
V_{31}^G(p.u.)	0.9921	V_{72}^G(p.u.)	1.0192	V_{110}^G (p.u.)	0.9831
V_{32}^G(p.u.)	0.9954	V_{73}^G(p.u.)	0.9904	V_{111}^G (p.u.)	0.9858
V_{34}^G(p.u.)	0.9839	V_{74}^G(p.u.)	0.9776	V_{112}^G (p.u.)	0.9860
V_{36}^G(p.u.)	0.9812	V_{76}^G(p.u.)	0.9712	V_{113}^G (p.u.)	0.9982
V_{40}^G(p.u.)	0.9672	V_{77}^G(p.u.)	1.0066	V_{116}^G (p.u.)	1.0008
Q_5^C(MVar)	-13.2283	Q_{82}^C(MVar)	7.6347	T_{8-5} (p.u.)	1.03
Q_{34}^C(MVar)	1.8485	Q_{83}^C(MVar)	0.2538	T_{26-25} (p.u.)	1.06
Q_{37}^C(MVar)	-16.6935	Q_{105}^C(MVar)	5.9079	T_{30-17} (p.u.)	1.02
Q_{44}^C(MVar)	2.3831	Q_{107}^C(MVar)	2.8754	T_{38-37} (p.u.)	1.00
Q_{45}^C(MVar)	8.8230	Q_{110}^C(MVar)	0.2057	T_{63-59} (p.u.)	1.01
Q_{46}^C(MVar)	2.5921			T_{64-61} (p.u.)	1.00
Q_{48}^C(MVar)	6.1688			T_{65-66} (p.u.)	0.99
Q_{74}^C(MVar)	3.1212			T_{68-69} (p.u.)	0.92
Q_{79}^C(MVar)	18.7955			T_{81-80} (p.u.)	0.98

5.5.4 Case study 4: IEEE 300-bus system

The last tested system is the huge IEEE 300-bus system, which includes 69 generators and the total of controlled variables is up to 213. Similarly, the data of the IEEE 300-bus system is taken from the MATPOWER Toolbox [61], while the lower bounds of

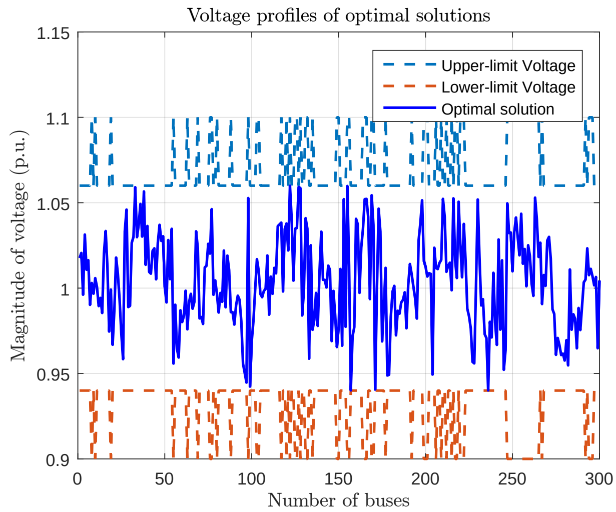

FIGURE 5.12: Voltage profiles of the optimal solution on the IEEE 300-bus system

generating real powers and the capacities of transmission lines are conducted from the IEEE testbed[65].

Numerical results in Tab. 5.11 show that the conventional CSA unsuccessfully solves this problems while the proposed SLCSA succeeds in searching the optimal solution. The optimal solution is in Tab. 5.11, and it also satisfies all of required operating constraints as Fig. 5.12, 5.13 and 5.14.

TABLE 5.10: Numerical results of the SCLCSA and the conventional CSA for IEEE 300-bus system

Methods	Best [$]	Mean [$]	Worst [$]	Std. dev.
SLCSA	722,899	730,864	827,287	15,771
CSA	1,963,015	3,964,877	7,229,361	1,342,516

TABLE 5.11: Optimal solution for the IEEE 300-bus system

Variables	Solution	Variables	Solution	Variables	Solution
P_8^G(MW)	40.3068	P_{171}^G(MW)	73.1298	P_{7002}^G (MW)	575.0587
P_{10}^G(MW)	44.8642	P_{176}^G(MW)	208.3053	P_{7003}^G (MW)	1058.4121
P_{20}^G(MW)	44.3019	P_{177}^G(MW)	90.7954	P_{7011}^G (MW)	246.8336
P_{63}^G(MW)	49.5046	P_{185}^G(MW)	207.9606	P_{7012}^G (MW)	393.7651
P_{76}^G(MW)	54.1091	P_{186}^G(MW)	1174.2478	P_{7017}^G (MW)	305.5999
P_{84}^G(MW)	373.2180	P_{187}^G(MW)	1208.6181	P_{7023}^G (MW)	192.6768

continued ...

Table 5.11 Continued: Optimal solution for the IEEE 300-bus system

Variables	Solution	Variables	Solution	Variables	Solution
P_{91}^G(MW)	152.0334	P_{190}^G(MW)	487.7060	P_{7024}^G (MW)	363.7661
P_{92}^G(MW)	280.1124	P_{191}^G(MW)	1909.3309	P_{7039}^G (MW)	484.5276
P_{98}^G(MW)	87.0508	P_{198}^G(MW)	452.4902	P_{7044}^G (MW)	43.9926
P_{108}^G(MW)	125.4805	P_{213}^G(MW)	288.7926	P_{7049}^G (MW)	78.5143
P_{119}^G(MW)	1867.3113	P_{220}^G(MW)	129.6215	P_{7055}^G (MW)	49.3134
P_{124}^G(MW)	256.5403	P_{221}^G(MW)	499.3277	P_{7057}^G (MW)	171.5392
P_{125}^G(MW)	54.1564	P_{222}^G(MW)	258.6833	P_{7061}^G (MW)	384.3697
P_{138}^G(MW)	31.8129	P_{227}^G(MW)	330.7820	P_{7062}^G (MW)	369.2490
P_{141}^G(MW)	281.7596	P_{230}^G(MW)	360.8058	P_{7071}^G (MW)	132.6656
P_{143}^G(MW)	681.6624	P_{233}^G(MW)	323.1361	P_{7130}^G (MW)	1210.0413
P_{146}^G(MW)	91.6161	P_{236}^G(MW)	571.6399	P_{7139}^G (MW)	673.9895
P_{147}^G(MW)	210.4158	P_{238}^G(MW)	242.0424	P_{7166}^G (MW)	603.1292
P_{149}^G(MW)	99.2045	P_{239}^G(MW)	564.0645	P_{9002}^G (MW)	44.4260
P_{152}^G(MW)	322.5976	P_{241}^G(MW)	623.2231	P_{9051}^G (MW)	54.4227
P_{153}^G(MW)	205.7379	P_{242}^G(MW)	176.9308	P_{9053}^G (MW)	42.2456
P_{156}^G(MW)	49.5701	P_{243}^G(MW)	92.2649	P_{9054}^G (MW)	69.4099
P_{170}^G(MW)	187.9672	P_{7001}^G(MW)	440.7553	P_{9055}^G (MW)	32.4047
V_{8}^G(p.u.)	1.0030	V_{171}^G(p.u.)	0.9772	V_{7002}^G (p.u.)	1.0322
V_{10}^G(p.u.)	1.0058	V_{176}^G(p.u.)	1.0598	V_{7003}^G (p.u.)	1.0326
V_{20}^G(p.u.)	0.9991	V_{177}^G(p.u.)	1.0132	V_{7011}^G (p.u.)	1.0098
V_{63}^G(p.u.)	0.9558	V_{185}^G(p.u.)	1.0348	V_{7012}^G (p.u.)	1.0327
V_{76}^G(p.u.)	0.9759	V_{186}^G(p.u.)	1.0521	V_{7017}^G (p.u.)	1.0413
V_{84}^G(p.u.)	1.0234	V_{187}^G(p.u.)	1.0522	V_{7023}^G (p.u.)	1.0299
V_{91}^G(p.u.)	1.0202	V_{190}^G(p.u.)	1.0544	V_{7024}^G (p.u.)	1.0192
V_{92}^G(p.u.)	1.0462	V_{191}^G(p.u.)	1.0370	V_{7039}^G (p.u.)	1.0435
V_{98}^G(p.u.)	0.9965	V_{198}^G(p.u.)	1.0119	V_{7044}^G (p.u.)	1.0142
V_{108}^G(p.u.)	0.9859	V_{213}^G(p.u.)	1.0081	V_{7049}^G (p.u.)	1.0229
V_{119}^G(p.u.)	1.0527	V_{220}^G(p.u.)	1.0160	V_{7055}^G (p.u.)	1.0011

continued . . .

Table 5.11 Continued: Optimal solution for the IEEE 300-bus system

Variables	Solution	Variables	Solution	Variables	Solution
V_{124}^G(p.u.)	1.0169	V_{221}^G(p.u.)	1.0125	V_{7057}^G (p.u.)	1.0251
V_{125}^G(p.u.)	1.0102	V_{222}^G(p.u.)	1.0068	V_{7061}^G (p.u.)	1.0188
V_{138}^G(p.u.)	1.0384	V_{227}^G(p.u.)	1.0118	V_{7062}^G (p.u.)	1.0026
V_{141}^G(p.u.)	1.0378	V_{230}^G(p.u.)	1.0165	V_{7071}^G (p.u.)	0.9954
V_{143}^G(p.u.)	1.0599	V_{233}^G(p.u.)	1.0095	V_{7130}^G (p.u.)	1.0530
V_{146}^G(p.u.)	1.0348	V_{236}^G(p.u.)	0.9987	V_{7139}^G (p.u.)	1.0402
V_{147}^G(p.u.)	1.0352	V_{238}^G(p.u.)	1.0161	V_{7166}^G (p.u.)	1.0182
V_{149}^G(p.u.)	1.0585	V_{239}^G(p.u.)	1.0059	V_{9002}^G (p.u.)	0.9907
V_{152}^G(p.u.)	1.0409	V_{241}^G(p.u.)	1.0255	V_{9051}^G (p.u.)	1.0050
V_{153}^G(p.u.)	1.0348	V_{242}^G(p.u.)	1.0063	V_{9053}^G (p.u.)	1.0076
V_{156}^G(p.u.)	0.9756	V_{243}^G(p.u.)	1.0376	V_{9054}^G (p.u.)	1.0113
V_{170}^G(p.u.)	0.9655	V_{7001}^G(p.u.)	1.0496	V_{9055}^G (p.u.)	1.0069
Q_{117}^C(MVar)	253.8616	Q_{173}^C(MVar)	39.1623	Q_{240}^C (MVar)	-40.4169
Q_{120}^C(MVar)	18.2194	Q_{179}^C(MVar)	44.8799	Q_{248}^C (MVar)	18.9005
Q_{154}^C(MVar)	17.4322	Q_{190}^C(MVar)	-30.5400	Q_{9003}^C (MVar)	0.9558
Q_{164}^C(MVar)	-63.5705	Q_{231}^C(MVar)	-58.3959	Q_{9034}^C (MVar)	0.9300
Q_{166}^C(MVar)	-29.1361	Q_{238}^C(MVar)	-36.6317	-	-
$T_{37-9001}$(p.u)	1.00	T_{45-44}(p.u)	0.94	$T_{189-210}$ (p.u)	1.01
$T_{9001-9006}$(p.u)	0.95	T_{62-61}(p.u)	0.95	$T_{193-196}$ (p.u)	1.04
$T_{9001-9012}$(p.u)	0.99	T_{63-64}(p.u)	0.97	$T_{195-212}$ (p.u)	0.98
$T_{9005-9051}$(p.u)	1.09	T_{87-94}(p.u)	0.99	T_{201-69} (p.u)	1.04
$T_{9005-9052}$(p.u)	0.92	$T_{114-207}$(p.u)	1.01	$T_{202-211}$ (p.u)	1.02
$T_{9005-9053}$(p.u)	1.07	$T_{116-124}$(p.u)	0.94	$T_{204-2040}$ (p.u)	1.07
$T_{9005-9054}$(p.u)	1.06	$T_{121-115}$(p.u)	0.99	$T_{209-198}$ (p.u)	1.03
$T_{9005-9055}$(p.u)	1.01	$T_{130-131}$(p.u)	1.05	$T_{218-219}$ (p.u)	1.04
$T_{9053-9533}$(p.u)	1.00	$T_{130-150}$(p.u)	1.06	$T_{229-230}$ (p.u)	0.98
T_{3-1}(p.u)	1.00	$T_{132-170}$(p.u)	1.02	$T_{234-236}$ (p.u)	1.03
T_{3-2}(p.u)	0.96	$T_{141-174}$(p.u)	0.97	$T_{238-239}$ (p.u)	1.02

continued ...

Table 5.11 Continued: Optimal solution for the IEEE 300-bus system

Variables	Solution	Variables	Solution	Variables	Solution
T_{3-4}(p.u)	0.97	$T_{143-144}$(p.u)	0.97	$T_{119-1190}$ (p.u)	1.07
T_{7-5}(p.u)	0.94	$T_{143-148}$(p.u)	0.97	$T_{120-1200}$ (p.u)	0.92
T_{7-6}(p.u)	0.97	$T_{151-170}$(p.u)	0.99	$T_{7062-62}$ (p.u)	0.94
T_{10-11}(p.u)	1.03	$T_{153-183}$(p.u)	1.03	$T_{7017-17}$ (p.u)	0.98
T_{12-10}(p.u)	0.98	$T_{155-156}$(p.u)	1.04	$T_{7039-39}$ (p.u)	0.95
T_{15-17}(p.u)	0.98	$T_{159-117}$(p.u)	1.01	$T_{7057-57}$ (p.u)	0.97
T_{16-15}(p.u)	0.98	$T_{160-124}$(p.u)	1.00	$T_{7044-44}$ (p.u)	0.96
T_{21-20}(p.u)	0.94	$T_{163-137}$(p.u)	0.93	$T_{7055-55}$ (p.u)	0.94
T_{24-23}(p.u)	1.02	$T_{164-155}$(p.u)	0.96	$T_{7071-71}$ (p.u)	0.96
T_{36-35}(p.u)	0.97	$T_{182-139}$(p.u)	1.06	-	-

5.6 Conclusion

The proposed Self-learning Cuckoo search algorithm successfully solves the optimal power flow problems in large-scale power systems. The proposed strategy to enhance Cuckoo eggs is clearly effective. According to the numerical results on four evaluated systems, the SLCSA is much better than the conventional CSA in finding optimal solutions with higher performance. Comparing with other algorithms in literature, the proposed method is also better than Evolution Programing, Differential Evolution, Gravitation Search Algorithm and Teaching-learning based optimization on the IEEE 30-bus and 57-bus tested systems. The proposed method also improves the global solutions on the problems, which consist of various types of variables and handle a huge of equal and unequal constraints. Discussing the effectiveness of learning factor p_l, when the factor p_l is over 0.5, the search engine gives better solutions than the lower value. However, when the factor p_l is near to 1.0, the Cuckoo eggs can be too excited and its performance is not good. Thus, we propose the learning factor p_l around 0.8 to give the better solution. On summary, the proposed SLCSA is favorable to non-convex and large-scale problems like the optimal power flow problem. In future, the proposed method should be continued evaluating on various

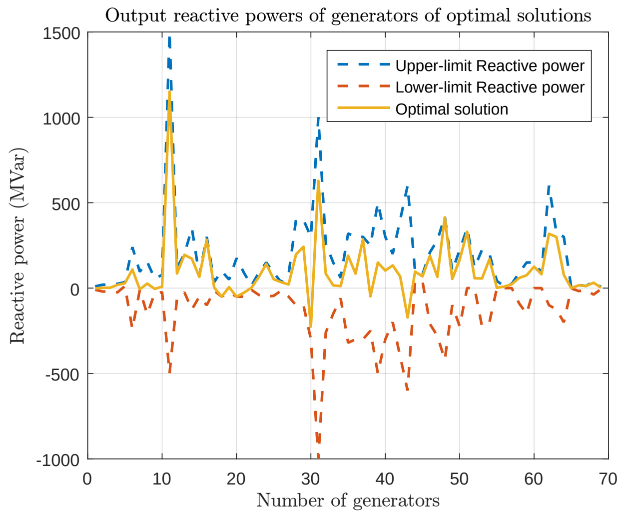

FIGURE 5.13: Generating reactive powers of generators on the IEEE 300-bus system

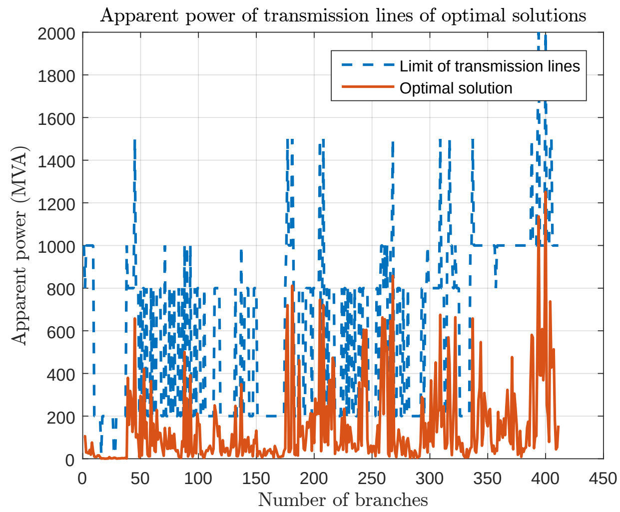

FIGURE 5.14: Apparent power through transmission lines of the optimal solution on the IEEE 300-bus system

benchmarks to identify its effectiveness on engineering problems.

Chapter 6

Optimal Reactive Power Dispatch

This chapter proposes a Self-Learning Cuckoo search algorithm to solve the optimal reactive power dispatch problem. Self-Learning Cuckoo search algorithm is a simple combination of the Cuckoo search algorithm and Teaching-learning-based optimization, where the learner phase of Teaching-learning-based optimization is added to improve performance of Cuckoo eggs. The proposed method has been applied for solving three tested cases of optimal reactive power dispatch problem. The objective of this problem is to minimize the power loss while satisfying generator operational constraints of generators, transformers, shunt capacitors and capacity of transmission lines. The results show that the proposed Self-Learning Cuckoo search algorithm is better than the conventional Cuckoo search algorithm.

This chapter includes six parts. The second part describes the objective function and operational constraints of this problem. The next part shows original pseudo codes of Cuckoo search algorithm and describes the proposed Self-Learning Cuckoo search algorithm. In the forth part, we describes our implementation of Self-Learning Cuckoo search algorithm for ORPD. Numerical results are shown in the fifth part and the last part is our conclusion and future work.

6.1 Previous works on optimal reactive power dispatch

Optimal reactive power dispatch (ORPD) is a type of optimal power flow. It focuses on controlling variables related with reactive power such as: output voltage of generators, load change tap of transformers, reactive power sources, etc. In literature, the objective of this problem is to minimize power loss and enhance performance of voltage profile. Therefore, ORPD tool is very useful and well-known in operating the power system.

Many optimization techniques have been proposed to solve the optimal reactive power dispatch problems. In the past, some classical methods such as linear programming [70], quadratic programming [71], Lagrange approach [72] have been applied for this problem. However, the disadvantages of these techniques are difficult to handle large systems, easy convergence to local optima. Some of them only calculate on continuous and differential objective functions. In recent years, despite of the development of computers, stochastic search methods have been widely employed for the ORPD. For example, El Ela et al. applied Differential evolution for ORPD in the IEEE 30-bus system [73]. A.H. Khazali and M. Kalantar proposed Harmony search algorithm for the IEEE 30-bus and 57-bus systems [74]. On another hand, John G. V. and Kwang Y. L. applied Evolutionary algorithm to solve the optimal real and reactive power for the IEEE 118-bus system [75]. Other modern algorithms have been employed to improve the global solution,e.g. Particle Swarm optimization [76], Teaching-learning-based optimization [77]. The development of stochastic methods gives the challenge to find an effective method while increasing the number of variables and constraints of the power system.

In this chapter, we propose an improvement of Cuckoo search algorithm to solve the optimal reactive power dispatch problem. The proposed method enhance performance of Cuckoo eggs by using the learner stage of Teaching-learning-based optimization. The learner stage help Cuckoo eggs learn together to focus on searching global solution. We name this improvement Self-Learning Cuckoo search algorithm. In order to investigate its effectiveness, we have applied it for the ORPD in three standard IEEE systems. The objective of ORPD is to minimize power loss while satisfying many operation constraints such as: the power balance constraint, limitations of generators, transformers, reactive power sources and capacity of transmission lines. The results have been compared with the conventional Cuckoo search algorithm and another modern approach, quasi-oppositional teaching learning based optimization [77].

6.2 Problem Formulation

6.2.1 Objective function

The main objective of the optimal reactive power dispatch is to minimize the power loss. Thus, the objective function is expressed as following:

$$\min F; F = P_{loss} = \sum_{l=1}^{N_{br}} R_l I_l^2 = \sum_{i=1}^{N_b} \sum_{\substack{j=1 \\ i \neq j}}^{N_b} \left[V_i^2 + V_j^2 - 2V_i V_j \cos\left(\delta_i - \delta_j\right)\right] Y_{ii} \cos\varphi_{ij} \quad (6.1)$$

Where N_{br} and N_b are the number of lines and buses, respectively; R_l is the resistance of line l_{th}; I_l is the current through line l^{th}; V_i and δ_i are the magnitude and angle of voltage at the i^{th} bus, respectively; Y_{ij} and φ_{ij} are the magnitude and angle of the line admittance between bus i^{th} and bus j^{th}, respectively.

6.2.2 Operational constraints

The optimal solutions have to satisfy all of operational constraints such as the power balance constraint, limitation of bus voltages and transmission lines.

6.2.2.1 Power balance constraint:

As other problems for operation in a power system, the balance of generating and demand powers must be satisfied at each node. Two below equations describe the balance of active and reactive powers in a power system:

$$P_i^G - P_i^D = V_i \sum_{i=1}^{N_b} \left[V_j \left[G_{ij} \cos\left(\delta_i - \delta_j\right) + B_{ij} \sin\left(\delta_i - \delta_j\right)\right]\right] \quad (6.2)$$

$$Q_i^G - Q_i^D = V_i \sum_{i=1}^{N_b} \left[V_j \left[G_{ij} \sin\left(\delta_i - \delta_j\right) - B_{ij} \sin\left(\delta_i - \delta_j\right) \right] \right] \tag{6.3}$$

Where P_i^G and Q_i^G are the active and reactive generating powers at the i^{th} bus, respectively; P_i^D and Q_i^D are the active and reactive of demand powers at the i^{th} bus, respectively. G_{ij} and B_{ij} represent the real and imaginary components of element Y_{ij} of the admittance matrix, respectively.

6.2.2.2 Limitation constrains of generators

Terminal voltage and reactive output power of a generator work in range as follows:

$$V_{i,\min}^G \leq V_i^G \leq V_{i,\max}^G \tag{6.4}$$

$$Q_{i,\min}^G \leq Q_i^G \leq Q_{i,\max}^G \tag{6.5}$$

6.2.2.3 Limitation of shunt-VAR compensators

The reactive power sources are bounded as follows:

$$Q_{i,\min}^C \leq Q_i^C \leq Q_{i,\max}^C \tag{6.6}$$

6.2.2.4 Limitation of transformer load changers

Upper and lower limits restrict transformer tap settings as shown below:

$$V_{i,\min}^T \leq V_i^T \leq V_{i,\max}^T \tag{6.7}$$

6.2.2.5 Limitation of load bus voltages

In order to keep the power system operate in stability and commit power quality, voltages at load buses must be maintained around a nominal value.

$$V_{i,\min}^L \leq V_i^L \leq V_{i,\max}^L \tag{6.8}$$

6.2.2.6 Limitation of transmission lines

Because of limited thermal condition, all transmission lines in the power system have to satisfy an upper bound as follow:

$$|S_{li}| \leq S_{li}^{\max} \tag{6.9}$$

6.3 Implementation of Self-Learning Cuckoo Search for ORPD

6.3.1 Constraint handling

During the optimizing process, all constraints must be satisfied. The real and reactive power balance constraints (6.2), (6.3) are implicitly satisfied by the power flow algorithm. The generator voltages, capacitor of shunt-VAR compensator and transformer lap setting are controlled variables. Thus their limitation constraints (6.4), (6.6), (6.7) are self-modified when generating Cuckoo eggs. Other constraints of dependent variables are restricted by including in the fitness function.

The fitness function FF combine the objective function and operational constraints of depend variables via penalty factors K_p. With the limits of load bus voltages, reactive power of generators and transmission line (6.8), (6.5), (6.9), we use a limited function, $V^{\lim}(x)$ as (6.11). Through all tested cases, all penalty factors are 100. The fitness function is as follow:

$$FF = P_{loss} + \sum_{i=1}^{N_g} \left(Q_i^G - V_i^{\lim}(Q_i^G)\right)^2 + K_p.\sum_{i=1}^{b} \left[V_i - V_i^{\lim}(V_i)\right]^2 + K_p.\sum_{i=1}^{br} (|S_{li}| - S_{li}^{\max})^2 \tag{6.10}$$

$$V^{\lim}(x) = \begin{cases} x_{\max}, \text{if} x > x_{\max} \\ x, \text{if} x_{\min} \leq x \leq x_{\max} \\ x_{\min}, \text{if} x < x_{\min} \end{cases} \tag{6.11}$$

Similar to other population-based methods, initial nests also lay randomly between upper and lower bounds as follows:

$$Nest_i = UpB + rand().\,(UpB - LowB) \tag{6.12}$$

Where:

- N_g is the number of generators.
- $Nest_i$ is the i^{th} nest in populations.
- UpB and $LowB$ are the upper and lower bound vectors created from (6.4), (6.6), (6.7).

6.3.2 Overall procedure

Figure 6.1 shows the overall procedure of the proposed Self-Learning Cuckoo search Algorithm for the optimal reactive power dispatch.

6.4 Numerical results

Proposed Self-Learning Cuckoo search algorithm has been applied to solve the optimal reactive power dispatch problem in three various IEEE power systems. The obtained numerical results are compared with conventional Cuckoo search algorithm and Quasi-oppositional Teaching-learning-based optimization (QOTLBO) [77]. Applications of SLCSA and CSA are coded in Matlab 2015a and run in a personal computer with a 3Ghz Core 2Duo processor and 4GB RAM. For each method, each benchmark is run 50 independent trials. In order to calculate power flow, we used the Newton-Raphson method by the Matpower toolbox [61].

6.4.1 Case study 1: IEEE 30-bus system

This case study is the standard IEEE 30-bus system [57]. The tested system consists of six generators, 41 branches and 24 load buses. There are nine installed reactive sources

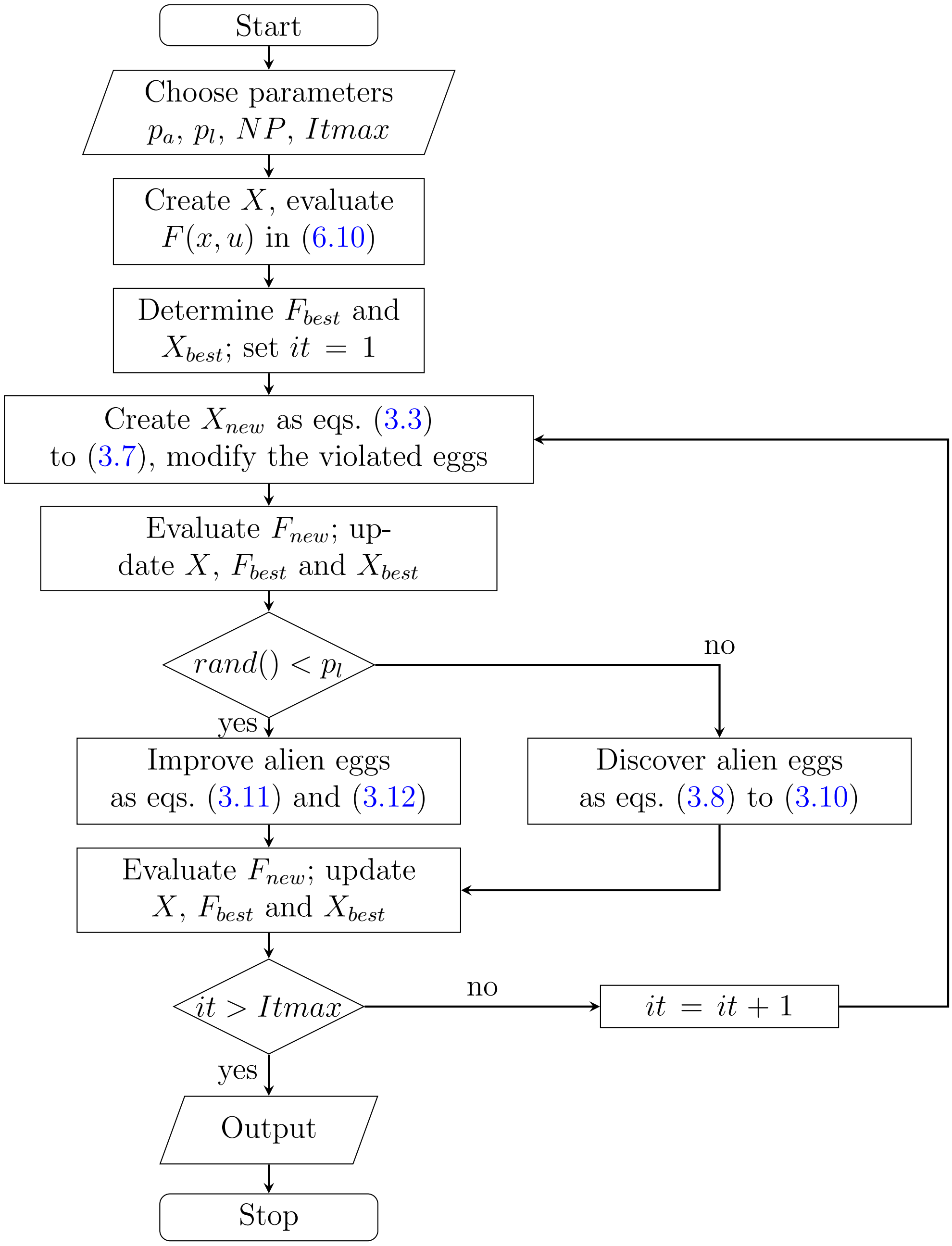

FIGURE 6.1: Flow chart

at the 10^{th}, 12^{th}, 15^{th}, 17^{th}, 20^{th}, 21^{th}, 23^{th}, 24^{th} and 29^{th} buses. Four branches are transformers with tap changers in lines (6, 9), (6, 10), (4, 12) and (27, 28). The reactive power generation limits are taken from [78] and the maximum apparent power flows of transmission lines are given in [79] The limitations of transformer lap changers, generator voltage and voltages at load buses are as follows:

$$
\begin{aligned}
0.95 \leq V_{Gi} \leq 1.1 \\
0.90 \leq V_{Ti} \leq 1.1 \\
0.95 \leq V_{li} \leq 1.1
\end{aligned}
\tag{6.13}
$$

Table 6.1: Numerical results of compared methods for IEEE 30-bus tested system

Methods	**SLCSA**	**CSA**
Best [MW]	4.5125	4.5152
Mean [MW]	4.5125	4.5199
Worst [MW]	4.5125	4.5168
Standard deviation	1.43722E-06	0.0015

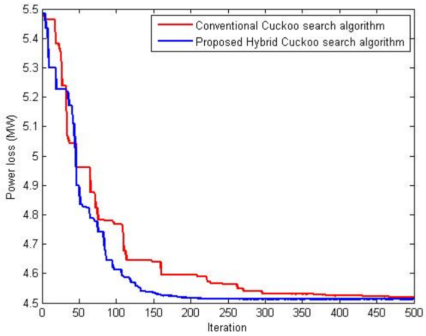

Figure 6.2: Convergence characteristics of CSA and SLCSA in the IEEE 30-bus system

According to numerical results in Tab. 6.1, the proposed Self-Learning Cuckoo search

Table 6.2: Optimal solutions of compared methods for IEEE 30-bus system

Control variables	SLCSA	CSA	Control variables	SLCSA	CSA
V_{G1} (p.u.)	1.1	1.1	Q_{C17} (MVar)	5.0	4.8892
V_{G2} (p.u.)	1.0943	1.0944	Q_{C20} (MVar)	4.0955	3.7108
V_{G5} (p.u.)	1.0747	1.0748	Q_{C21} (MVar)	5.0	4.9727
V_{G8} (p.u.)	1.0766	1.0770	Q_{C23} (MVar)	2.5327	3.0216
V_{G11} (p.u.)	1.1	1.0994	Q_{C24} (MVar)	5.0	4.9769
V_{G13} (p.u.)	1.1	1.1	Q_{C29} (MVar)	2.2118	2.6445
Q_{C10} (MVar)	5.0	5.0	T_{6-9} (p.u.)	1.0403	1.0222
Q_{C12} (MVar)	5.0	4.9871	T_{6-10} (p.u.)	0.9000	0.9145
Q_{C15} (MVar)	4.9778	4.5196	T_{4-12} (p.u.)	0.9758	0.9738
Loss (MW)	**4.5125**	**4.5152**	T_{28-27} (p.u.)	0.9636	0.9676

algorithm gives better solution than conventional Cuckoo search algorithm and QOTLBO. The convergence curve of Fig. 6.2 shows that the SLCSA converges faster than CSA. At the beginning of search process, CSA converges slightly faster than SLCSA. However, SLCSA can reach to the best solution at the end of process. Figure 6.2 shows the optimal solutions of compared methods.

6.4.2 Case study 2: IEEE 57-bus system

This benchmark is a lager scale power system, the standard IEEE 57-bus system with 7 generators, 57 buses and 80 transmission lines-transformers. 17 branches are under load change tap transformers. Three shunt reactive power sources are installed at buses 18, 25 and 53. The variable limits are taken from [80].

Table 6.3 shows the Monte Carlo numerical results. The Self-Learning Cuckoo search algorithm is clearly better than conventional Cuckoo search algorithm. It doesn't only give better solutions, but its performance also is higher than others. The best solution of SLCSA is given in Tab 6.4.

According to Fig. 6.3, it clearly shows that Self-Learning Cuckoo search algorithm is better than conventional Cuckoo search algorithm to find the global optimum.

TABLE 6.3: Numerical results of SLCSA and CSA for IEEE 57-bus system

	SLCSA	**CSA**
Best [MW]	24.3785	24.7651
Mean [MW]	24.4809	24.9496
Worst [MW]	25.2094	25.1935
Standard deviation	0.1178	0.1756

6.4.3 Case study 3: IEEE 118-bus system

The last tested case is the IEEE 118-bus system. It is a huge system with 54 generators, 64 load buses, 186 transmission lines and 9 transformers with load settings. There are 14 reactive power sources in the system. The placement and capacity of these sources are

Table 6.4: Optimal solutions of SLCSA and CSA for IEEE 57-bus system

Control variables	**SL-CSA**	**CSA**	**Control variables**	**SL-CSA**	**CSA**	**Control variables**	**SL-CSA**	**CSA**
V_{G1}(pu)	1.06	1.06	T_{24-25}(pu)	0.9695	0.9704	T_{4-18}(pu)	0.9389	0.9
V_{G2}(pu)	1.0498	1.0491	T_{24-25}(pu)	0.9530	0.9147	T_{11-43}(pu)	0.9471	0.9330
V_{G3}(pu)	1.0412	1.0382	T_{24-26}(pu)	1.0085	1.0332	T_{4-18}(pu)	0.9998	1.0831
V_{G6} (pu)	1.0366	1.0320	T_{7-29}(pu)	0.9617	0.9680	T_{40-56}(pu)	1.0011	1.0649
V_{G8} (pu)	1.0587	1.0459	T_{34-32}(pu)	0.9411	0.9425	T_{21-20}(pu)	1.0184	1.0619
V_{G9} (pu)	1.0253	1.0150	T_{11-41}(pu)	0.9001	0.9134	T_{39-57}(pu)	0.9744	1.0064
V_{G12} (pu)	1.0323	1.0266	T_{15-45} (pu)	0.9452	0.9414	T_{10-51}(pu)	0.9503	0.9580
Q_{C18} (MVar)	9.6068	4.4174	T_{14-46} (pu)	0.9383	0.9238	T_{13-49}(pu)	0.9090	0.9094
Q_{C25} (MVar)	5.8992	4.5008	Q_{C53} (MVar)	6.2757	4.7618	T_{9-55}(pu)	0.9569	0.9731

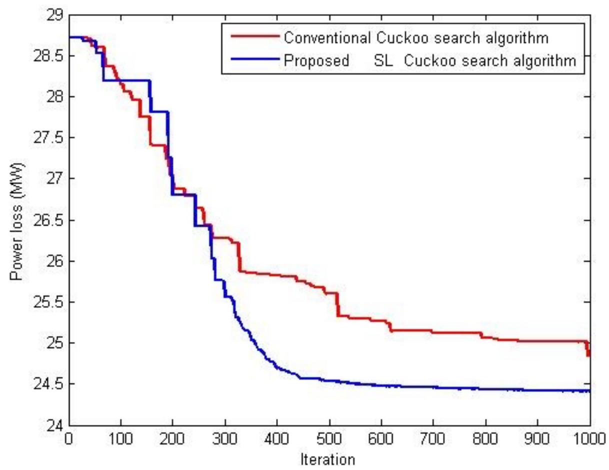

Figure 6.3: Convergence characteristics of CSA and SLCSA in the IEEE 57-bus system

given in Tab. 6.5. The variable limits are as follows:

$$
\begin{aligned}
0.95 &\leq V_{Gi} \leq 1.1 \\
0.90 &\leq V_{Ti} \leq 1.1 \qquad (6.14) \\
0.95 &\leq V_{li} \leq 1.1
\end{aligned}
$$

In this work, the Self-Learning Cuckoo search algorithm has just been run a few times. However, according to Tab. **??** its optimal result is better than the solution of QOTLBO.

TABLE 6.5: Reactive power generation limits in IEEE 118-bus system

Bus	5	34	37	44	45	46	48	74	79	82	83	105	107	110
$Q_{Ci,\max}$ [MVar]	0	14	0	10	10	10	15	12	20	20	10	20	6	6
$Q_{Ci,\min}$ [MVar]	-40	0	-25	0	0	0	0	0	0	0	0	0	0	0

6.5 Conclusions

The proposed Self-Learning Cuckoo search algorithm has been successful in solving the optimal reactive power dispatch. The proposed method employs the learner stage of Teach-learning-based optimization to enhance the performance of Cuckoo eggs. A learning factor p_h has been used to prevent Cuckoo eggs fall into local optima when employing the learner stage. According to three benchmarks of the ORPD, the Self-Learning CSA is much better than the conventional CSA in finding optimal solutions with higher performance. Comparing with the QOTLBO, the proposed method gives better solution in two tested systems. However, in IEEE 118-bus system, the proposed method should be continued simulating to obtain its effectiveness in large-scale power systems. The proposed method is a favorable for solving other types of the optimal reactive power dispatch.

Chapter 7

Optimal sizing and placement of shunt VAR compensators

This paper presents an application of Cuckoo search algorithm to determine optimal location and sizing of Static VAR Compensator. Cuckoo search algorithm is a modern heuristic technique basing Cuckoo species' parasitic strategy. The Lévy flight has been employed to generate random Cuckoo eggs. Moreover, the objective function is a multi-objective problem, which minimizes loss power, voltage deviation and investment cost of Static VAR Compensator while satisfying other operating constraints in power system. Cuckoo search algorithm is evaluated on three case studies and compared with the Teaching-learning-based optimization, Particle Swarm optimization and Improved Harmony search algorithm. The results show that Cuckoo search algorithm is better than other optimization techniques and its performance is also better.

7.1 Previous works on optimal reactive power dispatch

In reconfiguration of the electric power system, Flexible AC transmission system (FACTS) devices play an important role. FACTS give many benefits of dynamic stability and steady-state controls of a power system. Among FACTS devices, Static VAR Compensator

(SVC) is widely used because of its low cost, easy control and good performance. The first required problem to install SVC or other FACTS devices in power system is to determine place and size of them.

In literature, this problem has been mentioned in various ways. For example, Y. Del Valle et al. applied the particle swarm optimization for finding size and location of a Static Compensator (STATCOM) to improve the voltage profile of Brazilian power system [81]. In Taiwan, Huang C.H. et al. employed four various FACTS devices to save active power of generators and enhance voltage profile. The optimal solution given by Harmony Search algorithm is better than methods [82]. Another research of Pisica et al. proposed a multi-objective function to determine the optimal placement and size of a SVC device [83]. The multi-objective function includes the power loss, the voltage deviation and the investment cost of SVC. They solved this problem by a version of genetic algorithm. Following this approach, Reza Sirjani et al. proposed an improved version of the Harmony search algorithm to solve the problem [84, 85]. On summary, all of above studies successfully use evolutionary methods to determine optimal location and size of SVC or other FACTS devices.

However, each method can solve some problems effectively. Thus, the requirement to develop a new optimization technique and apply it for various problems increasingly continues. Since 2009, Yang and Deb have been developing a modern nature-inspired method, it names Cuckoo search algorithm [27, 28]. In 2013, a survey made by P. Civicioglu and E. Besdok gives comparison of four methods: Cuckoo search, particle swarm optimization, differential evolution and artificial bee colony algorithms [47]. After obtaining 50 mathematical functions, they conducted that differential evolution and the Cuckoo search are quite better than particle swarm optimization and artificial bee colony algorithm. Furthermore, many researchers have applied this method for solving optimized problems in power system. For instance, Moravej, Z., & Akhlaghi, A. basing on Cuckoo search give optimal location of distributed generators in distribution network [86]. Vo D.N. et al. proposed optimal commitment of thermal generators in power system [44]. Ahmed, J., & Salam, Z. applied Cuckoo search for maximum power tracking for photovoltaic modules [45].

In this paper, we propose Cuckoo search algorithm to solve the multi-objective function for optimal SVC devices in electrical power system. It also gives a comparison between Cuckoo search algorithm and other methods. Three systems of IEEE tested cases are obtained to figure out the effect of the proposed method when increasing search space. The first benchmark is the modified IEEE 30-bus system with five candidate SVC devices. The second case study is the IEEE 57-bus system with six candidate SVC devices. The last case study is the IEEE 118-bus system considering 10 candidate SVC devices.

This paper includes six parts. Current part provides a literature review about applications of SVC in the electric power system and Cuckoo search algorithm. The second part describes three objectives and regular operational constraints of this problem. The next part shows original pseudo codes of Cuckoo search algorithm. In the forth part, we describes our implementation of Cuckoo search algorithm for this problem. Numerical results are shown in the fifth part and the last part is our conclusion and future work.

7.2 Objectives and operational constraints

7.2.1 Objectives

The problem of optimal placement and sizing of SVC is described as a multi-objective problem. This problem is to minimize power losses, voltage deviations and investment cost. Where the objectives of decreasing power losses and voltage deviations are technical objectives, while the investment cost is an economic one.

7.2.1.1 The active power losses

The total power loss in a power system is given in literature as:

$$P_{loss} = \sum_{l=1}^{br} R_l I_l^2 = \sum_{i=1}^{b} \sum_{\substack{j=1 \\ i \neq j}}^{b} \left[V_i^2 + V_j^2 - 2V_i V_j \cos(\delta_i - \delta_j) \right] Y_{ii} \cos \varphi_{ij} \tag{7.1}$$

where br and b are the number of lines and buses, respectively; R_l is the resistance of line l_{th}; I_l is the current through line l^{th}; V_i and δ_i are the magnitude and angle of voltage at the i^{th} bus, respectively; Y_{ij} and φ_{ij} are the magnitude and angle of the line admittance between bus i^{th} and bus j^{th}, respectively.

7.2.1.2 The voltage deviation

The voltage deviation is a sum of voltage deviations at all buses in the power system from reference values. The below formula defines the voltage deviation objective:

$$\Delta V_{\Sigma} = \sum_{i=1}^{b} \left(\frac{V_{ref,i} - V_i}{V_{ref,i}} \right)^2 \tag{7.2}$$

where $V_{ref,i}$ is the reference voltage at the i^{th} bus.

7.2.1.3 The investment cost

The investment cost of each SVC device is a quadratic function of reactive power [87]. Thus, the total investment cost as below:

$$C_{SVC} = \sum_{k=1}^{n} 0.0003Q_k^2 - 0.3051Q_k + 127.38 \tag{7.3}$$

where n is the number of installed SVC, Q_k is injected reactive power of the k^{th} SVC.

7.2.2 Operational constraints

Optimizing placement and sizing of SVC needs to satisfy all of operational constraints such as the power balance constraint, limitation of bus voltages and limitation of transmission lines.

7.2.2.1 Power balance constraint

As other problems for operation in a power system, the balance of generating and demand powers must be satisfied at each node. Two below equations describe the balance of active and reactive powers in a power system:

$$P_{G,i} - P_{D,i} = V_i \sum_{i=1}^{b} \left[V_j \left[G_{ij} \cos\left(\delta_i - \delta_j\right) + B_{ij} \sin\left(\delta_i - \delta_j\right)\right]\right] \tag{7.4}$$

$$Q_{G,i} - Q_{D,i} = V_i \sum_{i=1}^{b} \left[V_j \left[G_{ij} \sin\left(\delta_i - \delta_j\right) - B_{ij} \sin\left(\delta_i - \delta_j\right)\right]\right] \tag{7.5}$$

where $P_{G,i}$ and $Q_{G,i}$ are the active and reactive generating powers at the i^{th} bus, respectively; $P_{D,i}$ and $Q_{D,i}$ are the active and reactive of demand powers at the i^{th} bus, respectively. G_{ij} and B_{ij} represent the real and imaginary components of element Y_{ij} of the admittance matrix, respectively.

7.2.2.2 Limitation of SVC devices

Each SVC device only works in a range of reactive power:

$$Q_{i,\min} \leq Q_i \leq Q_{i,\max} \tag{7.6}$$

7.2.2.3 Limitation of bus voltages

In order to keep the power system operate in stability and commit power quality, bus voltage at each bus must be maintained around a nominal value.

$$V_{i,\min} \leq V_i \leq V_{i,\max} \tag{7.7}$$

7.3 Implementation and the fitness function

7.3.1 Solution vector

A solution for this problem is a vector with $2n$ elements; where n is the number of candidate SVC devices. The first n elements are positions of SVC devices. Each element is a natural number that represents the bus number where a SVC device is connected.

The other elements are continuing values that represent optimal installed reactive power of SVC devices. Fig. 7.1 shows the structure of a solution vector.

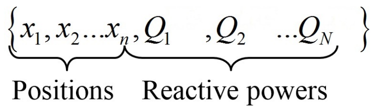

FIGURE 7.1: Structure of solution vector

With above structure of solution, it may lead the search engine to duplicated solutions. Table 7.1 shows an example of duplicated solutions. Two solutions actually give the same result that we need to install SVC at three buses {2, 4 and 7} with the same amount of injected reactive powers. Hence, to prevent this case, we proposed another constraint for positions of SVC as $x_1 < x_2 < \ldots < x_n$.

TABLE 7.1: Example of duplicated solutions

	Selected buses			**Injected reactive power (MW)**		
Solution 1	2	4	7	44.95	40.69	23.76
Solution 2	4	7	2	40.69	23.76	44.95

7.3.2 Fitness function

In order to describe three various objectives in a same mathematical function, we normalize each objective in a comparative manner with the base case (the system without SVC) and connect them together by weights. Equation (7.8) is the fitness function for this problem. With opinion that technical objectives are more important than economic one, the corresponding weights are set as $\alpha = 0.4, \beta = 0.4, \eta = 0.2$.

In order to handle operational constraints, we use penalty factors to combine with objective functions. The element *balance_flag* is a factor that equals to 0 if the power balance constraint is not violated and 1 otherwise. With the limits of bus voltages, we use a limited function, $V^{\text{lim}}(x)$. Equation (7.9) describes the limited function. With the constraint for positions, we use a counter to find out the number of positions are violated. Through all tested cases, all penalty factors are 100.

$$FF = \alpha \frac{P_{loss}}{P_{loss,base}} + \beta \frac{\Delta V}{\Delta V_{base}} + \eta \frac{C_{SVC}}{C_{\max}} + K_p.counter$$
$$+K_p.balance\_flag + K_p. \sum_{i=1}^{b} \left[V_i - V_i^{\lim} \left(V_i \right) \right]^2 \tag{7.8}$$

$$V^{\lim}(x) = \begin{cases} x_{\max}, \text{if} x > x_{\max} \\ x, \text{if} x_{\min} \leq x \leq x_{\max} \\ x_{\min}, \text{if} x < x_{\min} \end{cases} \tag{7.9}$$

where:

- P_{loss}: active power loss
- ΔV: voltage deviation index
- C_{SVC}: total SVC cost
- $P_{loss,base}$, ΔV_{base} and C_{max} are the total base case active power loss in the network, the total base case voltage deviation and the maximum investment cost, respectively.
- K_p: penalty factor

7.3.3 Limitation of solution vector and initialization

According to the structure of solution vector, the positions of candidate SVC devices cannot exceed the number of buses in the power system. Thus, x_{max} is the number of buses and x_{min} is equal to one. On other hand, the injected reactive power of SVC devices cannot exceed its capacitor in the constraint (7.6). Similar to other population-based methods, in the Cuckoo search algorithm, the nests also lay randomly between upper and lower bounds. However, for this problem, the first n elements of nests are natural numbers. Hence, we use the round function $round(x)$ to return the value x to the nearest natural number. Equation (7.10) and (7.11) describe the initialization of search space:

$$Nest_i = UpB + rand(). (UpB - LowB) \tag{7.10}$$

$$Nest_i \left(1 : n\right) = round \left(Nest_i(1 : n)\right) \tag{7.11}$$

where:

- $Nest_i$ is the i^{th} nest in populations.
- UpB and $LowB$ are the upper and lower bound vectors, as following:

$$UpB = \{x_{\max}, \dots, x_{\max}, Q_{\max}, \dots, Q_{\max}\} \tag{7.12}$$

$$LowB = \{x_{\min}, \dots, x_{\min}, Q_{\min}, \dots, Q_{\min}\} \tag{7.13}$$

7.3.4 Overall procedure

The overall procedure for the implementation of the Cuckoo search algorithm to determine optimal placement and sizing of SVC devices:

- **Step 1:** Choose controlling parameters for the Cuckoo search algorithm, such as: the probability of discovering Cuckoo eggs, the number of nests NP and the number of iterations It_{max}.
- **Step 2:** Create randomly initial nests $currentNest$.
- **Step 3:** Evaluate value of the fitness function FF in (7.8), while using Newton-Raphson method for calculating the power flow.
- **Step 4:** Determine the best value of the fitness function FF_{best} and the best nest $Nestbest$. Set the iteration counter $k = 1$.
- **Step 5:** Create Cuckoo eggs via Lévy flight and the new nests X_{new} as eqs. (3.3) to (3.7)
- **Step 6:** Modify the eggs that violate the limitations of SVC device constraints and the limitation of bus numbers.
- **Step 7:** Evaluate the fitness function for new nests $FFnew$
- **Step 8:** Compare the new values $FFnew$ to the current ones FF to pick up the better nests. Update the $currentNest$, the best value of fitness function $FFbest$ and the best nest $Nestbest$.

- **Step 9:** Discovery Cuckoo eggs by random biased walks, create new nests newNest as eqs. (3.8) to (3.10).

- **Step 10:** Modify the eggs that violate the limitations of SVC device constraints and the limitation of bus numbers.

- **Step 11:** Once again, evaluate the fitness function $FFnew$ for new nests $newNest$

- **Step 12:** Update values of the fitness function FF the $currentNest$, the best value of fitness function $FFbest$ and the best nest $Nestbest$.

- **Step 13:** Check if the iteration counter k is lower than the maximum iteration It_{max}, increase k and return step 5. Otherwise, stop.

7.4 Simulation results

Cuckoo search algorithm has been applied to identify optimal placement and sizing of SVC devices in three various IEEE power systems. The first tested system is the modified IEEE 30-bus system. This system consists of six generators, 41 transmission lines and transformers. It supplies for 189.2 MW load power. Another larger system is also a standard IEEE system with 7 generators, 57 buses and 80 transmission lines-transformers. The last benchmark is the standard IEEE 118-bus system. This system has 54 generators, 118 buses and 186 transmission lines-transformers.The obtained numerical results are compared with the Teaching-learning-based optimization (TLBO) [17, 69], self-organizing hierarchical particle swarm optimization with time-varying acceleration coefficients (SOHPSO-TVAC) [13] and Improved Harmony search algorithm (IHS) [16]. All applications are coded in Matlab 2015a and run in a personal computer with a 3Ghz Core 2Duo processor and 4GB RAM. For each method, each benchmark is run 100 independent trials. In order to calculate power flow, we used the Newton-Raphson method by the Matpower toolbox [61]. Table 7.2 shows the dimension, size of population, number of iterations and selected parameters of Cuckoo search algorithm for each benchmark.

TABLE 7.2: Size of search space and number of iterations

	30-bus system	**57-bus system**	**118-bus system**
Number of candidate SVC	5	6	10
Number of population	30	50	50
Iteration	500	5000	1000
Probability p_a	0.8	0.7	0.9

TABLE 7.3: Numerical results of CSA and TLBO for IEEE 30-bus system

	CSA	**TLBO**	**SOHPSO TVAC**	**IHS**
Best	1.4502	1.4502	1.4783	1.4626
Mean	1.4630	1.4810	1.5217	1.4764
Worst	1.4924	1.5089	1.5217	1.5139
SD	0.0080	0.0139	0.0165	0.0160

TABLE 7.4: Optimal solution of CSA in IEEE 30-bus case study

Selected bus	**Reactive power [MVar]**
8	46.8054
12	29.1442
19	11.8746
26	4.6557
30	7.1452

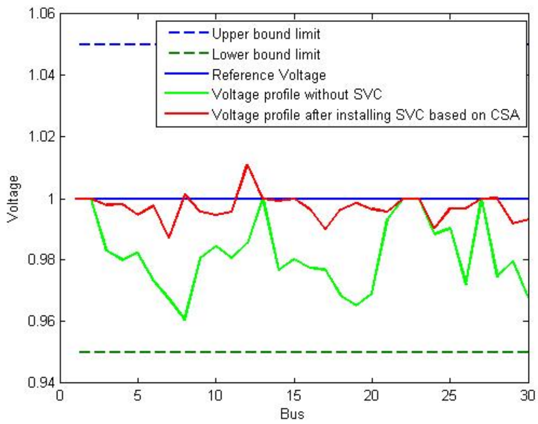

FIGURE 7.2: Voltage profiles of the best solution proposed by CSA in IEEE 30-bus case study

7.4.1 Case study 1: IEEE 30-bus system

According to numerical results in Tab. 7.3, Cuckoo search algorithm and TLBO give the same optimal solution and it is better than those given by SOHPSO-TVAC and IHS.

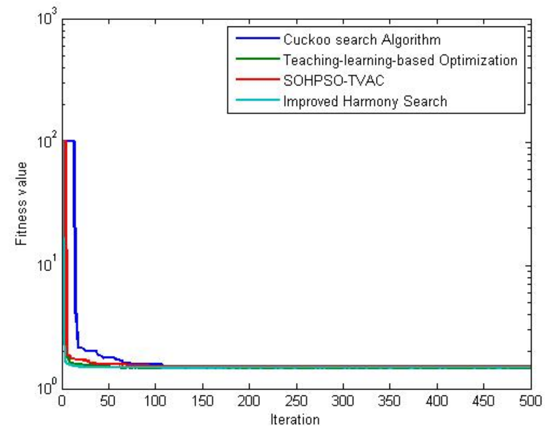

FIGURE 7.3: Comparison about convergences of proposed methods

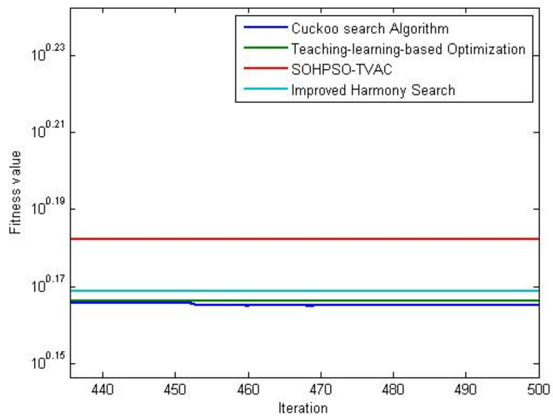

FIGURE 7.4: Zoomed image of convergences at the end of search process

However, in general, the Cuckoo search is better performance with lower average value and lower standard deviation.

Table 7.4 shows the best solutions proposed by Cuckoo search algorithm. Five selected buses are 8^{th}, 12^{th}, 19^{th}, 26^{th} and 30^{th} buses. After installing SVC, voltage magnitudes at these buses has been enhanced as Fig 7.2.

Figure 7.3 and Figure 7.4 consider the convergence of these methods, where Fig. 7.4 is a zoom image of Fig. 7.3 at the end of calculating process. Cuckoo search algorithm starts slower than other methods. However, it reaches the best solution at the end of process. Its solution is slightlt better than the ones proposed by Teaching-learning-based optimization and Improved Harmony search.

7.4.2 Case study 2: IEEE 57-bus system

TABLE 7.5: Numerical results of compared methods for IEEE 57-bus system

	CSA	**TLBO**	**SOHPSO TVAC**	**IHS**
Best	62.593	63.555	70.758	66.208
Mean	68.119	70.279	91.184	101.794
Worst	73.169	76.809	105.642	188.203
SD	3.141	4.520	8.259	42.231

TABLE 7.6: Optimal solution of CSA in IEEE 57-bus case study

Selected bus	**Reactive power [MVar]**
20	7.6985
31	5.0549
35	22.1316
42	6.5069
47	-49.9728
51	-31.7249

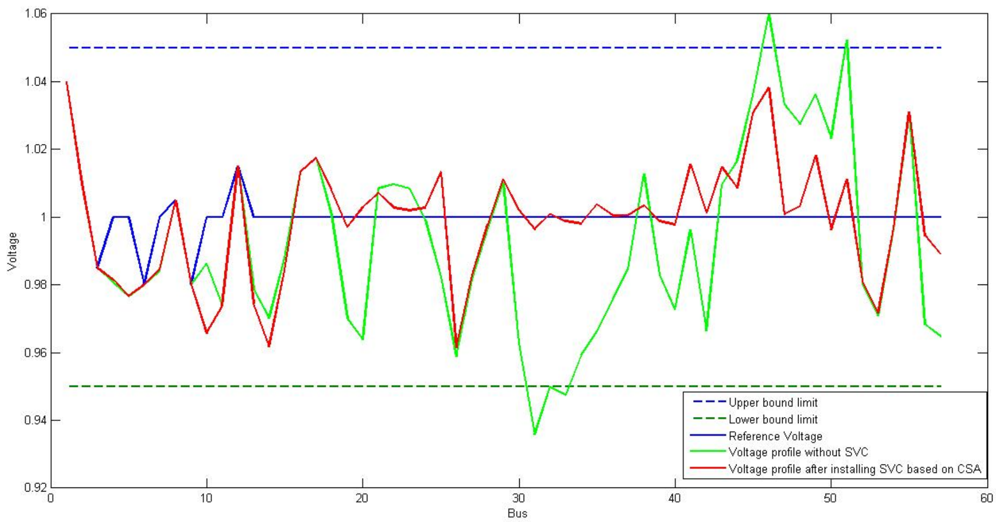

FIGURE 7.5: Voltage profiles of proposed methods in the IEEE 57-bus system

Table 7.5 shows the Monte Carlo numerical results. The Cuckoo search algorithm is clearly better than other compared search engines. The Cuckoo search algorithm does not only give better solutions, but its performance also is higher than others. The best solution of CSA is given in Tab 7.6. Cuckoo search algorithm suggests to inject reactive power at the 20^{th}, 31^{th}, 35^{th} and 42^{th} buses and absorb reactive power at the 47^{th} and

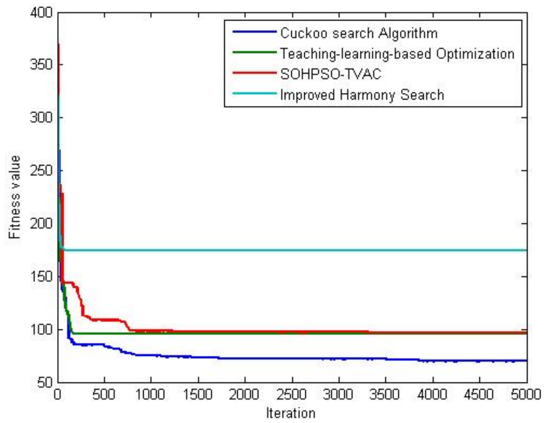

Figure 7.6: Comparison about convergences of CSA and TLBO

51^{th} buses.After installing SVC, voltage magnitudes at the 31^{th} and 47^{th} buses have been enhanced as Fig. 7.5.

According to Fig. 7.6, it clearly shows that Cuckoo search algorithm is better than other methods to find the global optimum. All of TLBO, SOHPSO-TVAC and IHS are easily stuck in local optima.

7.4.3 Case study 3: IEEE 118-bus system

Once again, Cuckoo search algorithm gives better solution than other methods. Detailed best solutions of compared methods are shown in Tab. 7.7. Both of the proposed method and the TLBO try to inject reactive power as much as possible but their proposed locations are different. However, the solution of Cuckoo search algorithm is slightly better than the one of TLBO, and clearly better than SOHPSO-TVAC and IHS.

7.5 Conclusions

The Cuckoo search algorithm is totally powerful and effective for determining location and size of SVC devices. Optimizing location and size of SVC devices is a complex problem. It combines continuous and discrete numbers with many equal and unequal constraints. It is easy to let the search engine to local optimums. However, according to three case studies,

TABLE 7.7: Best results of compared methods for IEEE 118-bus system

No. of installed SVC	CSA		TLBO		SOHPSO-TVAC	
	Selected bus	Reactive power	Selected bus	Reactive power	Selected bus	Reactive power
1	2	50	2	50	21	41.0593
2	13	50	13	50	37	-2.5962
3	20	50	14	32.4255	48	0.1190
4	28	50	20	50	52	40.2274
5	53	50	28	50	53	9.8975
6	58	50	39	50	57	19.4900
7	95	50	52	50	58	37.3924
8	106	50	109	50	75	27.9348
9	109	50	115	50	79	-17.0275
10	115	50	118	50	84	11.8723 50
Best	23.2405		23.9943		30.7140	

the Cuckoo search always gives the better solution with the higher performance. Comparing with Teaching-learning-based optimization, Cuckoo search algorithm may converge slower at the beginning, but it always give better solution at the end of search process. Comparing with SOHPSO-TVAC and IHS, Cuckoo search algorithm totally gives better solutions. On summary, the Cuckoo search algorithm is an effective optimization strategy to optimize location and size of SVC devices in a bulk power system. Furthermore, it is also favorable for the problem that combines continuous and discrete numbers.

Chapter 8

Conclusion

8.1 Alignment with research issues:

Following a design sciences research approach, the focus of this thesis is to propose and apply a new optimization technique to solve economic problems in the power system. This section now answers the research questions stated in the beginning of this thesis (see Chapter 1):

- About the Self-Learning Cuckoo search algorithm: The proposed method is an effective improvement of the Cuckoo search algorithm. The modification of Cuckoo eggs to follow the better solutions really enhances the efficiency of the search engine. The proposed learning factor p_l helps to control the performance of Cuckoo eggs and prevent them fall into local solutions. In addition, the proposed method is also more effective than the conventional on large-scale problems.

- About the Multi-Area Economic Dispatch: The proposed SLCSA is successful in a problem including many non-convex functions and equal constraints. Numerical results show that the proposed SLCSA gives better solutions than the conventional CSA and TLBO. Comparing the convergence characteristics, the SLCSA is faster than CSA but lower than TLBO at the beginning of seeking process, however, it can give the best solution at the end.

- About the Optimal Power Flow: Numerical results show that the proposed SLCSA achieves the OPF problems, especially in large-scale systems. The optimal solutions of this problem require to satisfy a huge of unequal constraints and the number of dimensions is up to 213 for the 300-bus system. The improvement boost Cuckoo eggs to solve the problem completely while the conventional is unsuccessful.

- About the Optimal Reactive Power Dispatch: According to numerical results, the SLCSA is in the first successful steps to solve the ORPD problems. On three evaluated case studies, the SLCSA is better than the conventional CSA. However, the proposed method needs to be compared with other algorithms to figure out its effectiveness.

- About the optimal sizing and placement of Shunt-VAR compensators: The proposed procedure based on the Cuckoo search algorithm is evaluated on three various IEEE power systems. According to numerical results, the Cuckoo search is entirely effective and powerful to solve the multi-objective function. Comparing to the Improve Harmony search algorithm and a version of Particle Swarm Optimization, it always gives better solutions and higher stability.

On summary, I have understood the Self-Learning Cuckoo search algorithm by modifying the controlling parameters, coding and propose an application for certain problems in the power system. The proposed procedure can be good for electric companies to operate the large-scale system and consulting companies to reconfigure the power system by FACTS devices.

8.2 Future research:

An overarching goal of this thesis is to continue applying the Self-learning Cuckoo search for various problems in power system; for instance, optimizing an environmental economic dispatch, volt-VAR control in distribution grids, . . . For successful case studies, the proposed method should be evaluated on larger and more practical systems.

On another hand, this proposed method should be tested on other engineering problems to investigate its efficiency. Furthermore, the author should do more simulation to figure out the effective range of the learning factor p_l and the probability of discovering alien eggs p_a.

Appendix A

Data of Multi-Area Economic Dispatch

A.1 Data of 6 generators considering Prohibited Operation Zones

TABLE A.1: Fuel cost coefficients of 6 generators

Index	a [\$/h]	b [\$/MWh]	c [$\$/(MW)^2h$]	$P_{\min}$ [MW]	$P_{\max}$ [MW]	Prohibited Operation Zones [P_{Ui}, P_{Li}]
$P_{1,1}$	550	8.10	0.00028	100	500	[210,240] [350,380]
$P_{1,2}$	350	7.50	0.00056	50	200	[90,110] [140,160]
$P_{1,3}$	310	8.10	0.00056	50	150	[80,90] [110,120]
$P_{2,1}$	240	7.74	0.00324	80	300	[150,170] [210,240]
$P_{2,2}$	200	8.00	0.00254	50	200	[90,110] [140,150]
$P_{2,3}$	126	8.60	0.00284	50	120	[75,85] [100,105]

TABLE A.2: Transmission loss coefficients of two areas

Area 1	Area 2
$B_1 = 1e^{-6} * \begin{bmatrix} 17 & 12 & 7 \\ 12 & 14 & 9 \\ 7 & 9 & 31 \end{bmatrix}$	$B_2 = 1e^{-6} * \begin{bmatrix} 24 & -6 & -8 \\ -6 & 129 & -2 \\ -8 & -2 & 150 \end{bmatrix}$
$B_{01} = 1e^{-3} * [-0.3908 - 0.12970.7047]$	$B_{02} = 1e^{-3} * [0.05910.2161 - 0.6635];$
$B_{001} = 0.045$	$B_{002} = 0.056;$

A.2 Data of 10 generators considering Multiple fuel cost functions

Table A.3: Fuel cost coefficients of 10 generators

Index		a	b	c	e	f
	[$/h]	[$/MWh]	[$/(MW)^2h$]	[MW]	[MW]	[P_{Ui}, P_{Li}]
1	100	0.2697e2	-0.3975	0.2176e-2	0.2697e-1	-0.3975e1
1	196	0.2113e2	-0.3059	0.1861e-2	0.2113e-1	-0.3059e1
2	50	0.1865e1	-0.3988e-1	0.1138e-2	0.1865e-2	-0.3988
2	114	0.1365e2	-0.1980e0	0.1620e-2	0.1365e-1	-0.1980e1
2	157	0.1184e3	-0.1269e1	0.4194e-2	0.1184	-0.1269e2
3	200	0.3979e2	-0.3116e0	0.1457e-2	0.3979e-1	-0.3116e1
3	332	-0.2875e1	0.3389e-1	0.8035e-3	-0.2876e-2	0.3389e0
3	388	-0.5914e2	0.4864e0	0.1176e-4	-0.5914e-1	0.4864e1
4	99	0.1983e1	-0.3114e-1	0.1049e-2	0.1983e-2	-0.3114e0
4	138	0.5285e2	-0.6348e0	0.2758e-2	0.5285e-1	-0.6348e1
4	200	0.2668e3	-0.2338e1	0.5935e-2	0.2668e0	-0.2338e2
5	190	0.1392e2	-0.8733e-1	0.1066e-2	0.1392e-1	-0.8733e0
5	338	0.9976e2	-0.5206e0	0.1597e-2	0.9976e-1	-0.5206e1
5	407	-0.5399e2	0.4462e0	0.1498e-3	-0.5399e-1	0.4462e1
6	85	0.1983e1	-0.3114e-1	0.1049e-2	0.1983e-2	-0.3114e0
6	138	0.5285e2	-0.6348e0	0.2758e-2	0.5285e-1	-0.6348e1
6	200	0.2668e3	-0.2338e1	0.5935e-2	0.2668e0	-0.2338e2
7	200	0.1893e2	-0.1325e0	0.1107e-2	0.1893e-1	-0.1325e1
7	331	0.4377e2	-0.2267e0	0.1165e-2	0.4377e-1	-0.2267e1
7	391	-0.4335e2	0.3559e0	0.2454e-3	-0.4335e-1	0.3559e1
8	99	0.1983e1	-0.3114e-1	0.1049e-2	0.1983e-2	-0.3114e0
8	138	0.5285e2	-0.6348e0	0.2758e-2	0.5285e-1	-0.6348e1
8	200	0.2668e3	-0.2338e1	0.5935e-2	0.2668e0	-0.2338e2
9	130	0.1423e2	-0.1817e-1	0.6121e-3	0.1423e-1	-0.1817e0
9	213	0.8853e2	-0.5675e0	0.1554e-2	0.8853e-1	-0.5675e1
9	370	0.1423e2	-0.1817e-1	0.6121e-3	0.1423e-1	-0.1817e0
10	200	0.1397e2	-0.9938e-1	0.1102e-2	0.1397e-1	-0.9938e0
10	362	0.4671e2	-0.2024e0	0.1137e-2	0.4671e-1	-0.2024e1
10	407	-0.6113e2	0.5084e0	0.4164e-4	-0.6113e-1	0.5084e1

$$B_1 = 1e{-}5 * \begin{bmatrix} 8.7 & 0.43 & -4.61 & 0.36 \\ 0.43 & 8.3 & -0.97 & 0.22 \\ -4.61 & -0.97 & 9.00 & -2.0 \\ 0.36 & 0.22 & -2.0 & 5.30 \end{bmatrix}; B01 = 1e{-}3 * [-0.3908 -0.1297 0.7047 0.0591]; B001 = 0.045 \tag{A.1}$$

$$B_2 = 1e-5 * \begin{bmatrix} 8.6 & -0.8 & 0.37 \\ -0.8 & 9.08 & -4.9 \\ 0.37 & -4.9 & 8.24 \end{bmatrix}; B02 = 1e-3*[0.2161-0.66350.5034]; B002 = 0.056 \quad (A.2)$$

$$B_3 = 1e-5 * \begin{bmatrix} 1.2 & -0.96 & 0.56 \\ -0.96 & 4.93 & -0.3 \\ 0.56 & -0.3 & 5.99 \end{bmatrix}; B03 = 1e-3*[-0.32160.46350.3503]; B003 = 0.055 \quad (A.3)$$

A.3 Data of 40 generators considering valve-point-effect fuel cost functions

TABLE A.4: Data of 40 generators

No	Pmin	Pmax	a	b	c	e	f
1	36	114	0.00690	6.73	94.705	100	0
2	36	114	0.00690	6.73	94.705	100	0
3	60	120	0.02028	7.07	309.540	100	0
4	80	190	0.00942	8.18	369.030	150	0
5	47	97	0.01140	5.35	148.890	120	0
6	68	140	0.01142	8.05	222.330	100	0
7	110	300	0.00357	8.03	287.710	200	0
8	135	300	0.00492	6.99	391.980	200	0
9	135	300	0.00573	6.60	455.760	200	0
10	130	300	0.00605	12.90	722.820	200	0
11	94	375	0.00515	12.90	635.200	200	0
12	94	375	0.00569	12.80	654.690	200	0
13	125	500	0.00421	12.50	913.400	300	0
14	125	500	0.00752	8.84	1760.400	300	0
15	125	500	0.00708	9.15	1728.300	300	0
16	125	500	0.00708	9.15	1728.300	300	0
17	220	500	0.00313	7.97	647.850	300	0

continued ...

Table 5.9 Continued: Optimal solution for the IEEE 118-bus system

No	Pmin	Pmax	a	b	c	e	f
18	220	500	0.00313	7.95	649.690	300	0
19	242	550	0.00313	7.97	647.830	300	0
20	242	550	0.00313	7.97	647.810	300	0
21	254	550	0.00298	6.63	785.960	300	0
22	254	550	0.00298	6.63	785.960	300	0
23	254	550	0.00284	6.66	794.530	300	0
24	254	550	0.00284	6.66	794.530	300	0
25	254	550	0.00277	7.10	801.320	300	0
26	254	550	0.00277	7.10	801.320	300	0
27	10	150	0.52124	3.33	1055.100	120	0
28	10	150	0.52124	3.33	1055.100	120	0
29	10	150	0.52124	3.33	1055.100	120	0
30	47	97	0.01140	5.35	148.890	120	0
31	60	190	0.00160	6.43	222.920	150	0
32	60	190	0.00160	6.43	222.920	150	0
33	60	190	0.00160	6.43	222.920	150	0
34	90	200	0.00010	8.95	107.870	200	0
35	90	200	0.00010	8.62	116.580	200	0
36	90	200	0.00010	8.62	116.580	200	0
37	25	110	0.01610	5.88	307.450	80	0
38	25	110	0.01610	5.88	307.450	80	0
39	25	110	0.01610	5.88	307.450	80	0
40	242	550	0.00313	7.97	647.830	300	0

A.4 Data of 140 generators considering valve-point-effect fuel cost functions

Table A.5: Data of 140 generators

No	Pmin	Pmax	a	b	c	e	f
1	94	203	1269.13200	89.83	0.014	0	0
2	94	203	1269.13200	89.83	0.014	0	0;
3	94	203	1269.13200	89.83	0.014	0	0;
4	244	379	4965.12400	64.13	0.030	0	0;
5	244	379	4965.12400	64.13	0.030	0	0;
6	244	379	4965.12400	64.13	0.030	0	0;
7	95	190	2243.18500	76.13	0.024	0	0;
8	95	189	2290.38100	81.81	0.002	600	0
9	116	194	1681.53300	81.14	0.022	0	0;
10	175	321	6743.30200	46.67	0.077	1200	0.043;
11	2	19	394.39800	78.41	0.953	0	0;
12	4	59	1243.16500	112.09	0.000	0	0;
13	15	83	1454.74000	90.87	0.072	0	0;
14	9	53	1011.05100	97.12	0.000	0	0;
15	12	37	909.26900	83.24	0.599	0	0;
16	10	34	689.37800	95.67	0.245	0	0;
17	112	373	1443.79200	91.20	0.000	0	0;
18	4	20	535.55300	104.50	0.085	0	0;
19	5	38	617.73400	83.02	0.525	0	0;
20	5	19	90.96600	127.80	0.177	0	0;
21	50	98	974.44700	77.93	0.063	0	0;
22	5	10	263.81000	92.78	2.740	0	0;
23	42	74	1335.59400	80.95	0.112	0	0;
24	42	74	1033.87100	89.07	0.042	0	0;
25	41	105	1391.32500	161.29	0.001	0	0;
26	17	51	4477.11000	161.83	0.005	0	0;
27	7	19	57.79400	84.97	0.235	0	0;
28	7	19	57.79400	84.97	0.235	0	0;
29	26	40	1258.43700	16.09	1.112	0	0;

continued ...

Table 5.9 Continued: Optimal solution for the IEEE 118-bus system

No	Pmin	Pmax	a	b	c	e	f
30	71	119	1220.64500	61.24	0.033	0	0;
31	120	189	1315.11800	41.10	0.008	0	0;
32	125	190	874.28800	46.31	0.004	0	0;
33	125	190	874.28800	46.31	0.004	0	0;
34	90	190	1976.46900	54.24	0.042	700	0
35	90	190	1338.08700	61.22	0.015	0	0;
36	280	490	1818.29900	11.79	0.007	0	0;
37	280	490	1133.97800	15.06	0.003	0	0;
38	260	496	1320.63600	13.23	0.005	0	0;
39	260	496	1320.63600	13.23	0.005	600	0
40	260	496	1320.63600	13.23	0.005	0	0;
41	260	496	1106.53900	14.50	0.004	0	0;
42	260	506	1176.50400	14.65	0.004	0	0;
43	260	509	1176.50400	14.65	0.004	0	0;
44	260	506	1176.50400	14.65	0.004	800	0
45	260	505	1176.50400	14.65	0.004	0	0;
46	260	506	1017.40600	15.67	0.002	0	0;
47	260	506	1017.40600	15.67	0.002	0	0;
48	260	505	1229.13100	14.66	0.004	0	0;
49	260	505	1229.13100	14.66	0.004	0	0;
50	260	505	1229.13100	14.66	0.004	0	0;
51	260	505	1229.13100	14.66	0.004	600	0
52	260	505	1267.89400	14.38	0.004	0	0;
53	260	505	1229.13100	14.66	0.004	0	0;
54	280	537	975.92600	16.26	0.002	0	0;
55	280	537	1532.09300	13.36	0.005	0	0;
56	280	549	641.98900	17.20	0.001	0	0;
57	280	549	641.98900	17.20	0.001	0	0;
58	260	501	911.53300	15.27	0.002	0	0;

continued . . .

Table 5.9 Continued: Optimal solution for the IEEE 118-bus system

No	Pmin	Pmax	a	b	c	e	f
59	260	501	910.53300	15.21	0.003	0	0;
60	260	506	1074.81000	15.03	0.004	0	0;
61	260	506	1074.81000	15.03	0.004	0	0;
62	260	506	1074.81000	15.03	0.004	600	0
63	260	506	1074.81000	15.03	0.004	0	0;
64	260	500	1278.46000	13.99	0.003	0	0;
65	260	500	861.74200	15.68	0.001	0	0;
66	120	241	408.83400	16.54	0.003	0	0;
67	120	241	408.83400	16.54	0.003	0	0;
68	423	774	1288.81500	16.52	0.001	0	0;
69	423	769	1436.25100	15.82	0.002	600	0
70	3	19	669.98800	75.46	0.902	0	0;
71	3	28	134.54400	129.54	0.110	0	0;
72	160	250	3427.91200	56.61	0.024	0	0;
73	160	250	3751.77200	54.45	0.029	0	0;
74	160	250	3918.78000	54.74	0.025	0	0;
75	160	250	3379.58000	58.03	0.017	0	0;
76	160	250	3345.29600	55.98	0.027	0	0;
77	160	250	3138.75400	61.52	0.008	0	0;
78	160	250	3453.05000	58.64	0.016	0	0;
79	160	250	5119.30000	44.65	0.046	0	0;
80	165	504	1898.41500	71.58	0.000	0	0;
81	165	504	1898.41500	71.58	0.000	1100	0
82	165	504	1898.41500	71.58	0.000	0	0;
83	165	504	1898.41500	71.58	0.000	0	0;
84	180	471	2473.39000	85.12	0.003	0	0;
85	180	561	2781.70500	87.68	0.000	0	0;
86	103	341	5515.50800	69.53	0.010	0	0;
87	198	617	3478.30000	78.34	0.008	0	0;

continued . . .

Table 5.9 Continued: Optimal solution for the IEEE 118-bus system

No	Pmin	Pmax	a	b	c	e	f
88	100	312	6240.90900	58.17	0.012	0	0;
89	153	471	9960.11000	46.64	0.039	0	0;
90	163	500	3671.99700	76.95	0.007	0	0;
91	95	302	1837.38300	80.76	0.000	0	0;
92	160	511	3108.39500	70.14	0.000	0	0;
93	160	511	3108.39500	70.14	0.000	0	0;
94	196	490	7095.48400	49.84	0.019	0	0;
95	196	490	3392.73200	65.40	0.011	0	0;
96	196	490	7095.48400	49.84	0.019	0	0;
97	196	490	7095.48400	49.84	0.019	0	0;
98	130	432	4288.32000	66.47	0.035	0	0;
99	130	432	13813.00100	22.94	0.082	1200	0
100	137	455	4435.49300	64.31	0.024	0	0;
101	137	455	9750.75000	45.02	0.035	1000	0
102	195	541	1042.36600	70.64	0.001	0	0;
103	175	536	1159.89500	70.96	0.000	0	0;
104	175	540	1159.89500	70.96	0.000	0	0;
105	175	538	1303.99000	70.30	0.001	0	0;
106	175	540	1156.19300	70.66	0.000	0	0;
107	330	574	2118.96800	71.10	0.000	0	0;
108	160	531	779.51900	37.85	0.001	0	0;
109	160	531	829.88800	37.77	0.000	0	0;
110	200	542	2333.69000	67.98	0.001	0	0;
111	56	132	2028.94500	77.84	0.132	0	0;
112	115	245	4412.01700	63.67	0.097	0	0;
113	115	245	2982.21900	79.46	0.055	1000	0
114	115	245	2982.21900	79.46	0.055	0	0;
115	207	307	3174.93900	93.97	0.014	0	0;
116	207	307	3218.35900	94.72	0.013	0	0;

continued . . .

Table 5.9 Continued: Optimal solution for the IEEE 118-bus system

No	Pmin	Pmax	a	b	c	e	f
117	175	345	3723.82200	66.92	0.016	0	0;
118	175	345	3551.40500	68.19	0.014	0	0;
119	175	345	4322.61500	60.82	0.028	0	0;
120	175	345	3493.73900	68.55	0.013	0	0;
121	360	580	226.79900	2.84	0.000	0	0;
122	415	645	382.93200	2.95	0.000	0	0;
123	795	984	156.98700	3.10	0.000	0	0;
124	795	978	154.48400	3.04	0.000	0	0;
125	578	682	332.83400	1.71	0.000	0	0;
126	615	720	326.59900	1.67	0.000	0	0;
127	612	718	345.30600	1.79	0.000	0	0;
128	612	720	350.37200	1.82	0.000	0	0;
129	758	964	370.37700	2.73	0.000	0	0;
130	755	958	367.06700	2.73	0.000	0	0;
131	750	1007	124.87500	2.65	0.000	0	0;
132	750	1006	130.78500	2.80	0.000	0	0;
133	713	1013	878.74600	1.60	0.001	0	0
134	718	1020	827.95900	1.50	0.001	0	0;
135	791	954	432.00700	2.43	0.000	0	0;
136	786	952	445.60600	2.50	0.000	0	0;
137	795	1006	467.22300	2.67	0.000	0	0;
138	795	1013	475.94000	2.69	0.000	0	0;
139	795	1021	899.46200	1.63	0.001	0	0;
140	795	1015	1000.36700	1.82	0.001	0	0

Appendix B

Data of the IEEE 30-bus system

B.1 Bus Data

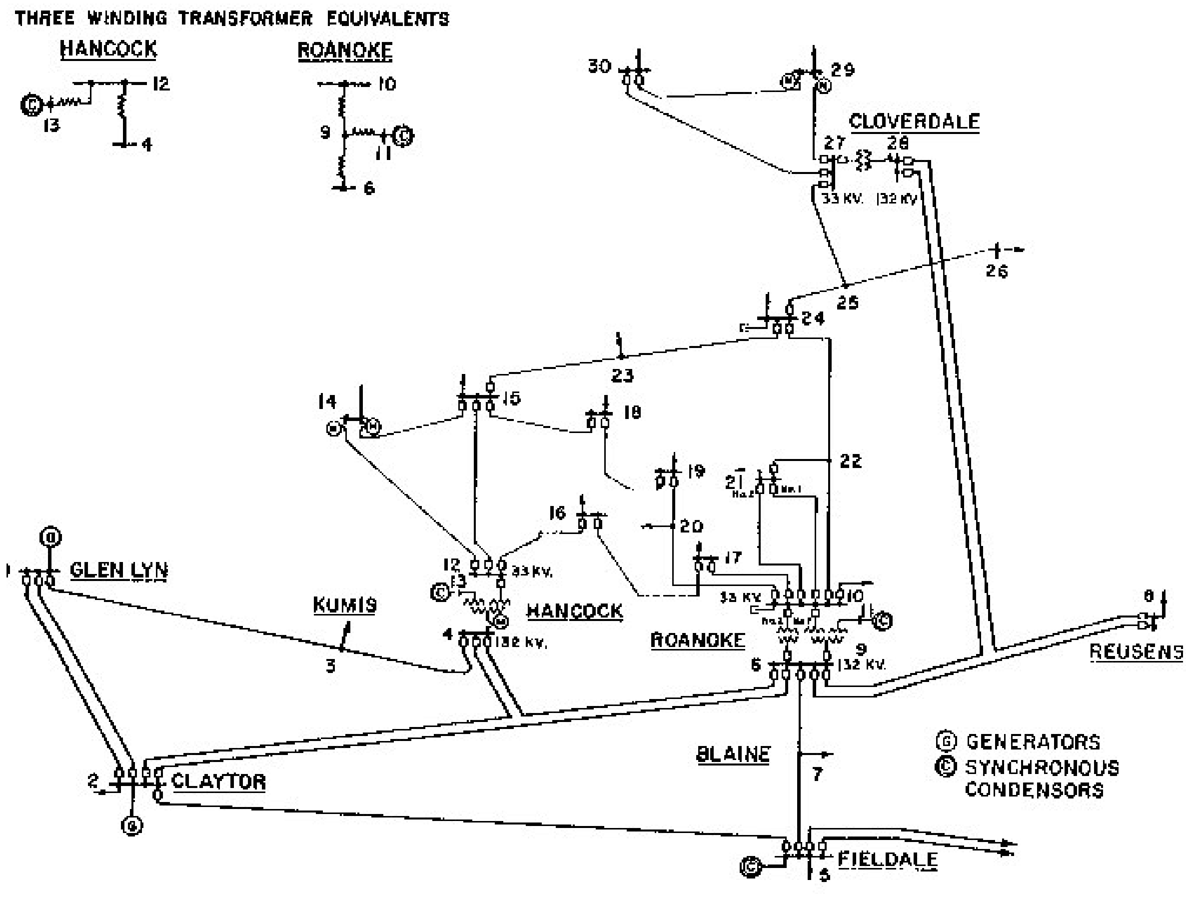

FIGURE B.1: One-line diagram of IEEE 30-bus system

TABLE B.1: Data of buses of the IEEE 30-bus system

Bus ID	Bus type	P_{load} (MW)	Q_{load} (MVAr)	Gs	Bs	Initial V_m (p.u.)	Initial V_a	baseKV	$V_{\max}$ (p.u.)	V_{min} (p.u)
1	3	0	0	0	0	1.060	0.00	132.00	1.05	0.95
2	2	22	13	0	0	1.043	-5.48	132.00	1.10	0.95
3	1	2	1	0	0	1.021	-7.96	132.00	1.05	0.95
4	1	8	2	0	0	1.012	-9.62	132.00	1.05	0.95
5	2	94	19	0	0	1.010	-14.37	132.00	1.10	0.95
6	1	0	0	0	0	1.010	-11.34	132.00	1.05	0.95
7	1	23	11	0	0	1.002	-13.12	132.00	1.05	0.95
8	2	30	30	0	0	1.010	-12.10	132.00	1.10	0.95
9	1	0	0	0	0	1.051	-14.38	1.00	1.05	0.95
10	1	6	2	0	19	1.045	-15.97	33.00	1.05	0.95
11	2	0	0	0	0	1.082	-14.39	11.00	1.10	0.95
12	1	11	8	0	0	1.057	-15.24	33.00	1.05	0.95
13	2	0	0	0	0	1.071	-15.24	11.00	1.10	0.95
14	1	6	2	0	0	1.042	-16.13	33.00	1.05	0.95
15	1	8	3	0	0	1.038	-16.22	33.00	1.05	0.95
16	1	4	2	0	0	1.045	-15.83	33.00	1.05	0.95
17	1	9	6	0	0	1.040	-16.14	33.00	1.05	0.95
18	1	3	1	0	0	1.028	-16.82	33.00	1.05	0.95
19	1	10	3	0	0	1.026	-17.00	33.00	1.05	0.95
20	1	2	1	0	0	1.030	-16.80	33.00	1.05	0.95
21	1	18	11	0	0	1.033	-16.42	33.00	1.05	0.95
22	1	0	0	0	0	1.033	-16.41	33.00	1.05	0.95
23	1	3	2	0	0	1.027	-16.61	33.00	1.05	0.95
24	1	9	7	0	4	1.021	-16.78	33.00	1.05	0.95
25	1	0	0	0	0	1.017	-16.35	33.00	1.05	0.95
26	1	4	2	0	0	1.000	-16.77	33.00	1.05	0.95
27	1	0	0	0	0	1.023	-15.82	33.00	1.05	0.95
28	1	0	0	0	0	1.007	-11.97	132.00	1.05	0.95

continued . . .

Table B.1 Continued: Data of buses of the IEEE 30-bus system

Bus ID	Bus type	P_{load} (MW)	Q_{load} (MVAr)	Gs	Bs	Initial Vm (p.u.)	Initial Va	baseKV	$V_{\max}$ (p.u.)	V_{min} (p.u)
29	1	2	1	0	0	1.003	-17.06	33.00	1.05	0.95
30	1	11	2	0	0	0.992	-17.94	33.00	1.05	0.95

B.2 Transmission lines

Table B.2: Data of transformers and transmission lines of IEEE 30-bus system

From bus	To bus	R (p.u.)	X (p.u.)	B (p.u.)	$S_{li}^{\max}$ (MVA)	Transformer tap
1	2	0.01920	0.0575	0.053	130	0.0000
1	3	0.04520	0.1652	0.041	130	0.0000
2	4	0.05700	0.1737	0.037	65	0.0000
3	4	0.01320	0.0379	0.008	130	0.0000
2	5	0.04720	0.1983	0.042	130	0.0000
2	6	0.05810	0.1763	0.037	65	0.0000
4	6	0.01190	0.0414	0.009	90	0.0000
5	7	0.04600	0.1160	0.020	70	0.0000
6	7	0.02670	0.0820	0.017	130	0.0000
6	8	0.01200	0.0420	0.009	32	0.0000
6	9	0.00000	0.2080	0.000	65	0.9780
6	10	0.00000	0.5560	0.000	32	0.9690
9	11	0.00000	0.2080	0.000	65	0.0000
9	10	0.00000	0.1100	0.000	65	0.0000
4	12	0.00000	0.2560	0.000	65	0.9320
12	13	0.00000	0.1400	0.000	65	0.0000
12	14	0.12310	0.2559	0.000	32	0.0000
12	15	0.06620	0.1304	0.000	32	0.0000
12	16	0.09450	0.1987	0.000	32	0.0000

continued . . .

Table B.2 Continued: Data of transformers and transmission lines of IEEE 30-bus system

From bus	To bus	R (p.u.)	X (p.u.)	B (p.u.)	$S_{li}^{\max}$ (MVA)	Transformer tap
14	15	0.22100	0.1997	0.000	16	0.0000
16	17	0.05240	0.1923	0.000	16	0.0000
15	18	0.10730	0.2185	0.000	16	0.0000
18	19	0.06390	0.1292	0.000	16	0.0000
19	20	0.03400	0.0680	0.000	32	0.0000
10	20	0.09360	0.2090	0.000	32	0.0000
10	17	0.03240	0.0845	0.000	32	0.0000
10	21	0.03480	0.0749	0.000	32	0.0000
10	22	0.07270	0.1499	0.000	32	0.0000
21	22	0.01160	0.0236	0.000	32	0.0000
15	23	0.10000	0.2020	0.000	16	0.0000
22	24	0.11500	0.1790	0.000	16	0.0000
23	24	0.13200	0.2700	0.000	16	0.0000
24	25	0.18850	0.3292	0.000	16	0.0000
25	26	0.25440	0.3800	0.000	16	0.0000
25	27	0.10930	0.2087	0.000	16	0.0000
28	27	0.00000	0.3960	0.000	65	0.9680
27	29	0.21980	0.4153	0.000	16	0.0000
27	30	0.32020	0.6027	0.000	16	0.0000
29	30	0.23990	0.4533	0.000	16	0.0000
8	28	0.06360	0.2000	0.043	32	0.0000
6	28	0.01690	0.0599	0.013	32	0.0000

B.3 Generators

1	260.2	-16.1	200	-20	1.050	100.000	1.00	200.00	50.000
2	80.0	50.0	100	-20	1.045	100.000	1.00	80.00	20.000
5	50.0	37.0	80	-15	1.010	100.000	1.00	50.00	15.000
8	20.0	37.3	60	-15	1.010	100.000	1.00	35.00	10.000
11	20.0	16.2	50	-10	1.050	100.000	1.00	30.00	10.000
13	20.0	10.6	60	-15	1.050	100.000	1.00	40.00	12.000

Table B.3: Quadratic functions

2	0	0	3	0	2.00	0.00375
2	0	0	3	0	1.75	0.01750
2	0	0	3	0	1.00	0.06250
2	0	0	3	0	3.25	0.00834
2	0	0	3	0	3.00	0.02500
2	0	0	3	0	3.00	0.02500

Table B.4: Valve-point-effect functions

2	0	0	3	150	2.00	0.00160	50	0
2	0	0	3	25	2.50	0.01000	40	0
2	0	0	3	0	1.00	0.06250	0	0
2	0	0	3	0	3.25	0.00834	0	0
2	0	0	3	0	3.00	0.02500	0	0
2	0	0	3	0	3.00	0.02500	0	0

Table B.5: Piecewise functions

1	50	0	3	55.0	0.70	0.00500
1	140	0	3	82.5	1.05	0.00750
2	20	0	3	40.0	0.30	0.01000
2	55	0	3	80.0	0.60	0.02000
5	15	0	3	0.0	1.00	0.06250
8	10	0	3	0.0	3.25	0.00834
11	10	0	3	0.0	3.00	0.02500
13	12	0	3	0.0	3.00	0.02500

Appendix C

Data of the IEEE 57-bus system

C.1 Bus Data

Table C.1: Data of buses of the IEEE 57-bus system

Bus ID	Bus type	P_{load} (MW)	Q_{load} (MVAr)	Gs	Bs	Initial V_m (p.u.)	Initial V_a	baseKV	$V_{\max}$ (p.u.)	V_{min} (p.u)
1	3	55	17	0	0	1.040	0.00	0.00	1.06	0.94
2	2	3	88	0	0	1.010	-1.18	0.00	1.06	0.94
3	2	41	21	0	0	0.985	-5.97	0.00	1.06	0.94
4	1	0	0	0	0	0.981	-7.32	0.00	1.06	0.94
5	1	13	4	0	0	0.976	-8.52	0.00	1.06	0.94
6	2	75	2	0	0	0.980	-8.65	0.00	1.06	0.94
7	1	0	0	0	0	0.984	-7.58	0.00	1.06	0.94
8	2	150	22	0	0	1.005	-4.45	0.00	1.06	0.94
9	2	121	26	0	0	0.980	-9.56	0.00	1.06	0.94
10	1	5	2	0	0	0.986	-11.43	0.00	1.06	0.94
11	1	0	0	0	0	0.974	-10.17	0.00	1.06	0.94
12	2	377	24	0	0	1.015	-10.46	0.00	1.06	0.94
13	1	18	2	0	0	0.979	-9.79	0.00	1.06	0.94
14	1	11	5	0	0	0.970	-9.33	0.00	1.06	0.94

continued . . .

Table C.1 Continued: Data of buses of the IEEE 57-bus system

Bus ID	Bus type	P_{load} (MW)	Q_{load} (MVAr)	Gs	Bs	Initial Vm (p.u.)	Initial Va	baseKV	$V_{\max}$ (p.u.)	V_{min} (p.u)
15	1	22	5	0	0	0.988	-7.18	0.00	1.06	0.94
16	1	43	3	0	0	1.013	-8.85	0.00	1.06	0.94
17	1	42	8	0	0	1.017	-5.39	0.00	1.06	0.94
18	1	27	10	0	10	1.001	-11.71	0.00	1.06	0.94
19	1	3	1	0	0	0.970	-13.20	0.00	1.06	0.94
20	1	2	1	0	0	0.964	-13.41	0.00	1.06	0.94
21	1	0	0	0	0	1.008	-12.89	0.00	1.06	0.94
22	1	0	0	0	0	1.010	-12.84	0.00	1.06	0.94
23	1	6	2	0	0	1.008	-12.91	0.00	1.06	0.94
24	1	0	0	0	0	0.999	-13.25	0.00	1.06	0.94
25	1	6	3	0	6	0.982	-18.13	0.00	1.06	0.94
26	1	0	0	0	0	0.959	-12.95	0.00	1.06	0.94
27	1	9	1	0	0	0.982	-11.48	0.00	1.06	0.94
28	1	5	2	0	0	0.997	-10.45	0.00	1.06	0.94
29	1	17	3	0	0	1.010	-9.75	0.00	1.06	0.94
30	1	4	2	0	0	0.962	-18.68	0.00	1.06	0.94
31	1	6	3	0	0	0.936	-19.34	0.00	1.06	0.94
32	1	2	1	0	0	0.949	-18.46	0.00	1.06	0.94
33	1	4	2	0	0	0.947	-18.50	0.00	1.06	0.94
34	1	0	0	0	0	0.959	-14.10	0.00	1.06	0.94
35	1	6	3	0	0	0.966	-13.86	0.00	1.06	0.94
36	1	0	0	0	0	0.976	-13.59	0.00	1.06	0.94
37	1	0	0	0	0	0.985	-13.41	0.00	1.06	0.94
38	1	14	7	0	0	1.013	-12.71	0.00	1.06	0.94
39	1	0	0	0	0	0.983	-13.46	0.00	1.06	0.94
40	1	0	0	0	0	0.973	-13.62	0.00	1.06	0.94
41	1	6	3	0	0	0.996	-14.05	0.00	1.06	0.94
42	1	7	4	0	0	0.966	-15.50	0.00	1.06	0.94

continued . . .

Table C.1 Continued: Data of buses of the IEEE 57-bus system

Bus ID	Bus type	P_{load} (MW)	Q_{load} (MVAr)	Gs	Bs	Initial Vm (p.u.)	Initial Va	baseKV	$V_{\max}$ (p.u.)	V_{min} (p.u)
43	1	2	1	0	0	1.010	-11.33	0.00	1.06	0.94
44	1	12	2	0	0	1.017	-11.86	0.00	1.06	0.94
45	1	0	0	0	0	1.036	-9.25	0.00	1.06	0.94
46	1	0	0	0	0	1.050	-11.89	0.00	1.06	0.94
47	1	30	12	0	0	1.033	-12.49	0.00	1.06	0.94
48	1	0	0	0	0	1.027	-12.59	0.00	1.06	0.94
49	1	18	9	0	0	1.036	-12.92	0.00	1.06	0.94
50	1	21	11	0	0	1.023	-13.39	0.00	1.06	0.94
51	1	18	5	0	0	1.052	-12.52	0.00	1.06	0.94
52	1	5	2	0	0	0.980	-11.47	0.00	1.06	0.94
53	1	20	10	0	6	0.971	-12.23	0.00	1.06	0.94
54	1	4	1	0	0	0.996	-11.69	0.00	1.06	0.94
55	1	7	3	0	0	1.031	-10.78	0.00	1.06	0.94
56	1	8	2	0	0	0.968	-16.04	0.00	1.06	0.94
57	1	7	2	0	0	0.965	-16.56	0.00	1.06	0.94

C.2 Transmission lines

Table C.2: Data of transformers and transmission lines of IEEE 57-bus system

From bus	To bus	R (p.u.)	X (p.u.)	B (p.u.)	$S_{li}^{\max}$ (MVA)	Transformer tap
1	2	0.00830	0.0280	0.129	9900	0.0000
2	3	0.02980	0.0850	0.082	9900	0.0000
3	4	0.01120	0.0366	0.038	9900	0.0000
4	5	0.06250	0.1320	0.026	9900	0.0000
4	6	0.04300	0.1480	0.035	9900	0.0000
6	7	0.02000	0.1020	0.028	9900	0.0000

continued ...

Table C.2 Continued: Data of transformers and transmission lines of IEEE 57-bus system

From bus	To bus	R (p.u.)	X (p.u.)	B (p.u.)	$S_{li}^{\max}$ (MVA)	Transformer tap
6	8	0.03390	0.1730	0.047	9900	0.0000
8	9	0.00990	0.0505	0.055	9900	0.0000
9	10	0.03690	0.1679	0.044	9900	0.0000
9	11	0.02580	0.0848	0.022	9900	0.0000
9	12	0.06480	0.2950	0.077	9900	0.0000
9	13	0.04810	0.1580	0.041	9900	0.0000
13	14	0.01320	0.0434	0.011	9900	0.0000
13	15	0.02690	0.0869	0.023	9900	0.0000
1	15	0.01780	0.0910	0.099	9900	0.0000
1	16	0.04540	0.2060	0.055	9900	0.0000
1	17	0.02380	0.1080	0.029	9900	0.0000
3	15	0.01620	0.0530	0.054	9900	0.0000
4	18	0.00000	0.5550	0.000	9900	0.9700
4	18	0.00000	0.4300	0.000	9900	0.9780
5	6	0.03020	0.0641	0.012	9900	0.0000
7	8	0.01390	0.0712	0.019	9900	0.0000
10	12	0.02770	0.1262	0.033	9900	0.0000
11	13	0.02230	0.0732	0.019	9900	0.0000
12	13	0.01780	0.0580	0.060	9900	0.0000
12	16	0.01800	0.0813	0.022	9900	0.0000
12	17	0.03970	0.1790	0.048	9900	0.0000
14	15	0.01710	0.0547	0.015	9900	0.0000
18	19	0.46100	0.6850	0.000	9900	0.0000
19	20	0.28300	0.4340	0.000	9900	0.0000
21	20	0.00000	0.7767	0.000	9900	1.0430
21	22	0.07360	0.1170	0.000	9900	0.0000
22	23	0.00990	0.0152	0.000	9900	0.0000

continued . . .

Table C.2 Continued: Data of transformers and transmission lines of IEEE 57-bus system

From bus	To bus	R (p.u.)	X (p.u.)	B (p.u.)	$S_{li}^{\max}$ (MVA)	Transformer tap
23	24	0.16600	0.2560	0.008	9900	0.0000
24	25	0.00000	1.1820	0.000	9900	1.0000
24	25	0.00000	1.2300	0.000	9900	1.0000
24	26	0.00000	0.0473	0.000	9900	1.0430
26	27	0.16500	0.2540	0.000	9900	0.0000
27	28	0.06180	0.0954	0.000	9900	0.0000
28	29	0.04180	0.0587	0.000	9900	0.0000
7	29	0.00000	0.0648	0.000	9900	0.9670
25	30	0.13500	0.2020	0.000	9900	0.0000
30	31	0.32600	0.4970	0.000	9900	0.0000
31	32	0.50700	0.7550	0.000	9900	0.0000
32	33	0.03920	0.0360	0.000	9900	0.0000
34	32	0.00000	0.9530	0.000	9900	0.9750
34	35	0.05200	0.0780	0.003	9900	0.0000
35	36	0.04300	0.0537	0.002	9900	0.0000
36	37	0.02900	0.0366	0.000	9900	0.0000
37	38	0.06510	0.1009	0.002	9900	0.0000
37	39	0.02390	0.0379	0.000	9900	0.0000
36	40	0.03000	0.0466	0.000	9900	0.0000
22	38	0.01920	0.0295	0.000	9900	0.0000
11	41	0.00000	0.7490	0.000	9900	0.9550
41	42	0.20700	0.3520	0.000	9900	0.0000
41	43	0.00000	0.4120	0.000	9900	0.0000
38	44	0.02890	0.0585	0.002	9900	0.0000
15	45	0.00000	0.1042	0.000	9900	0.9550
14	46	0.00000	0.0735	0.000	9900	0.9000
46	47	0.02300	0.0680	0.003	9900	0.0000

continued . . .

Table C.2 Continued: Data of transformers and transmission lines of IEEE 57-bus system

From bus	To bus	R (p.u.)	X (p.u.)	B (p.u.)	$S_{li}^{\max}$ (MVA)	Transformer tap
47	48	0.01820	0.0233	0.000	9900	0.0000
48	49	0.08340	0.1290	0.005	9900	0.0000
49	50	0.08010	0.1280	0.000	9900	0.0000
50	51	0.13860	0.2200	0.000	9900	0.0000
10	51	0.00000	0.0712	0.000	9900	0.9300
13	49	0.00000	0.1910	0.000	9900	0.8950
29	52	0.14420	0.1870	0.000	9900	0.0000
52	53	0.07620	0.0984	0.000	9900	0.0000
53	54	0.18780	0.2320	0.000	9900	0.0000
54	55	0.17320	0.2265	0.000	9900	0.0000
11	43	0.00000	0.1530	0.000	9900	0.9580
44	45	0.06240	0.1242	0.004	9900	0.0000
40	56	0.00000	1.1950	0.000	9900	0.9580
56	41	0.55300	0.5490	0.000	9900	0.0000
56	42	0.21250	0.3540	0.000	9900	0.0000
39	57	0.00000	1.3550	0.000	9900	0.9800
57	56	0.17400	0.2600	0.000	9900	0.0000
38	49	0.11500	0.1770	0.003	9900	0.0000
38	48	0.03120	0.0482	0.000	9900	0.0000
9	55	0.00000	0.1205	0.000	9900	0.9400

C.3 Generators

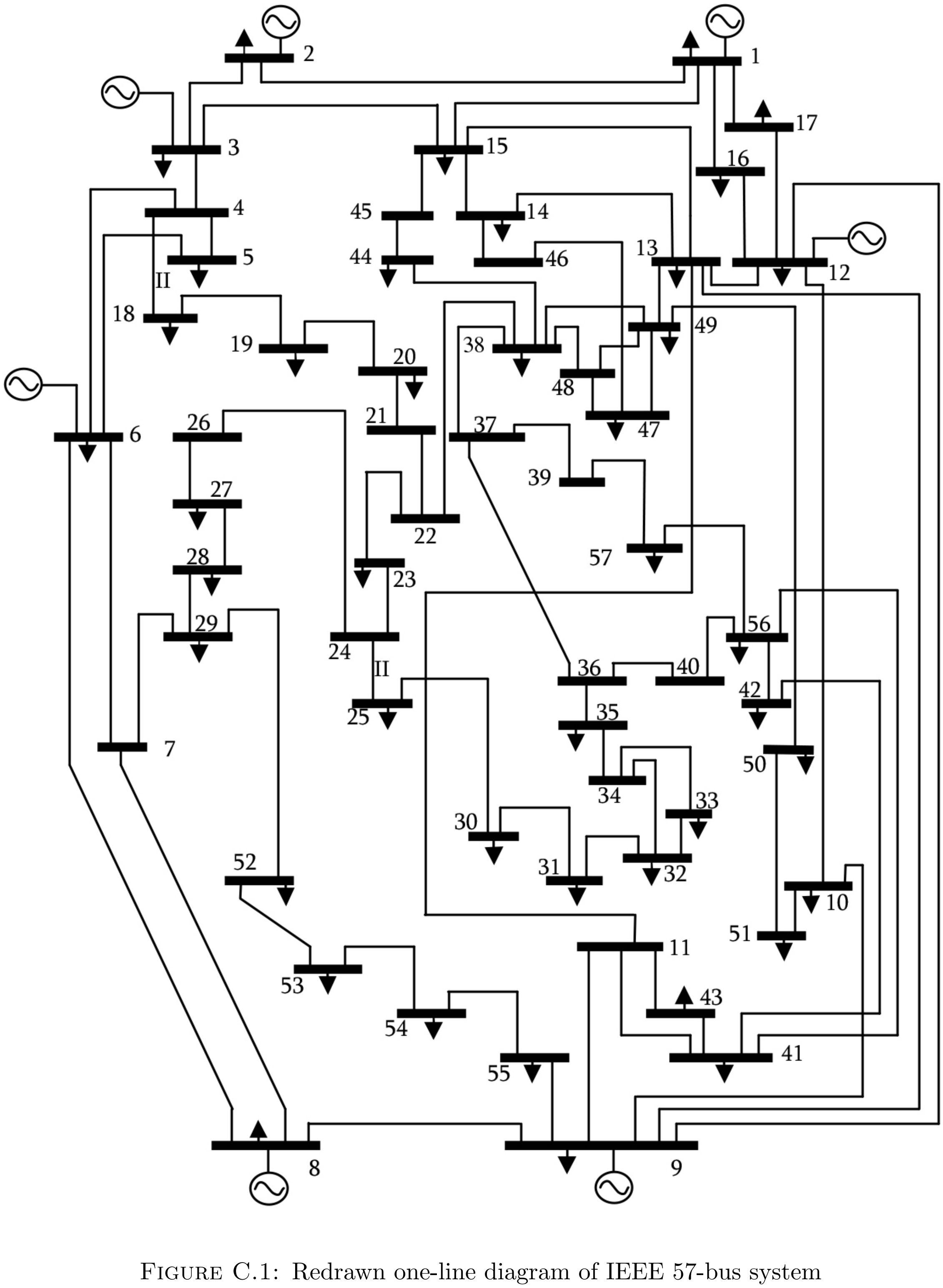

FIGURE C.1: Redrawn one-line diagram of IEEE 57-bus system

TABLE C.3: Data of generators of the IEEE 57-bus system

Bus ID	Initial P (MW)	$Q_{\max}$ (MVAr)	$Q_{\min}$ (MVAr)	Initial V_g (p.u.)	$P_{\max}$ (MW)	$P_{\min}$ (MW)	Coefficients		
							a	b	c
1	129	200	-140	1.04000	575.880	0	0	20	0.077580
2	0	50	-17	1.01000	100.000	0	0	40	0.010000
3	40	60	-10	0.98500	140.000	0	0	20	0.250000
6	0	25	-8	0.98000	100.000	0	0	40	0.010000
8	450	200	-140	1.00500	550.000	0	0	20	0.022222
9	0	9	-3	0.98000	100.000	0	0	40	0.010000
12	310	155	-150	1.01500	410.000	0	0	20	0.032258

Appendix D

Data of the IEEE 118-bus system

D.1 Bus Data

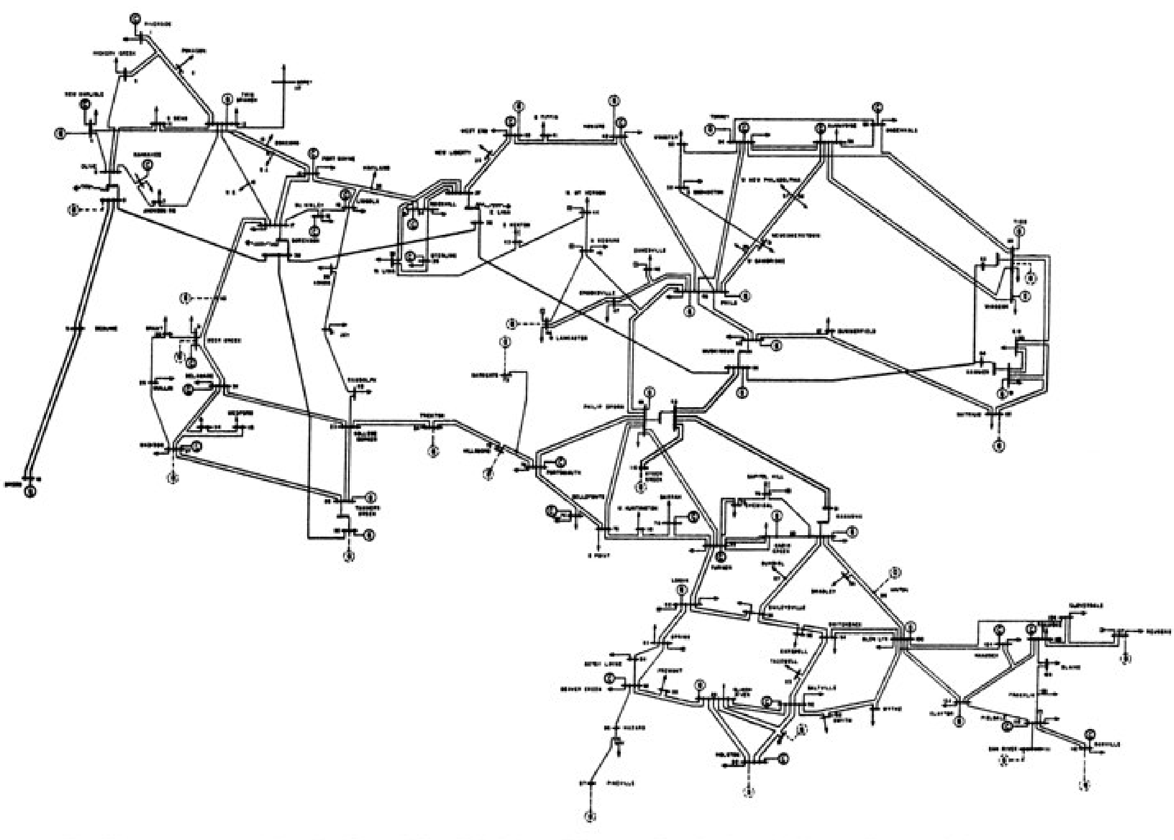

FIGURE D.1: One-line diagram of IEEE 118-bus system

Table D.1: Data of buses of the IEEE 118-bus system

Bus ID	Bus type	P_{load} (MW)	Q_{load} (MVAr)	Gs	Bs	Initial V_m (p.u.)	Initial V_a	baseKV	$V_{\max}$ (p.u.)	V_{min} (p.u)
1	2	51	27	0	0	0.955	10.67	138.00	1.06	0.94
2	1	20	9	0	0	0.971	11.22	138.00	1.06	0.94
3	1	39	10	0	0	0.968	11.56	138.00	1.06	0.94
4	2	39	12	0	0	0.998	15.28	138.00	1.06	0.94
5	1	0	0	0	-40	1.002	15.73	138.00	1.06	0.94
6	2	52	22	0	0	0.990	13.00	138.00	1.06	0.94
7	1	19	2	0	0	0.989	12.56	138.00	1.06	0.94
8	2	28	0	0	0	1.015	20.77	345.00	1.06	0.94
9	1	0	0	0	0	1.043	28.02	345.00	1.06	0.94
10	2	0	0	0	0	1.050	35.61	345.00	1.06	0.94
11	1	70	23	0	0	0.985	12.72	138.00	1.06	0.94
12	2	47	10	0	0	0.990	12.20	138.00	1.06	0.94
13	1	34	16	0	0	0.968	11.35	138.00	1.06	0.94
14	1	14	1	0	0	0.984	11.50	138.00	1.06	0.94
15	2	90	30	0	0	0.970	11.23	138.00	1.06	0.94
16	1	25	10	0	0	0.984	11.91	138.00	1.06	0.94
17	1	11	3	0	0	0.995	13.74	138.00	1.06	0.94
18	2	60	34	0	0	0.973	11.53	138.00	1.06	0.94
19	2	45	25	0	0	0.963	11.05	138.00	1.06	0.94
20	1	18	3	0	0	0.958	11.93	138.00	1.06	0.94
21	1	14	8	0	0	0.959	13.52	138.00	1.06	0.94
22	1	10	5	0	0	0.970	16.08	138.00	1.06	0.94
23	1	7	3	0	0	1.000	21.00	138.00	1.06	0.94
24	2	13	0	0	0	0.992	20.89	138.00	1.06	0.94
25	2	0	0	0	0	1.050	27.93	138.00	1.06	0.94
26	2	0	0	0	0	1.015	29.71	345.00	1.06	0.94
27	2	71	13	0	0	0.968	15.35	138.00	1.06	0.94
28	1	17	7	0	0	0.962	13.62	138.00	1.06	0.94

continued ...

Table D.1 Continued: Data of buses of the IEEE 118-bus system

Bus ID	Bus type	P_{load} (MW)	Q_{load} (MVAr)	Gs	Bs	Initial Vm (p.u.)	Initial Va	baseKV	$V_{\max}$ (p.u.)	V_{min} (p.u)
29	1	24	4	0	0	0.963	12.63	138.00	1.06	0.94
30	1	0	0	0	0	0.968	18.79	345.00	1.06	0.94
31	2	43	27	0	0	0.967	12.75	138.00	1.06	0.94
32	2	59	23	0	0	0.964	14.80	138.00	1.06	0.94
33	1	23	9	0	0	0.972	10.63	138.00	1.06	0.94
34	2	59	26	0	14	0.986	11.30	138.00	1.06	0.94
35	1	33	9	0	0	0.981	10.87	138.00	1.06	0.94
36	2	31	17	0	0	0.980	10.87	138.00	1.06	0.94
37	1	0	0	0	-25	0.992	11.77	138.00	1.06	0.94
38	1	0	0	0	0	0.962	16.91	345.00	1.06	0.94
39	1	27	11	0	0	0.970	8.41	138.00	1.06	0.94
40	2	66	23	0	0	0.970	7.35	138.00	1.06	0.94
41	1	37	10	0	0	0.967	6.92	138.00	1.06	0.94
42	2	96	23	0	0	0.985	8.53	138.00	1.06	0.94
43	1	18	7	0	0	0.978	11.28	138.00	1.06	0.94
44	1	16	8	0	10	0.985	13.82	138.00	1.06	0.94
45	1	53	22	0	10	0.987	15.67	138.00	1.06	0.94
46	2	28	10	0	10	1.005	18.49	138.00	1.06	0.94
47	1	34	0	0	0	1.017	20.73	138.00	1.06	0.94
48	1	20	11	0	15	1.021	19.93	138.00	1.06	0.94
49	2	87	30	0	0	1.025	20.94	138.00	1.06	0.94
50	1	17	4	0	0	1.001	18.90	138.00	1.06	0.94
51	1	17	8	0	0	0.967	16.28	138.00	1.06	0.94
52	1	18	5	0	0	0.957	15.32	138.00	1.06	0.94
53	1	23	11	0	0	0.946	14.35	138.00	1.06	0.94
54	2	113	32	0	0	0.955	15.26	138.00	1.06	0.94
55	2	63	22	0	0	0.952	14.97	138.00	1.06	0.94
56	2	84	18	0	0	0.954	15.16	138.00	1.06	0.94

continued . . .

Table D.1 Continued: Data of buses of the IEEE 118-bus system

Bus ID	Bus type	P_{load} (MW)	Q_{load} (MVAr)	Gs	Bs	Initial Vm (p.u.)	Initial Va	baseKV	$V_{\max}$ (p.u.)	V_{min} (p.u)
57	1	12	3	0	0	0.971	16.36	138.00	1.06	0.94
58	1	12	3	0	0	0.959	15.51	138.00	1.06	0.94
59	2	277	113	0	0	0.985	19.37	138.00	1.06	0.94
60	1	78	3	0	0	0.993	23.15	138.00	1.06	0.94
61	2	0	0	0	0	0.995	24.04	138.00	1.06	0.94
62	2	77	14	0	0	0.998	23.43	138.00	1.06	0.94
63	1	0	0	0	0	0.969	22.75	345.00	1.06	0.94
64	1	0	0	0	0	0.984	24.52	345.00	1.06	0.94
65	2	0	0	0	0	1.005	27.65	345.00	1.06	0.94
66	2	39	18	0	0	1.050	27.48	138.00	1.06	0.94
67	1	28	7	0	0	1.020	24.84	138.00	1.06	0.94
68	1	0	0	0	0	1.003	27.55	345.00	1.06	0.94
69	3	0	0	0	0	1.035	30.00	138.00	1.06	0.94
70	2	66	20	0	0	0.984	22.58	138.00	1.06	0.94
71	1	0	0	0	0	0.987	22.15	138.00	1.06	0.94
72	2	12	0	0	0	0.980	20.98	138.00	1.06	0.94
73	2	6	0	0	0	0.991	21.94	138.00	1.06	0.94
74	2	68	27	0	12	0.958	21.64	138.00	1.06	0.94
75	1	47	11	0	0	0.967	22.91	138.00	1.06	0.94
76	2	68	36	0	0	0.943	21.77	138.00	1.06	0.94
77	2	61	28	0	0	1.006	26.72	138.00	1.06	0.94
78	1	71	26	0	0	1.003	26.42	138.00	1.06	0.94
79	1	39	32	0	20	1.009	26.72	138.00	1.06	0.94
80	2	130	26	0	0	1.040	28.96	138.00	1.06	0.94
81	1	0	0	0	0	0.997	28.10	345.00	1.06	0.94
82	1	54	27	0	20	0.989	27.24	138.00	1.06	0.94
83	1	20	10	0	10	0.985	28.42	138.00	1.06	0.94
84	1	11	7	0	0	0.980	30.95	138.00	1.06	0.94

continued . . .

Table D.1 Continued: Data of buses of the IEEE 118-bus system

Bus ID	Bus type	P_{load} (MW)	Q_{load} (MVAr)	Gs	Bs	Initial Vm (p.u.)	Initial Va	baseKV	$V_{\max}$ (p.u.)	V_{min} (p.u)
85	2	24	15	0	0	0.985	32.51	138.00	1.06	0.94
86	1	21	10	0	0	0.987	31.14	138.00	1.06	0.94
87	2	0	0	0	0	1.015	31.40	161.00	1.06	0.94
88	1	48	10	0	0	0.987	35.64	138.00	1.06	0.94
89	2	0	0	0	0	1.005	39.69	138.00	1.06	0.94
90	2	163	42	0	0	0.985	33.29	138.00	1.06	0.94
91	2	10	0	0	0	0.980	33.31	138.00	1.06	0.94
92	2	65	10	0	0	0.993	33.80	138.00	1.06	0.94
93	1	12	7	0	0	0.987	30.79	138.00	1.06	0.94
94	1	30	16	0	0	0.991	28.64	138.00	1.06	0.94
95	1	42	31	0	0	0.981	27.67	138.00	1.06	0.94
96	1	38	15	0	0	0.993	27.51	138.00	1.06	0.94
97	1	15	9	0	0	1.011	27.88	138.00	1.06	0.94
98	1	34	8	0	0	1.024	27.40	138.00	1.06	0.94
99	2	42	0	0	0	1.010	27.04	138.00	1.06	0.94
100	2	37	18	0	0	1.017	28.03	138.00	1.06	0.94
101	1	22	15	0	0	0.993	29.61	138.00	1.06	0.94
102	1	5	3	0	0	0.991	32.30	138.00	1.06	0.94
103	2	23	16	0	0	1.001	24.44	138.00	1.06	0.94
104	2	38	25	0	0	0.971	21.69	138.00	1.06	0.94
105	2	31	26	0	20	0.965	20.57	138.00	1.06	0.94
106	1	43	16	0	0	0.962	20.32	138.00	1.06	0.94
107	2	50	12	0	6	0.952	17.53	138.00	1.06	0.94
108	1	2	1	0	0	0.967	19.38	138.00	1.06	0.94
109	1	8	3	0	0	0.967	18.93	138.00	1.06	0.94
110	2	39	30	0	6	0.973	18.09	138.00	1.06	0.94
111	2	0	0	0	0	0.980	19.74	138.00	1.06	0.94
112	2	68	13	0	0	0.975	14.99	138.00	1.06	0.94

continued . . .

Table D.1 Continued: Data of buses of the IEEE 118-bus system

Bus ID	Bus type	P_{load} (MW)	Q_{load} (MVAr)	Gs	Bs	Initial Vm (p.u.)	Initial Va	baseKV	$V_{\max}$ (p.u.)	V_{min} (p.u)
113	2	6	0	0	0	0.993	13.74	138.00	1.06	0.94
114	1	8	3	0	0	0.960	14.46	138.00	1.06	0.94
115	1	22	7	0	0	0.960	14.46	138.00	1.06	0.94
116	2	184	0	0	0	1.005	27.12	138.00	1.06	0.94
117	1	20	8	0	0	0.974	10.67	138.00	1.06	0.94
118	1	33	15	0	0	0.949	21.92	138.00	1.06	0.94

D.2 Transmission lines

TABLE D.2: Data of transformers and transmission lines of IEEE 118-bus system

From bus	To bus	R (p.u.)	X (p.u.)	B (p.u.)	$S_{li}^{\max}$ (MVA)	Transformer tap
1	2	0.03030	0.0999	0.025	9900	0.0000
1	3	0.01290	0.0424	0.011	9900	0.0000
4	5	0.00176	0.0080	0.002	9900	0.0000
3	5	0.02410	0.1080	0.028	9900	0.0000
5	6	0.01190	0.0540	0.014	9900	0.0000
6	7	0.00459	0.0208	0.006	9900	0.0000
8	9	0.00244	0.0305	1.162	9900	0.0000
8	5	0.00000	0.0267	0.000	9900	0.9850
9	10	0.00258	0.0322	1.230	9900	0.0000
4	11	0.02090	0.0688	0.017	9900	0.0000
5	11	0.02030	0.0682	0.017	9900	0.0000
11	12	0.00595	0.0196	0.005	9900	0.0000
2	12	0.01870	0.0616	0.016	9900	0.0000
3	12	0.04840	0.1600	0.041	9900	0.0000
7	12	0.00862	0.0340	0.009	9900	0.0000

continued . . .

Table D.2 Continued: Data of transformers and transmission lines of IEEE 118-bus system

From bus	To bus	R (p.u.)	X (p.u.)	B (p.u.)	$S_{li}^{\max}$ (MVA)	Transformer tap
11	13	0.02225	0.0731	0.019	9900	0.0000
12	14	0.02150	0.0707	0.018	9900	0.0000
13	15	0.07440	0.2444	0.063	9900	0.0000
14	15	0.05950	0.1950	0.050	9900	0.0000
12	16	0.02120	0.0834	0.021	9900	0.0000
15	17	0.01320	0.0437	0.044	9900	0.0000
16	17	0.04540	0.1801	0.047	9900	0.0000
17	18	0.01230	0.0505	0.013	9900	0.0000
18	19	0.01119	0.0493	0.011	9900	0.0000
19	20	0.02520	0.1170	0.030	9900	0.0000
15	19	0.01200	0.0394	0.010	9900	0.0000
20	21	0.01830	0.0849	0.022	9900	0.0000
21	22	0.02090	0.0970	0.025	9900	0.0000
22	23	0.03420	0.1590	0.040	9900	0.0000
23	24	0.01350	0.0492	0.050	9900	0.0000
23	25	0.01560	0.0800	0.086	9900	0.0000
26	25	0.00000	0.0382	0.000	9900	0.9600
25	27	0.03180	0.1630	0.176	9900	0.0000
27	28	0.01913	0.0855	0.022	9900	0.0000
28	29	0.02370	0.0943	0.024	9900	0.0000
30	17	0.00000	0.0388	0.000	9900	0.9600
8	30	0.00431	0.0504	0.514	9900	0.0000
26	30	0.00799	0.0860	0.908	9900	0.0000
17	31	0.04740	0.1563	0.040	9900	0.0000
29	31	0.01080	0.0331	0.008	9900	0.0000
23	32	0.03170	0.1153	0.117	9900	0.0000
31	32	0.02980	0.0985	0.025	9900	0.0000

continued . . .

Table D.2 Continued: Data of transformers and transmission lines of IEEE 118-bus system

From bus	To bus	R (p.u.)	X (p.u.)	B (p.u.)	$S_{li}^{\max}$ (MVA)	Transformer tap
27	32	0.02290	0.0755	0.019	9900	0.0000
15	33	0.03800	0.1244	0.032	9900	0.0000
19	34	0.07520	0.2470	0.063	9900	0.0000
35	36	0.00224	0.0102	0.003	9900	0.0000
35	37	0.01100	0.0497	0.013	9900	0.0000
33	37	0.04150	0.1420	0.037	9900	0.0000
34	36	0.00871	0.0268	0.006	9900	0.0000
34	37	0.00256	0.0094	0.010	9900	0.0000
38	37	0.00000	0.0375	0.000	9900	0.9350
37	39	0.03210	0.1060	0.027	9900	0.0000
37	40	0.05930	0.1680	0.042	9900	0.0000
30	38	0.00464	0.0540	0.422	9900	0.0000
39	40	0.01840	0.0605	0.016	9900	0.0000
40	41	0.01450	0.0487	0.012	9900	0.0000
40	42	0.05550	0.1830	0.047	9900	0.0000
41	42	0.04100	0.1350	0.034	9900	0.0000
43	44	0.06080	0.2454	0.061	9900	0.0000
34	43	0.04130	0.1681	0.042	9900	0.0000
44	45	0.02240	0.0901	0.022	9900	0.0000
45	46	0.04000	0.1356	0.033	9900	0.0000
46	47	0.03800	0.1270	0.032	9900	0.0000
46	48	0.06010	0.1890	0.047	9900	0.0000
47	49	0.01910	0.0625	0.016	9900	0.0000
42	49	0.07150	0.3230	0.086	9900	0.0000
42	49	0.07150	0.3230	0.086	9900	0.0000
45	49	0.06840	0.1860	0.044	9900	0.0000
48	49	0.01790	0.0505	0.013	9900	0.0000

continued . . .

Table D.2 Continued: Data of transformers and transmission lines of IEEE 118-bus system

From bus	To bus	R (p.u.)	X (p.u.)	B (p.u.)	$S_{li}^{\max}$ (MVA)	Transformer tap
49	50	0.02670	0.0752	0.019	9900	0.0000
49	51	0.04860	0.1370	0.034	9900	0.0000
51	52	0.02030	0.0588	0.014	9900	0.0000
52	53	0.04050	0.1635	0.041	9900	0.0000
53	54	0.02630	0.1220	0.031	9900	0.0000
49	54	0.07300	0.2890	0.074	9900	0.0000
49	54	0.08690	0.2910	0.073	9900	0.0000
54	55	0.01690	0.0707	0.020	9900	0.0000
54	56	0.00275	0.0096	0.007	9900	0.0000
55	56	0.00488	0.0151	0.004	9900	0.0000
56	57	0.03430	0.0966	0.024	9900	0.0000
50	57	0.04740	0.1340	0.033	9900	0.0000
56	58	0.03430	0.0966	0.024	9900	0.0000
51	58	0.02550	0.0719	0.018	9900	0.0000
54	59	0.05030	0.2293	0.060	9900	0.0000
56	59	0.08250	0.2510	0.057	9900	0.0000
56	59	0.08030	0.2390	0.054	9900	0.0000
55	59	0.04739	0.2158	0.056	9900	0.0000
59	60	0.03170	0.1450	0.038	9900	0.0000
59	61	0.03280	0.1500	0.039	9900	0.0000
60	61	0.00264	0.0135	0.015	9900	0.0000
60	62	0.01230	0.0561	0.015	9900	0.0000
61	62	0.00824	0.0376	0.010	9900	0.0000
63	59	0.00000	0.0386	0.000	9900	0.9600
63	64	0.00172	0.0200	0.216	9900	0.0000
64	61	0.00000	0.0268	0.000	9900	0.9850
38	65	0.00901	0.0986	1.046	9900	0.0000

continued . . .

Table D.2 Continued: Data of transformers and transmission lines of IEEE 118-bus system

From bus	To bus	R (p.u.)	X (p.u.)	B (p.u.)	$S_{li}^{\max}$ (MVA)	Transformer tap
64	65	0.00269	0.0302	0.380	9900	0.0000
49	66	0.01800	0.0919	0.025	9900	0.0000
49	66	0.01800	0.0919	0.025	9900	0.0000
62	66	0.04820	0.2180	0.058	9900	0.0000
62	67	0.02580	0.1170	0.031	9900	0.0000
65	66	0.00000	0.0370	0.000	9900	0.9350
66	67	0.02240	0.1015	0.027	9900	0.0000
65	68	0.00138	0.0160	0.638	9900	0.0000
47	69	0.08440	0.2778	0.071	9900	0.0000
49	69	0.09850	0.3240	0.083	9900	0.0000
68	69	0.00000	0.0370	0.000	9900	0.9350
69	70	0.03000	0.1270	0.122	9900	0.0000
24	70	0.00221	0.4115	0.102	9900	0.0000
70	71	0.00882	0.0355	0.009	9900	0.0000
24	72	0.04880	0.1960	0.049	9900	0.0000
71	72	0.04460	0.1800	0.044	9900	0.0000
71	73	0.00866	0.0454	0.012	9900	0.0000
70	74	0.04010	0.1323	0.034	9900	0.0000
70	75	0.04280	0.1410	0.036	9900	0.0000
69	75	0.04050	0.1220	0.124	9900	0.0000
74	75	0.01230	0.0406	0.010	9900	0.0000
76	77	0.04440	0.1480	0.037	9900	0.0000
69	77	0.03090	0.1010	0.104	9900	0.0000
75	77	0.06010	0.1999	0.050	9900	0.0000
77	78	0.00376	0.0124	0.013	9900	0.0000
78	79	0.00546	0.0244	0.006	9900	0.0000
77	80	0.01700	0.0485	0.047	9900	0.0000

continued ...

Table D.2 Continued: Data of transformers and transmission lines of IEEE 118-bus system

From bus	To bus	R (p.u.)	X (p.u.)	B (p.u.)	$S_{li}^{\max}$ (MVA)	Transformer tap
77	80	0.02940	0.1050	0.023	9900	0.0000
79	80	0.01560	0.0704	0.019	9900	0.0000
68	81	0.00175	0.0202	0.808	9900	0.0000
81	80	0.00000	0.0370	0.000	9900	0.9350
77	82	0.02980	0.0853	0.082	9900	0.0000
82	83	0.01120	0.0367	0.038	9900	0.0000
83	84	0.06250	0.1320	0.026	9900	0.0000
83	85	0.04300	0.1480	0.035	9900	0.0000
84	85	0.03020	0.0641	0.012	9900	0.0000
85	86	0.03500	0.1230	0.028	9900	0.0000
86	87	0.02828	0.2074	0.045	9900	0.0000
85	88	0.02000	0.1020	0.028	9900	0.0000
85	89	0.02390	0.1730	0.047	9900	0.0000
88	89	0.01390	0.0712	0.019	9900	0.0000
89	90	0.05180	0.1880	0.053	9900	0.0000
89	90	0.02380	0.0997	0.106	9900	0.0000
90	91	0.02540	0.0836	0.021	9900	0.0000
89	92	0.00990	0.0505	0.055	9900	0.0000
89	92	0.03930	0.1581	0.041	9900	0.0000
91	92	0.03870	0.1272	0.033	9900	0.0000
92	93	0.02580	0.0848	0.022	9900	0.0000
92	94	0.04810	0.1580	0.041	9900	0.0000
93	94	0.02230	0.0732	0.019	9900	0.0000
94	95	0.01320	0.0434	0.011	9900	0.0000
80	96	0.03560	0.1820	0.049	9900	0.0000
82	96	0.01620	0.0530	0.054	9900	0.0000
94	96	0.02690	0.0869	0.023	9900	0.0000

continued . . .

Table D.2 Continued: Data of transformers and transmission lines of IEEE 118-bus system

From bus	To bus	R (p.u.)	X (p.u.)	B (p.u.)	$S_{li}^{\max}$ (MVA)	Transformer tap
80	97	0.01830	0.0934	0.025	9900	0.0000
80	98	0.02380	0.1080	0.029	9900	0.0000
80	99	0.04540	0.2060	0.055	9900	0.0000
92	100	0.06480	0.2950	0.047	9900	0.0000
94	100	0.01780	0.0580	0.060	9900	0.0000
95	96	0.01710	0.0547	0.015	9900	0.0000
96	97	0.01730	0.0885	0.024	9900	0.0000
98	100	0.03970	0.1790	0.048	9900	0.0000
99	100	0.01800	0.0813	0.022	9900	0.0000
100	101	0.02770	0.1262	0.033	9900	0.0000
92	102	0.01230	0.0559	0.015	9900	0.0000
101	102	0.02460	0.1120	0.029	9900	0.0000
100	103	0.01600	0.0525	0.054	9900	0.0000
100	104	0.04510	0.2040	0.054	9900	0.0000
103	104	0.04660	0.1584	0.041	9900	0.0000
103	105	0.05350	0.1625	0.041	9900	0.0000
100	106	0.06050	0.2290	0.062	9900	0.0000
104	105	0.00994	0.0378	0.010	9900	0.0000
105	106	0.01400	0.0547	0.014	9900	0.0000
105	107	0.05300	0.1830	0.047	9900	0.0000
105	108	0.02610	0.0703	0.018	9900	0.0000
106	107	0.05300	0.1830	0.047	9900	0.0000
108	109	0.01050	0.0288	0.008	9900	0.0000
103	110	0.03906	0.1813	0.046	9900	0.0000
109	110	0.02780	0.0762	0.020	9900	0.0000
110	111	0.02200	0.0755	0.020	9900	0.0000
110	112	0.02470	0.0640	0.062	9900	0.0000

continued . . .

Table D.2 Continued: Data of transformers and transmission lines of IEEE 118-bus system

From bus	To bus	R (p.u.)	X (p.u.)	B (p.u.)	$S_{li}^{\max}$ (MVA)	Transformer tap
17	113	0.00913	0.0301	0.008	9900	0.0000
32	113	0.06150	0.2030	0.052	9900	0.0000
32	114	0.01350	0.0612	0.016	9900	0.0000
27	115	0.01640	0.0741	0.020	9900	0.0000
114	115	0.00230	0.0104	0.003	9900	0.0000
68	116	0.00034	0.0041	0.164	9900	0.0000
12	117	0.03290	0.1400	0.036	9900	0.0000
75	118	0.01450	0.0481	0.012	9900	0.0000
76	118	0.01640	0.0544	0.014	9900	0.0000

D.3 Generators

Table D.3: Data of generators of the IEEE 118-bus system

Bus ID	Initial P (MW)	$Q_{\max}$ (MVAr)	$Q_{\min}$ (MVAr)	Initial V_g (p.u.)	$P_{\max}$ (MW)	$P_{\min}$ (MW)	Coefficients a	b	c
1	0	15	-5	0.95500	100.000	0	0	40	0.010000
4	0	300	-300	0.99800	100.000	0	0	40	0.010000
6	0	50	-13	0.99000	100.000	0	0	40	0.010000
8	0	300	-300	1.01500	100.000	0	0	40	0.010000
10	450	200	-147	1.05000	550.000	0	0	20	0.022222
12	85	120	-35	0.99000	185.000	0	0	20	0.117647
15	0	30	-10	0.97000	100.000	0	0	40	0.010000
18	0	50	-16	0.97300	100.000	0	0	40	0.010000
19	0	24	-8	0.96200	100.000	0	0	40	0.010000
24	0	300	-300	0.99200	100.000	0	0	40	0.010000
25	220	140	-47	1.05000	320.000	0	0	20	0.045455
26	314	1000	-1000	1.01500	414.000	0	0	20	0.031847

continued . . .

Table D.3 Continued: Data of generators of the IEEE 118-bus system

Bus ID	Initial P (MW)	$Q_{\max}$ (MVAr)	$Q_{\min}$ (MVAr)	Initial V_g (p.u.)	$P_{\max}$ (MW)	$P_{\min}$ (MW)	Coefficients		
							a	b	c
27	0	300	-300	0.96800	100.000	0	0	40	0.010000
31	7	300	-300	0.96700	107.000	0	0	20	1.428570
32	0	42	-14	0.96300	100.000	0	0	40	0.010000
34	0	24	-8	0.98400	100.000	0	0	40	0.010000
36	0	24	-8	0.98000	100.000	0	0	40	0.010000
40	0	300	-300	0.97000	100.000	0	0	40	0.010000
42	0	300	-300	0.98500	100.000	0	0	40	0.010000
46	19	100	-100	1.00500	119.000	0	0	20	0.526316
49	204	210	-85	1.02500	304.000	0	0	20	0.049020
54	48	300	-300	0.95500	148.000	0	0	20	0.208333
55	0	23	-8	0.95200	100.000	0	0	40	0.010000
56	0	15	-8	0.95400	100.000	0	0	40	0.010000
59	155	180	-60	0.98500	255.000	0	0	20	0.064516
61	160	300	-100	0.99500	260.000	0	0	20	0.062500
62	0	20	-20	0.99800	100.000	0	0	40	0.010000
65	391	200	-67	1.00500	491.000	0	0	20	0.025575
66	392	200	-67	1.05000	492.000	0	0	20	0.025510
69	516	300	-300	1.03500	805.200	0	0	20	0.019365
70	0	32	-10	0.98400	100.000	0	0	40	0.010000
72	0	100	-100	0.98000	100.000	0	0	40	0.010000
73	0	100	-100	0.99100	100.000	0	0	40	0.010000
74	0	9	-6	0.95800	100.000	0	0	40	0.010000
76	0	23	-8	0.94300	100.000	0	0	40	0.010000
77	0	70	-20	1.00600	100.000	0	0	40	0.010000
80	477	280	-165	1.04000	577.000	0	0	20	0.020964
85	0	23	-8	0.98500	100.000	0	0	40	0.010000
87	4	1000	-100	1.01500	104.000	0	0	20	2.500000
89	607	300	-210	1.00500	707.000	0	0	20	0.016475

continued . . .

Table D.3 Continued: Data of generators of the IEEE 118-bus system

Bus ID	Initial P (MW)	$Q_{\max}$ (MVAr)	$Q_{\min}$ (MVAr)	Initial V_g (p.u.)	$P_{\max}$ (MW)	$P_{\min}$ (MW)	Coefficients a	b	c
90	0	300	-300	0.98500	100.000	0	0	40	0.010000
91	0	100	-100	0.98000	100.000	0	0	40	0.010000
92	0	9	-3	0.99000	100.000	0	0	40	0.010000
99	0	100	-100	1.01000	100.000	0	0	40	0.010000
100	252	155	-50	1.01700	352.000	0	0	20	0.039683
103	40	40	-15	1.01000	140.000	0	0	20	0.250000
104	0	23	-8	0.97100	100.000	0	0	40	0.010000
105	0	23	-8	0.96500	100.000	0	0	40	0.010000
107	0	200	-200	0.95200	100.000	0	0	40	0.010000
110	0	23	-8	0.97300	100.000	0	0	40	0.010000
111	36	1000	-100	0.98000	136.000	0	0	20	0.277778
112	0	1000	-100	0.97500	100.000	0	0	40	0.010000
113	0	200	-100	0.99300	100.000	0	0	40	0.010000
116	0	1000	-1000	1.00500	100.000	0	0	40	0.010000

Appendix E

Data of the IEEE 300-bus system

E.1 Bus Data

Table E.1: Data of buses of the IEEE 300-bus system

Bus ID	Bus type	P_{load} (MW)	Q_{load} (MVAr)	Gs	Bs	Initial V_m (p.u.)	Initial V_a	baseKV	$V_{\max}$ (p.u.)	V_{min} (p.u)
1	1	90	49	0	0	1.028	5.95	115.00	1.06	0.94
2	1	56	15	0	0	1.035	7.74	115.00	1.06	0.94
3	1	20	0	0	0	0.997	6.64	230.00	1.06	0.94
4	1	0	0	0	0	1.031	4.71	345.00	1.06	0.94
5	1	353	130	0	0	1.019	4.68	115.00	1.06	0.94
6	1	120	41	0	0	1.031	6.99	115.00	1.06	0.94
7	1	0	0	0	0	0.993	6.19	230.00	1.06	0.94
8	2	63	14	0	0	1.015	2.40	115.00	1.06	0.94
9	1	96	43	0	0	1.003	2.85	115.00	1.06	0.94
10	2	153	33	0	0	1.021	1.35	230.00	1.06	0.94
11	1	83	21	0	0	1.006	2.46	115.00	1.06	0.94
12	1	0	0	0	0	0.997	5.21	230.00	1.06	0.94
13	1	58	10	0	0	0.998	-0.55	115.00	1.06	0.94
14	1	160	60	0	0	0.999	-4.81	115.00	1.06	0.94

continued ...

Table E.1 Continued: Data of buses of the IEEE 300-bus system

Bus ID	Bus type	P_{load} (MW)	Q_{load} (MVAr)	Gs	Bs	Initial Vm (p.u.)	Initial Va	baseKV	$V_{\max}$ (p.u.)	V_{min} (p.u)
15	1	127	23	0	0	1.034	-8.59	115.00	1.06	0.94
16	1	0	0	0	0	1.032	-2.65	345.00	1.06	0.94
17	1	561	220	0	0	1.065	-13.10	115.00	1.06	0.94
19	1	0	0	0	0	0.982	1.08	230.00	1.06	0.94
20	2	605	120	0	0	1.001	-2.46	115.00	1.06	0.94
21	1	77	1	0	0	0.975	1.62	230.00	1.06	0.94
22	1	81	23	0	0	0.996	-1.97	115.00	1.06	0.94
23	1	21	7	0	0	1.050	3.94	115.00	1.06	0.94
24	1	0	0	0	0	1.006	6.02	230.00	1.06	0.94
25	1	45	12	0	0	1.023	1.44	115.00	1.06	0.94
26	1	28	9	0	0	0.999	-1.73	115.00	1.06	0.94
27	1	69	13	0	0	0.975	-4.90	115.00	1.06	0.94
33	1	55	6	0	0	1.024	-12.02	115.00	1.06	0.94
34	1	0	0	0	0	1.041	-7.94	345.00	1.06	0.94
35	1	0	0	0	0	0.976	-25.72	115.00	1.06	0.94
36	1	0	0	0	0	1.001	-22.59	230.00	1.06	0.94
37	1	85	32	0	0	1.020	-11.23	115.00	1.06	0.94
38	1	155	18	0	0	1.020	-12.56	115.00	1.06	0.94
39	1	0	0	0	0	1.054	-5.81	345.00	1.06	0.94
40	1	46	-21	0	0	1.022	-12.78	115.00	1.06	0.94
41	1	86	0	0	0	1.029	-10.45	115.00	1.06	0.94
42	1	0	0	0	0	1.045	-7.44	345.00	1.06	0.94
43	1	39	9	0	0	1.001	-16.79	115.00	1.06	0.94
44	1	195	29	0	0	1.009	-17.47	115.00	1.06	0.94
45	1	0	0	0	0	1.022	-14.74	230.00	1.06	0.94
46	1	0	0	0	0	1.034	-11.75	345.00	1.06	0.94
47	1	58	12	0	0	0.978	-23.17	115.00	1.06	0.94
48	1	41	19	0	0	1.002	-16.09	115.00	1.06	0.94

continued . . .

Table E.1 Continued: Data of buses of the IEEE 300-bus system

Bus ID	Bus type	P_{load} (MW)	Q_{load} (MVAr)	Gs	Bs	Initial Vm (p.u.)	Initial Va	baseKV	$V_{\max}$ (p.u.)	V_{min} (p.u)
49	1	92	26	0	0	1.048	-2.95	115.00	1.06	0.94
51	1	-5	5	0	0	1.025	-8.15	115.00	1.06	0.94
52	1	61	28	0	0	0.998	-11.86	115.00	1.06	0.94
53	1	69	3	0	0	0.996	-17.60	115.00	1.06	0.94
54	1	10	1	0	0	1.005	-16.25	115.00	1.06	0.94
55	1	22	10	0	0	1.015	-12.21	115.00	1.06	0.94
57	1	98	20	0	0	1.034	-8.00	115.00	1.06	0.94
58	1	14	1	0	0	0.992	-5.99	115.00	1.06	0.94
59	1	218	106	0	0	0.979	-5.29	115.00	1.06	0.94
60	1	0	0	0	0	1.025	-9.56	230.00	1.06	0.94
61	1	227	110	0	0	0.991	-3.47	115.00	1.06	0.94
62	1	0	0	0	0	1.016	-1.10	230.00	1.06	0.94
63	2	70	30	0	0	0.958	-17.62	115.00	1.06	0.94
64	1	0	0	0	0	0.948	-12.97	230.00	1.06	0.94
69	1	0	0	0	0	0.963	-25.66	115.00	1.06	0.94
70	1	56	20	0	0	0.951	-35.16	115.00	1.06	0.94
71	1	116	38	0	0	0.979	-29.88	115.00	1.06	0.94
72	1	57	19	0	0	0.970	-27.48	115.00	1.06	0.94
73	1	224	71	0	0	0.978	-25.77	115.00	1.06	0.94
74	1	0	0	0	0	0.996	-22.00	230.00	1.06	0.94
76	2	208	107	0	0	0.963	-26.54	115.00	1.06	0.94
77	1	74	28	0	0	0.984	-24.94	115.00	1.06	0.94
78	1	0	0	0	0	0.990	-24.05	115.00	1.06	0.94
79	1	48	14	0	0	0.982	-24.97	115.00	1.06	0.94
80	1	28	7	0	0	0.987	-24.97	115.00	1.06	0.94
81	1	0	0	0	0	1.034	-18.89	345.00	1.06	0.94
84	2	37	13	0	0	1.025	-17.16	115.00	1.06	0.94
85	1	0	0	0	0	0.987	-17.68	230.00	1.06	0.94

continued . . .

Table E.1 Continued: Data of buses of the IEEE 300-bus system

Bus ID	Bus type	P_{load} (MW)	Q_{load} (MVAr)	Gs	Bs	Initial Vm (p.u.)	Initial Va	baseKV	$V_{\max}$ (p.u.)	V_{min} (p.u)
86	1	0	0	0	0	0.991	-14.19	230.00	1.06	0.94
87	1	0	0	0	0	0.992	-7.77	230.00	1.06	0.94
88	1	0	0	0	0	1.015	-20.96	230.00	1.06	0.94
89	1	44	0	0	0	1.032	-11.13	115.00	1.06	0.94
90	1	66	0	0	0	1.027	-11.23	115.00	1.06	0.94
91	2	17	0	0	0	1.052	-9.40	115.00	1.06	0.94
92	2	16	0	0	0	1.052	-6.20	115.00	1.06	0.94
94	1	60	0	0	0	0.993	-9.42	115.00	1.06	0.94
97	1	40	0	0	0	1.018	-13.24	115.00	1.06	0.94
98	2	67	0	0	0	1.000	-14.60	115.00	1.06	0.94
99	1	84	0	0	0	0.989	-20.27	115.00	1.06	0.94
100	1	0	0	0	0	1.006	-14.45	115.00	1.06	0.94
102	1	78	0	0	0	1.001	-15.23	115.00	1.06	0.94
103	1	32	0	0	0	1.029	-12.06	115.00	1.06	0.94
104	1	9	0	0	0	0.996	-17.33	115.00	1.06	0.94
105	1	50	0	0	0	1.022	-12.94	115.00	1.06	0.94
107	1	5	0	0	0	1.010	-16.03	115.00	1.06	0.94
108	2	112	0	0	0	0.990	-20.26	115.00	1.06	0.94
109	1	31	0	0	0	0.975	-26.06	115.00	1.06	0.94
110	1	63	0	0	0	0.973	-24.72	115.00	1.06	0.94
112	1	20	0	0	0	0.973	-28.69	115.00	1.06	0.94
113	1	26	0	0	0	0.970	-25.38	115.00	1.06	0.94
114	1	18	0	0	0	0.975	-28.59	115.00	1.06	0.94
115	1	0	0	0	0	0.960	-13.57	115.00	1.06	0.94
116	1	0	0	0	0	1.025	-12.69	115.00	1.06	0.94
117	1	0	0	0	325	0.935	-4.72	115.00	1.06	0.94
118	1	14	650	0	0	0.930	-4.12	115.00	1.06	0.94
119	2	0	0	0	0	1.044	5.17	115.00	1.06	0.94

continued . . .

Table E.1 Continued: Data of buses of the IEEE 300-bus system

Bus ID	Bus type	P_{load} (MW)	Q_{load} (MVAr)	Gs	Bs	Initial Vm (p.u.)	Initial Va	baseKV	$V_{\max}$ (p.u.)	V_{min} (p.u)
120	1	777	215	0	55	0.958	-8.77	115.00	1.06	0.94
121	1	535	55	0	0	0.987	-12.64	115.00	1.06	0.94
122	1	229	12	0	0	0.973	-14.36	115.00	1.06	0.94
123	1	78	1	0	0	1.001	-17.64	115.00	1.06	0.94
124	2	276	59	0	0	1.023	-13.49	115.00	1.06	0.94
125	2	515	83	0	0	1.010	-18.43	115.00	1.06	0.94
126	1	58	5	0	0	0.998	-12.86	115.00	1.06	0.94
127	1	381	37	0	0	1.000	-10.52	230.00	1.06	0.94
128	1	0	0	0	0	1.002	-4.78	230.00	1.06	0.94
129	1	0	0	0	0	1.003	-4.40	230.00	1.06	0.94
130	1	0	0	0	0	1.019	5.56	230.00	1.06	0.94
131	1	0	0	0	0	0.986	6.06	230.00	1.06	0.94
132	1	0	0	0	0	1.005	3.04	230.00	1.06	0.94
133	1	0	0	0	0	1.002	-5.46	230.00	1.06	0.94
134	1	0	0	0	0	1.022	-8.04	230.00	1.06	0.94
135	1	169	42	0	0	1.019	-6.76	230.00	1.06	0.94
136	1	55	18	0	0	1.048	1.54	230.00	1.06	0.94
137	1	274	100	0	0	1.047	-1.45	230.00	1.06	0.94
138	2	1019	135	0	0	1.055	-6.35	230.00	1.06	0.94
139	1	595	83	0	0	1.012	-3.57	115.00	1.06	0.94
140	1	388	115	0	0	1.043	-3.44	230.00	1.06	0.94
141	2	145	58	0	0	1.051	0.05	230.00	1.06	0.94
142	1	57	25	0	0	1.016	-2.77	230.00	1.06	0.94
143	2	90	36	0	0	1.044	4.03	230.00	1.06	0.94
144	1	0	0	0	0	1.016	-0.70	230.00	1.06	0.94
145	1	24	14	0	0	1.008	-0.16	230.00	1.06	0.94
146	2	0	0	0	0	1.053	4.32	230.00	1.06	0.94
147	2	0	0	0	0	1.053	8.36	230.00	1.06	0.94

continued . . .

Table E.1 Continued: Data of buses of the IEEE 300-bus system

Bus ID	Bus type	P_{load} (MW)	Q_{load} (MVAr)	Gs	Bs	Initial Vm (p.u.)	Initial Va	baseKV	$V_{\max}$ (p.u.)	V_{min} (p.u)
148	1	63	25	0	0	1.058	0.28	230.00	1.06	0.94
149	2	0	0	0	0	1.074	5.23	230.00	1.06	0.94
150	1	0	0	0	0	0.987	6.34	230.00	1.06	0.94
151	1	0	0	0	0	1.005	4.13	230.00	1.06	0.94
152	2	17	9	0	0	1.054	9.24	230.00	1.06	0.94
153	2	0	0	0	0	1.044	10.46	230.00	1.06	0.94
154	1	70	5	0	35	0.966	-1.80	115.00	1.06	0.94
155	1	200	50	0	0	1.018	6.75	230.00	1.06	0.94
156	2	75	50	0	0	0.963	5.15	115.00	1.06	0.94
157	1	124	-24	0	0	0.985	-11.93	230.00	1.06	0.94
158	1	0	0	0	0	0.999	-11.40	230.00	1.06	0.94
159	1	33	17	0	0	0.987	-9.82	230.00	1.06	0.94
160	1	0	0	0	0	1.000	-12.55	230.00	1.06	0.94
161	1	35	15	0	0	1.036	8.85	230.00	1.06	0.94
162	1	85	24	0	0	0.992	18.50	230.00	1.06	0.94
163	1	0	0	0	0	1.041	2.91	230.00	1.06	0.94
164	1	0	0	0	-212	0.984	9.66	230.00	1.06	0.94
165	1	0	0	0	0	1.000	26.31	230.00	1.06	0.94
166	1	0	0	0	-103	0.997	30.22	230.00	1.06	0.94
167	1	300	96	0	0	0.972	-6.91	230.00	1.06	0.94
168	1	0	0	0	0	1.002	-4.80	230.00	1.06	0.94
169	1	0	0	0	0	0.988	-6.68	230.00	1.06	0.94
170	2	482	205	0	0	0.929	0.09	115.00	1.06	0.94
171	2	764	291	0	0	0.983	-9.94	115.00	1.06	0.94
172	1	27	0	0	0	1.024	-6.22	115.00	1.06	0.94
173	1	164	43	0	53	0.984	-12.75	115.00	1.06	0.94
174	1	0	0	0	0	1.062	-2.69	115.00	1.06	0.94
175	1	176	83	0	0	0.973	-7.21	115.00	1.06	0.94

continued ...

Table E.1 Continued: Data of buses of the IEEE 300-bus system

Bus ID	Bus type	P_{load} (MW)	Q_{load} (MVAr)	Gs	Bs	Initial Vm (p.u.)	Initial Va	baseKV	$V_{\max}$ (p.u.)	V_{min} (p.u)
176	2	5	4	0	0	1.052	4.67	115.00	1.06	0.94
177	2	28	12	0	0	1.008	0.62	115.00	1.06	0.94
178	1	427	174	0	0	0.940	-6.56	115.00	1.06	0.94
179	1	74	29	0	45	0.970	-9.37	115.00	1.06	0.94
180	1	70	49	0	0	0.979	-3.09	115.00	1.06	0.94
181	1	73	0	0	0	1.052	-1.33	230.00	1.06	0.94
182	1	241	89	0	0	1.045	-4.19	230.00	1.06	0.94
183	1	40	4	0	0	0.972	7.12	115.00	1.06	0.94
184	1	137	17	0	0	1.039	-6.85	230.00	1.06	0.94
185	2	0	0	0	0	1.052	-4.33	230.00	1.06	0.94
186	2	60	24	0	0	1.065	2.17	230.00	1.06	0.94
187	2	60	24	0	0	1.065	1.40	230.00	1.06	0.94
188	1	183	44	0	0	1.053	-0.72	230.00	1.06	0.94
189	1	7	2	0	0	0.998	-25.84	66.00	1.06	0.94
190	2	0	0	0	-150	1.055	-20.62	345.00	1.06	0.94
191	2	489	53	0	0	1.044	12.25	230.00	1.06	0.94
192	1	800	72	0	0	0.937	-11.18	230.00	1.06	0.94
193	1	0	0	0	0	0.990	-26.09	66.00	1.06	0.94
194	1	0	0	0	0	1.049	-19.21	345.00	1.06	0.94
195	1	0	0	0	0	1.036	-20.79	345.00	1.06	0.94
196	1	10	3	0	0	0.970	-25.32	115.00	1.06	0.94
197	1	43	14	0	0	0.991	-23.72	115.00	1.06	0.94
198	2	64	21	0	0	1.015	-20.58	115.00	1.06	0.94
199	1	35	12	0	0	0.953	-26.05	115.00	1.06	0.94
200	1	27	12	0	0	0.955	-25.93	115.00	1.06	0.94
201	1	41	14	0	0	0.969	-27.49	66.00	1.06	0.94
202	1	38	13	0	0	0.991	-25.33	66.00	1.06	0.94
203	1	42	14	0	0	1.003	-22.35	115.00	1.06	0.94

continued . . .

Table E.1 Continued: Data of buses of the IEEE 300-bus system

Bus ID	Bus type	P_{load} (MW)	Q_{load} (MVAr)	Gs	Bs	Initial Vm (p.u.)	Initial Va	baseKV	$V_{\max}$ (p.u.)	V_{min} (p.u)
204	1	72	24	0	0	0.972	-25.70	66.00	1.06	0.94
205	1	0	-5	0	0	0.984	-26.07	66.00	1.06	0.94
206	1	12	2	0	0	0.999	-27.41	66.00	1.06	0.94
207	1	-21	-14	0	0	1.014	-27.44	66.00	1.06	0.94
208	1	7	2	0	0	0.993	-26.28	66.00	1.06	0.94
209	1	38	13	0	0	1.000	-25.66	66.00	1.06	0.94
210	1	0	0	0	0	0.979	-24.22	115.00	1.06	0.94
211	1	96	7	0	0	1.002	-23.31	115.00	1.06	0.94
212	1	0	0	0	0	1.013	-22.51	138.00	1.06	0.94
213	2	0	0	0	0	1.010	-11.67	16.50	1.06	0.94
214	1	22	16	0	0	0.992	-17.53	138.00	1.06	0.94
215	1	47	26	0	0	0.987	-20.23	138.00	1.06	0.94
216	1	176	105	0	0	0.975	-22.53	138.00	1.06	0.94
217	1	100	75	0	0	1.022	-22.20	138.00	1.06	0.94
218	1	131	96	0	0	1.008	-22.63	138.00	1.06	0.94
219	1	0	0	0	0	1.055	-21.15	345.00	1.06	0.94
220	2	285	100	0	0	1.008	-21.73	138.00	1.06	0.94
221	2	171	70	0	0	1.000	-22.49	138.00	1.06	0.94
222	2	328	188	0	0	1.050	-23.17	20.00	1.06	0.94
223	1	428	232	0	0	0.997	-22.70	138.00	1.06	0.94
224	1	173	99	0	0	1.000	-21.55	230.00	1.06	0.94
225	1	410	40	0	0	0.945	-11.34	230.00	1.06	0.94
226	1	0	0	0	0	1.018	-21.61	230.00	1.06	0.94
227	2	538	369	0	0	1.000	-27.22	27.00	1.06	0.94
228	1	223	148	0	0	1.042	-20.94	138.00	1.06	0.94
229	1	96	46	0	0	1.050	-19.94	138.00	1.06	0.94
230	2	0	0	0	0	1.040	-13.82	20.00	1.06	0.94
231	1	159	107	0	-300	1.054	-21.22	345.00	1.06	0.94

continued . . .

Table E.1 Continued: Data of buses of the IEEE 300-bus system

Bus ID	Bus type	P_{load} (MW)	Q_{load} (MVAr)	Gs	Bs	Initial Vm (p.u.)	Initial Va	baseKV	$V_{\max}$ (p.u.)	V_{min} (p.u)
232	1	448	143	0	0	1.041	-23.19	138.00	1.06	0.94
233	2	404	212	0	0	1.000	-25.90	66.00	1.06	0.94
234	1	572	244	0	0	1.039	-20.89	138.00	1.06	0.94
235	1	269	157	0	0	1.010	-21.03	138.00	1.06	0.94
236	2	0	0	0	0	1.017	-15.40	20.00	1.06	0.94
237	1	0	0	0	0	1.056	-21.10	345.00	1.06	0.94
238	2	255	149	0	-150	1.010	-20.94	138.00	1.06	0.94
239	2	0	0	0	0	1.000	-15.86	138.00	1.06	0.94
240	1	0	0	0	-140	1.024	-20.14	230.00	1.06	0.94
241	2	0	0	0	0	1.050	-16.50	20.00	1.06	0.94
242	2	0	0	0	0	0.993	-17.53	138.00	1.06	0.94
243	2	8	3	0	0	1.010	-19.27	66.00	1.06	0.94
244	1	0	0	0	0	0.992	-20.21	66.00	1.06	0.94
245	1	61	30	0	0	0.971	-20.90	66.00	1.06	0.94
246	1	77	33	0	0	0.965	-21.74	66.00	1.06	0.94
247	1	61	30	0	0	0.969	-21.67	66.00	1.06	0.94
248	1	29	14	0	46	0.976	-25.23	66.00	1.06	0.94
249	1	29	14	0	0	0.975	-25.65	66.00	1.06	0.94
250	1	-23	-17	0	0	1.020	-23.80	66.00	1.06	0.94
281	1	-33	-29	0	0	1.025	-20.06	230.00	1.06	0.94
319	1	116	-24	0	0	1.015	1.48	230.00	1.06	0.94
320	1	2	-13	0	0	1.015	-2.23	115.00	1.06	0.94
322	1	2	-4	0	0	1.001	-17.61	115.00	1.06	0.94
323	1	-15	27	0	0	0.981	-13.69	230.00	1.06	0.94
324	1	25	-1	0	0	0.975	-23.42	115.00	1.06	0.94
526	1	145	-35	0	0	0.943	-34.31	115.00	1.06	0.94
528	1	28	-21	0	0	0.972	-37.58	115.00	1.06	0.94
531	1	14	3	0	0	0.960	-29.10	115.00	1.06	0.94

continued . . .

Table E.1 Continued: Data of buses of the IEEE 300-bus system

Bus ID	Bus type	P_{load} (MW)	Q_{load} (MVAr)	Gs	Bs	Initial Vm (p.u.)	Initial Va	baseKV	$V_{\max}$ (p.u.)	V_{min} (p.u)
552	1	-11	-1	0	0	1.001	-23.36	115.00	1.06	0.94
562	1	51	17	0	0	0.978	-28.00	230.00	1.06	0.94
609	1	30	1	0	0	0.958	-28.79	115.00	1.06	0.94
664	1	-114	77	0	0	1.031	-17.00	345.00	1.06	0.94
1190	1	100	29	0	0	1.013	3.90	86.00	1.06	0.94
1200	1	-100	34	0	0	1.024	-7.52	86.00	1.06	0.94
1201	1	0	0	0	0	1.012	-15.18	115.00	1.06	0.94
2040	1	0	0	0	0	0.965	-14.94	115.00	1.06	0.94
7001	2	0	0	0	0	1.051	10.79	13.80	1.06	0.94
7002	2	0	0	0	0	1.051	12.48	13.80	1.06	0.94
7003	2	0	0	0	0	1.032	13.76	13.80	1.06	0.94
7011	2	0	0	0	0	1.015	4.99	13.80	1.06	0.94
7012	2	0	0	0	0	1.051	11.57	13.80	1.06	0.94
7017	2	0	0	0	0	1.051	-10.47	13.80	1.06	0.94
7023	2	0	0	0	0	1.051	6.15	13.80	1.06	0.94
7024	2	0	0	0	0	1.029	12.60	13.80	1.06	0.94
7039	2	0	0	0	0	1.050	2.11	20.00	1.06	0.94
7044	2	0	0	0	0	1.015	-13.92	13.80	1.06	0.94
7049	3	0	0	0	0	1.051	0.00	13.80	1.06	0.94
7055	2	0	0	0	0	0.997	-7.50	13.80	1.06	0.94
7057	2	0	0	0	0	1.021	-3.44	13.80	1.06	0.94
7061	2	0	0	0	0	1.015	1.97	13.80	1.06	0.94
7062	2	0	0	0	0	1.002	5.80	13.80	1.06	0.94
7071	2	0	0	0	0	0.989	-25.35	13.80	1.06	0.94
7130	2	0	0	0	0	1.051	19.02	13.80	1.06	0.94
7139	2	0	0	0	0	1.051	2.75	13.80	1.06	0.94
7166	2	0	0	0	0	1.015	35.05	13.80	1.06	0.94
9001	1	0	0	0	0	1.012	-11.25	115.00	1.06	0.94

continued . . .

Table E.1 Continued: Data of buses of the IEEE 300-bus system

Bus ID	Bus type	P_{load} (MW)	Q_{load} (MVAr)	Gs	Bs	Initial Vm (p.u.)	Initial Va	baseKV	$V_{\max}$ (p.u.)	V_{min} (p.u)
9002	2	4	0	0	0	0.995	-18.86	6.60	1.06	0.94
9003	1	3	1	0	2	0.983	-19.68	6.60	1.06	0.94
9004	1	1	0	0	0	0.977	-19.82	6.60	1.06	0.94
9005	1	0	0	0	0	1.012	-11.32	115.00	1.06	0.94
9006	1	0	0	0	0	1.003	-17.42	6.60	1.06	0.94
9007	1	0	0	0	0	0.991	-18.69	6.60	1.06	0.94
9012	1	0	0	0	0	1.002	-17.27	6.60	1.06	0.94
9021	1	5	2	0	0	0.989	-19.09	6.60	1.06	0.94
9022	1	2	1	0	0	0.965	-21.67	0.60	1.06	0.94
9023	1	0	0	0	0	0.975	-19.41	6.60	1.06	0.94
9024	1	1	0	0	0	0.971	-21.43	0.60	1.06	0.94
9025	1	0	0	0	0	0.965	-20.48	0.60	1.06	0.94
9026	1	0	0	0	0	0.966	-20.39	0.60	1.06	0.94
9031	1	2	1	0	0	0.932	-25.03	0.60	1.06	0.94
9032	1	1	0	0	0	0.944	-23.84	0.60	1.06	0.94
9033	1	2	1	0	0	0.929	-25.33	0.60	1.06	0.94
9034	1	2	1	0	2	0.997	-21.10	0.60	1.06	0.94
9035	1	2	1	0	0	0.951	-23.19	0.60	1.06	0.94
9036	1	3	1	0	0	0.960	-22.67	2.30	1.06	0.94
9037	1	2	1	0	0	0.957	-22.58	0.60	1.06	0.94
9038	1	3	1	0	0	0.939	-24.41	0.60	1.06	0.94
9041	1	1	0	0	0	0.964	-21.33	0.60	1.06	0.94
9042	1	1	0	0	0	0.950	-22.50	0.60	1.06	0.94
9043	1	2	1	0	0	0.965	-21.42	2.30	1.06	0.94
9044	1	0	0	0	0	0.979	-19.78	6.60	1.06	0.94
9051	2	36	0	0	0	1.000	-19.40	13.80	1.06	0.94
9052	1	30	23	0	0	0.979	-17.25	13.80	1.06	0.94
9053	2	26	0	0	0	1.000	-17.68	13.80	1.06	0.94

continued . . .

Table E.1 Continued: Data of buses of the IEEE 300-bus system

Bus ID	Bus type	P_{load} (MW)	Q_{load} (MVAr)	Gs	Bs	Initial Vm (p.u.)	Initial Va	baseKV	$V_{\max}$ (p.u.)	V_{min} (p.u)
9054	2	0	0	0	0	1.000	-6.83	13.80	1.06	0.94
9055	2	0	0	0	0	1.000	-7.54	13.80	1.06	0.94
9071	1	1	0	0	0	0.975	-20.48	0.60	1.06	0.94
9072	1	1	0	0	0	0.980	-19.92	0.60	1.06	0.94
9121	1	4	1	0	0	0.980	-19.30	6.60	1.06	0.94
9533	1	1	0	0	0	1.040	-18.24	2.30	1.06	0.94

E.2 Transmission lines

Table E.2: Data of transformers and transmission lines of IEEE 300-bus system

From bus	To bus	R (p.u.)	X (p.u.)	B (p.u.)	$S_{li}^{\max}$ (MVA)	Transformer tap
37	9001	0.00006	0.0005	0.000	1000	1.0082
9001	9005	0.00080	0.0035	0.000	800	0.0000
9001	9006	0.02439	0.4368	0.000	1000	0.9668
9001	9012	0.03624	0.6490	0.000	1000	0.9796
9005	9051	0.01578	0.3749	0.000	1000	1.0435
9005	9052	0.01578	0.3749	0.000	1000	0.9391
9005	9053	0.01602	0.3805	0.000	1000	1.0435
9005	9054	0.00000	0.1520	0.000	1000	1.0435
9005	9055	0.00000	0.8000	0.000	1000	1.0435
9006	9007	0.05558	0.2467	0.000	200	0.0000
9006	9003	0.11118	0.4933	0.000	200	0.0000
9006	9003	0.11118	0.4933	0.000	200	0.0000
9012	9002	0.07622	0.4329	0.000	200	0.0000
9012	9002	0.07622	0.4329	0.000	200	0.0000
9002	9021	0.05370	0.0703	0.000	200	0.0000

continued . . .

Table E.2 Continued: Data of transformers and transmission lines of IEEE 300-bus system

From bus	To bus	R (p.u.)	X (p.u.)	B (p.u.)	$S_{li}^{\max}$ (MVA)	Transformer tap
9021	9023	1.10680	0.9528	0.000	20	0.0000
9021	9022	0.44364	2.8152	0.000	200	1.0000
9002	9024	0.50748	3.2202	0.000	200	1.0000
9023	9025	0.66688	3.9440	0.000	200	1.0000
9023	9026	0.61130	3.6152	0.000	200	1.0000
9007	9071	0.44120	2.9668	0.000	200	1.0000
9007	9072	0.30792	2.0570	0.000	200	1.0000
9007	9003	0.05580	0.2467	0.000	200	0.0000
9003	9031	0.73633	4.6724	0.000	200	1.0000
9003	9032	0.76978	4.8846	0.000	200	1.0000
9003	9033	0.75732	4.8056	0.000	200	1.0000
9003	9044	0.07378	0.0635	0.000	20	0.0000
9044	9004	0.03832	0.0289	0.000	20	0.0000
9004	9041	0.36614	2.4560	0.000	200	1.0000
9004	9042	1.05930	5.4536	0.000	200	1.0000
9004	9043	0.15670	1.6994	0.000	200	1.0000
9003	9034	0.13006	1.3912	0.000	200	1.0000
9003	9035	0.54484	3.4572	0.000	200	1.0000
9003	9036	0.15426	1.6729	0.000	200	1.0000
9003	9037	0.38490	2.5712	0.000	200	1.0000
9003	9038	0.44120	2.9668	0.000	200	1.0000
9012	9121	0.23552	0.9904	0.000	200	0.0000
9053	9533	0.00000	0.7500	0.000	1000	0.9583
1	5	0.00100	0.0060	0.000	800	0.0000
2	6	0.00100	0.0090	0.000	800	0.0000
2	8	0.00600	0.0270	0.054	800	0.0000
3	7	0.00000	0.0030	0.000	800	0.0000

continued ...

Table E.2 Continued: Data of transformers and transmission lines of IEEE 300-bus system

From bus	To bus	R (p.u.)	X (p.u.)	B (p.u.)	$S_{li}^{\max}$ (MVA)	Transformer tap
3	19	0.00800	0.0690	0.139	800	0.0000
3	150	0.00100	0.0070	0.000	800	0.0000
4	16	0.00200	0.0190	1.127	1500	0.0000
5	9	0.00600	0.0290	0.018	800	0.0000
7	12	0.00100	0.0090	0.070	800	0.0000
7	131	0.00100	0.0070	0.014	800	0.0000
8	11	0.01300	0.0595	0.033	200	0.0000
8	14	0.01300	0.0420	0.081	800	0.0000
9	11	0.00600	0.0270	0.013	200	0.0000
11	13	0.00800	0.0340	0.018	800	0.0000
12	21	0.00200	0.0150	0.118	800	0.0000
13	20	0.00600	0.0340	0.016	200	0.0000
14	15	0.01400	0.0420	0.097	800	0.0000
15	37	0.06500	0.2480	0.121	200	0.0000
15	89	0.09900	0.2480	0.035	200	0.0000
15	90	0.09600	0.3630	0.048	200	0.0000
16	42	0.00200	0.0220	1.280	800	0.0000
19	21	0.00200	0.0180	0.036	200	0.0000
19	87	0.01300	0.0800	0.151	800	0.0000
20	22	0.01600	0.0330	0.015	200	0.0000
20	27	0.06900	0.1860	0.098	200	0.0000
21	24	0.00400	0.0340	0.280	800	0.0000
22	23	0.05200	0.1110	0.050	800	0.0000
23	25	0.01900	0.0390	0.018	800	0.0000
24	319	0.00700	0.0680	0.134	800	0.0000
25	26	0.03600	0.0710	0.034	200	0.0000
26	27	0.04500	0.1200	0.065	200	0.0000

continued . . .

Table E.2 Continued: Data of transformers and transmission lines of IEEE 300-bus system

From bus	To bus	R (p.u.)	X (p.u.)	B (p.u.)	$S_{li}^{\max}$ (MVA)	Transformer tap
26	320	0.04300	0.1300	0.014	200	0.0000
33	34	0.00000	0.0630	0.000	1000	0.0000
33	38	0.00250	0.0120	0.013	200	0.0000
33	40	0.00600	0.0290	0.020	200	0.0000
33	41	0.00700	0.0430	0.026	200	0.0000
34	42	0.00100	0.0080	0.042	800	0.0000
35	72	0.01200	0.0600	0.008	200	0.0000
35	76	0.00600	0.0140	0.002	800	0.0000
35	77	0.01000	0.0290	0.003	200	0.0000
36	88	0.00400	0.0270	0.043	800	0.0000
37	38	0.00800	0.0470	0.008	200	0.0000
37	40	0.02200	0.0640	0.007	200	0.0000
37	41	0.01000	0.0360	0.020	200	0.0000
37	49	0.01700	0.0810	0.048	800	0.0000
37	89	0.10200	0.2540	0.033	200	0.0000
37	90	0.04700	0.1270	0.016	200	0.0000
38	41	0.00800	0.0370	0.020	800	0.0000
38	43	0.03200	0.0870	0.040	200	0.0000
39	42	0.00060	0.0064	0.404	1000	0.0000
40	48	0.02600	0.1540	0.022	200	0.0000
41	42	0.00000	0.0290	0.000	1000	0.0000
41	49	0.06500	0.1910	0.020	200	0.0000
41	51	0.03100	0.0890	0.036	200	0.0000
42	46	0.00200	0.0140	0.806	1000	0.0000
43	44	0.02600	0.0720	0.035	200	0.0000
43	48	0.09500	0.2620	0.032	200	0.0000
43	53	0.01300	0.0390	0.016	200	0.0000

continued . . .

Table E.2 Continued: Data of transformers and transmission lines of IEEE 300-bus system

From bus	To bus	R (p.u.)	X (p.u.)	B (p.u.)	$S_{li}^{\max}$ (MVA)	Transformer tap
44	47	0.02700	0.0840	0.039	800	0.0000
44	54	0.02800	0.0840	0.037	200	0.0000
45	60	0.00700	0.0410	0.312	800	0.0000
45	74	0.00900	0.0540	0.411	800	0.0000
46	81	0.00500	0.0420	0.690	800	0.0000
47	73	0.05200	0.1450	0.073	200	0.0000
47	113	0.04300	0.1180	0.013	200	0.0000
48	107	0.02500	0.0620	0.007	200	0.0000
49	51	0.03100	0.0940	0.043	800	0.0000
51	52	0.03700	0.1090	0.049	200	0.0000
52	55	0.02700	0.0800	0.036	200	0.0000
53	54	0.02500	0.0730	0.035	200	0.0000
54	55	0.03500	0.1030	0.047	200	0.0000
55	57	0.06500	0.1690	0.082	200	0.0000
57	58	0.04600	0.0800	0.036	200	0.0000
57	63	0.15900	0.5370	0.071	200	0.0000
58	59	0.00900	0.0260	0.005	200	0.0000
59	61	0.00200	0.0130	0.015	800	0.0000
60	62	0.00900	0.0650	0.485	800	0.0000
62	64	0.01600	0.1050	0.203	800	0.0000
62	144	0.00100	0.0070	0.013	800	0.0000
63	526	0.02650	0.1720	0.026	800	0.0000
69	211	0.05100	0.2320	0.028	200	0.0000
69	79	0.05100	0.1570	0.023	200	0.0000
70	71	0.03200	0.1000	0.062	200	0.0000
70	528	0.02000	0.1234	0.028	200	0.0000
71	72	0.03600	0.1310	0.068	200	0.0000

continued ...

Table E.2 Continued: Data of transformers and transmission lines of IEEE 300-bus system

From bus	To bus	R (p.u.)	X (p.u.)	B (p.u.)	$S_{li}^{\max}$ (MVA)	Transformer tap
71	73	0.03400	0.0990	0.047	200	0.0000
72	77	0.01800	0.0870	0.011	200	0.0000
72	531	0.02560	0.1930	0.000	200	0.0000
73	76	0.02100	0.0570	0.030	200	0.0000
73	79	0.01800	0.0520	0.018	200	0.0000
74	88	0.00400	0.0270	0.050	200	0.0000
74	562	0.02860	0.2013	0.379	200	0.0000
76	77	0.01600	0.0430	0.004	200	0.0000
77	78	0.00100	0.0060	0.007	800	0.0000
77	80	0.01400	0.0700	0.038	200	0.0000
77	552	0.08910	0.2676	0.029	200	0.0000
77	609	0.07820	0.2127	0.022	200	0.0000
78	79	0.00600	0.0220	0.011	200	0.0000
78	84	0.00000	0.0360	0.000	1000	0.0000
79	211	0.09900	0.3750	0.051	200	0.0000
80	211	0.02200	0.1070	0.058	200	0.0000
81	194	0.00350	0.0330	0.530	800	0.0000
81	195	0.00350	0.0330	0.530	800	0.0000
85	86	0.00800	0.0640	0.128	800	0.0000
86	87	0.01200	0.0930	0.183	800	0.0000
86	323	0.00600	0.0480	0.092	200	0.0000
89	91	0.04700	0.1190	0.014	200	0.0000
90	92	0.03200	0.1740	0.024	200	0.0000
91	94	0.10000	0.2530	0.031	200	0.0000
91	97	0.02200	0.0770	0.039	800	0.0000
92	103	0.01900	0.1440	0.017	800	0.0000
92	105	0.01700	0.0920	0.012	800	0.0000

continued ...

Table E.2 Continued: Data of transformers and transmission lines of IEEE 300-bus system

From bus	To bus	R (p.u.)	X (p.u.)	B (p.u.)	$S_{li}^{\max}$ (MVA)	Transformer tap
94	97	0.27800	0.4270	0.043	200	0.0000
97	100	0.02200	0.0530	0.007	200	0.0000
97	102	0.03800	0.0920	0.012	200	0.0000
97	103	0.04800	0.1220	0.015	200	0.0000
98	100	0.02400	0.0640	0.007	200	0.0000
98	102	0.03400	0.1210	0.015	200	0.0000
99	107	0.05300	0.1350	0.017	200	0.0000
99	108	0.00200	0.0040	0.002	200	0.0000
99	109	0.04500	0.3540	0.044	200	0.0000
99	110	0.05000	0.1740	0.022	200	0.0000
100	102	0.01600	0.0380	0.004	200	0.0000
102	104	0.04300	0.0640	0.027	200	0.0000
103	105	0.01900	0.0620	0.008	200	0.0000
104	108	0.07600	0.1300	0.044	200	0.0000
104	322	0.04400	0.1240	0.015	200	0.0000
105	107	0.01200	0.0880	0.011	200	0.0000
105	110	0.15700	0.4000	0.047	200	0.0000
108	324	0.07400	0.2080	0.026	200	0.0000
109	110	0.07000	0.1840	0.021	200	0.0000
109	113	0.10000	0.2740	0.031	200	0.0000
109	114	0.10900	0.3930	0.036	200	0.0000
110	112	0.14200	0.4040	0.050	200	0.0000
112	114	0.01700	0.0420	0.006	200	0.0000
115	122	0.00360	0.0199	0.004	200	0.0000
116	120	0.00200	0.1049	0.001	800	0.0000
117	118	0.00010	0.0018	0.017	1000	0.0000
118	119	0.00000	0.0271	0.000	1500	0.0000

continued . . .

Table E.2 Continued: Data of transformers and transmission lines of IEEE 300-bus system

From bus	To bus	R (p.u.)	X (p.u.)	B (p.u.)	$S_{li}^{\max}$ (MVA)	Transformer tap
118	1201	0.00000	0.6163	0.000	1000	0.0000
1201	120	0.00000	-0.3697	0.000	1000	0.0000
118	121	0.00220	0.2915	0.000	1000	0.0000
119	120	0.00000	0.0339	0.000	1500	0.0000
119	121	0.00000	0.0582	0.000	1000	0.0000
122	123	0.08080	0.2344	0.029	200	0.0000
122	125	0.09650	0.3669	0.054	200	0.0000
123	124	0.03600	0.1076	0.117	200	0.0000
123	125	0.04760	0.1414	0.149	200	0.0000
125	126	0.00060	0.0197	0.000	800	0.0000
126	127	0.00590	0.0405	0.250	800	0.0000
126	129	0.01150	0.1106	0.185	800	0.0000
126	132	0.01980	0.1688	0.321	800	0.0000
126	157	0.00500	0.0500	0.330	200	0.0000
126	158	0.00770	0.0538	0.335	200	0.0000
126	169	0.01650	0.1157	0.171	800	0.0000
127	128	0.00590	0.0577	0.095	800	0.0000
127	134	0.00490	0.0336	0.208	800	0.0000
127	168	0.00590	0.0577	0.095	800	0.0000
128	130	0.00780	0.0773	0.126	800	0.0000
128	133	0.00260	0.0193	0.030	200	0.0000
129	130	0.00760	0.0752	0.122	800	0.0000
129	133	0.00210	0.0186	0.030	800	0.0000
130	132	0.00160	0.0164	0.026	800	0.0000
130	151	0.00170	0.0165	0.026	800	0.0000
130	167	0.00790	0.0793	0.127	800	0.0000
130	168	0.00780	0.0784	0.125	800	0.0000

continued . . .

Table E.2 Continued: Data of transformers and transmission lines of IEEE 300-bus system

From bus	To bus	R (p.u.)	X (p.u.)	B (p.u.)	$S_{li}^{\max}$ (MVA)	Transformer tap
133	137	0.00170	0.0117	0.289	1500	0.0000
133	168	0.00260	0.0193	0.030	200	0.0000
133	169	0.00210	0.0186	0.030	800	0.0000
133	171	0.00020	0.0101	0.000	1500	0.0000
134	135	0.00430	0.0293	0.180	200	0.0000
134	184	0.00390	0.0381	0.258	200	0.0000
135	136	0.00910	0.0623	0.385	800	0.0000
136	137	0.01250	0.0890	0.540	200	0.0000
136	152	0.00560	0.0390	0.953	800	0.0000
137	140	0.00150	0.0114	0.284	800	0.0000
137	181	0.00050	0.0034	0.021	800	0.0000
137	186	0.00070	0.0151	0.126	800	0.0000
137	188	0.00050	0.0034	0.021	800	0.0000
139	172	0.05620	0.2248	0.081	200	0.0000
140	141	0.01200	0.0836	0.123	200	0.0000
140	142	0.01520	0.1132	0.684	200	0.0000
140	145	0.04680	0.3369	0.519	200	0.0000
140	146	0.04300	0.3031	0.463	200	0.0000
140	147	0.04890	0.3492	0.538	200	0.0000
140	182	0.00130	0.0089	0.119	800	0.0000
141	146	0.02910	0.2267	0.342	200	0.0000
142	143	0.00600	0.0570	0.767	800	0.0000
143	145	0.00750	0.0773	0.119	800	0.0000
143	149	0.01270	0.0909	0.135	200	0.0000
145	146	0.00850	0.0588	0.087	800	0.0000
145	149	0.02180	0.1511	0.223	200	0.0000
146	147	0.00730	0.0504	0.074	800	0.0000

continued ...

Table E.2 Continued: Data of transformers and transmission lines of IEEE 300-bus system

From bus	To bus	R (p.u.)	X (p.u.)	B (p.u.)	$S_{li}^{\max}$ (MVA)	Transformer tap
148	178	0.05230	0.1526	0.074	800	0.0000
148	179	0.13710	0.3919	0.076	200	0.0000
152	153	0.01370	0.0957	0.141	200	0.0000
153	161	0.00550	0.0288	0.190	800	0.0000
154	156	0.17460	0.3161	0.040	200	0.0000
154	183	0.08040	0.3054	0.045	200	0.0000
155	161	0.01100	0.0568	0.388	200	0.0000
157	159	0.00080	0.0098	0.069	800	0.0000
158	159	0.00290	0.0285	0.190	800	0.0000
158	160	0.00660	0.0448	0.277	200	0.0000
162	164	0.00240	0.0326	0.236	800	0.0000
162	165	0.00180	0.0245	1.662	800	0.0000
163	164	0.00440	0.0514	3.597	800	0.0000
165	166	0.00020	0.0123	0.000	800	0.0000
167	169	0.00180	0.0178	0.029	800	0.0000
172	173	0.06690	0.4843	0.063	200	0.0000
172	174	0.05580	0.2210	0.031	200	0.0000
173	174	0.08070	0.3331	0.049	200	0.0000
173	175	0.07390	0.3071	0.043	200	0.0000
173	176	0.17990	0.5017	0.069	200	0.0000
175	176	0.09040	0.3626	0.048	200	0.0000
175	179	0.07700	0.3092	0.054	200	0.0000
176	177	0.02510	0.0829	0.047	800	0.0000
177	178	0.02220	0.0847	0.050	800	0.0000
178	179	0.04980	0.1855	0.029	200	0.0000
178	180	0.00610	0.0290	0.084	800	0.0000
181	138	0.00040	0.0202	0.000	1000	0.0000

continued . . .

Table E.2 Continued: Data of transformers and transmission lines of IEEE 300-bus system

From bus	To bus	R (p.u.)	X (p.u.)	B (p.u.)	$S_{li}^{\max}$ (MVA)	Transformer tap
181	187	0.00040	0.0083	0.115	1000	0.0000
184	185	0.00250	0.0245	0.164	800	0.0000
186	188	0.00070	0.0086	0.115	1000	0.0000
187	188	0.00070	0.0086	0.115	800	0.0000
188	138	0.00040	0.0202	0.000	1000	0.0000
189	208	0.03300	0.0950	0.000	200	0.0000
189	209	0.04600	0.0690	0.000	200	0.0000
190	231	0.00040	0.0022	6.200	1000	0.0000
190	240	0.00000	0.0275	0.000	1000	0.0000
191	192	0.00300	0.0480	0.000	1500	0.0000
192	225	0.00200	0.0090	0.000	200	0.0000
193	205	0.04500	0.0630	0.000	200	0.0000
193	208	0.04800	0.1270	0.000	200	0.0000
194	219	0.00310	0.0286	0.500	800	0.0000
194	664	0.00240	0.0355	0.360	800	0.0000
195	219	0.00310	0.0286	0.500	800	0.0000
196	197	0.01400	0.0400	0.004	200	0.0000
196	210	0.03000	0.0810	0.010	200	0.0000
197	198	0.01000	0.0600	0.009	800	0.0000
197	211	0.01500	0.0400	0.006	200	0.0000
198	202	0.33200	0.6880	0.000	200	0.0000
198	203	0.00900	0.0460	0.025	200	0.0000
198	210	0.02000	0.0730	0.008	800	0.0000
198	211	0.03400	0.1090	0.032	200	0.0000
199	200	0.07600	0.1350	0.009	200	0.0000
199	210	0.04000	0.1020	0.005	200	0.0000
200	210	0.08100	0.1280	0.014	200	0.0000

continued . . .

Table E.2 Continued: Data of transformers and transmission lines of IEEE 300-bus system

From bus	To bus	R (p.u.)	X (p.u.)	B (p.u.)	$S_{li}^{\max}$ (MVA)	Transformer tap
201	204	0.12400	0.1830	0.000	200	0.0000
203	211	0.01000	0.0590	0.008	200	0.0000
204	205	0.04600	0.0680	0.000	200	0.0000
205	206	0.30200	0.4460	0.000	200	0.0000
206	207	0.07300	0.0930	0.000	200	0.0000
206	208	0.24000	0.4210	0.000	200	0.0000
212	215	0.01390	0.0778	0.086	200	0.0000
213	214	0.00250	0.0380	0.000	800	1.0000
214	215	0.00170	0.0185	0.020	800	0.0000
214	242	0.00150	0.0108	0.002	200	0.0000
215	216	0.00450	0.0249	0.026	800	0.0000
216	217	0.00400	0.0497	0.018	800	0.0000
217	218	0.00000	0.0456	0.000	1000	0.0000
217	219	0.00050	0.0177	0.020	800	0.0000
217	220	0.00270	0.0395	0.832	800	0.0000
219	237	0.00030	0.0018	5.200	800	0.0000
220	218	0.00370	0.0484	0.430	800	0.0000
220	221	0.00100	0.0295	0.503	800	0.0000
220	238	0.00160	0.0046	0.402	800	0.0000
221	223	0.00030	0.0013	1.000	800	0.0000
222	237	0.00140	0.0514	0.330	800	1.0000
224	225	0.01000	0.0640	0.480	800	0.0000
224	226	0.00190	0.0081	0.860	800	0.0000
225	191	0.00100	0.0610	0.000	1500	0.0000
226	231	0.00050	0.0212	0.000	800	0.0000
227	231	0.00090	0.0472	0.186	800	1.0000
228	229	0.00190	0.0087	1.280	800	0.0000

continued . . .

Table E.2 Continued: Data of transformers and transmission lines of IEEE 300-bus system

From bus	To bus	R (p.u.)	X (p.u.)	B (p.u.)	$S_{li}^{\max}$ (MVA)	Transformer tap
228	231	0.00260	0.0917	0.000	200	0.0000
228	234	0.00130	0.0288	0.810	200	0.0000
229	190	0.00000	0.0626	0.000	1000	0.0000
231	232	0.00020	0.0069	1.364	1000	0.0000
231	237	0.00010	0.0006	3.570	1500	0.0000
232	233	0.00170	0.0485	0.000	1000	0.0000
234	235	0.00020	0.0259	0.144	1000	0.0000
234	237	0.00060	0.0272	0.000	800	0.0000
235	238	0.00020	0.0006	0.800	800	0.0000
241	237	0.00050	0.0154	0.000	1000	1.0000
240	281	0.00030	0.0043	0.009	800	0.0000
242	245	0.00820	0.0851	0.000	800	0.0000
242	247	0.01120	0.0723	0.000	800	0.0000
243	244	0.01270	0.0355	0.000	200	0.0000
243	245	0.03260	0.1804	0.000	200	0.0000
244	246	0.01950	0.0551	0.000	200	0.0000
245	246	0.01570	0.0732	0.000	200	0.0000
245	247	0.03600	0.2119	0.000	200	0.0000
246	247	0.02680	0.1285	0.000	200	0.0000
247	248	0.04280	0.1215	0.000	200	0.0000
248	249	0.03510	0.1004	0.000	200	0.0000
249	250	0.06160	0.1857	0.000	200	0.0000
3	1	0.00000	0.0520	0.000	1000	0.9470
3	2	0.00000	0.0520	0.000	1000	0.9560
3	4	0.00000	0.0050	0.000	1500	0.9710
7	5	0.00000	0.0390	0.000	1000	0.9480
7	6	0.00000	0.0390	0.000	1000	0.9590

continued . . .

Table E.2 Continued: Data of transformers and transmission lines of IEEE 300-bus system

From bus	To bus	R (p.u.)	X (p.u.)	B (p.u.)	$S_{li}^{\max}$ (MVA)	Transformer tap
10	11	0.00000	0.0890	0.000	1000	1.0460
12	10	0.00000	0.0530	0.000	1000	0.9850
15	17	0.01940	0.0311	0.000	1000	0.9561
16	15	0.00100	0.0380	0.000	1000	0.9710
21	20	0.00000	0.0140	0.000	1000	0.9520
24	23	0.00000	0.0640	0.000	1000	0.9430
36	35	0.00000	0.0470	0.000	1000	1.0100
45	44	0.00000	0.0200	0.000	1000	1.0080
45	46	0.00000	0.0210	0.000	1000	1.0000
62	61	0.00000	0.0590	0.000	1000	0.9750
63	64	0.00000	0.0380	0.000	1000	1.0170
73	74	0.00000	0.0244	0.000	1000	1.0000
81	88	0.00000	0.0200	0.000	1000	1.0000
85	99	0.00000	0.0480	0.000	1000	1.0000
86	102	0.00000	0.0480	0.000	1000	1.0000
87	94	0.00000	0.0460	0.000	1000	1.0150
114	207	0.00000	0.1490	0.000	1000	0.9670
116	124	0.00520	0.0174	0.000	800	1.0100
121	115	0.00000	0.0280	0.000	1000	1.0500
122	157	0.00050	0.0195	0.000	1000	1.0000
130	131	0.00000	0.0180	0.000	1000	1.0522
130	150	0.00000	0.0140	0.000	1000	1.0522
132	170	0.00100	0.0402	0.000	1000	1.0500
141	174	0.00240	0.0603	0.000	1000	0.9750
142	175	0.00240	0.0498	-0.087	1000	1.0000
143	144	0.00000	0.0833	0.000	1000	1.0350
143	148	0.00130	0.0371	0.000	1000	0.9565

continued . . .

Table E.2 Continued: Data of transformers and transmission lines of IEEE 300-bus system

From bus	To bus	R (p.u.)	X (p.u.)	B (p.u.)	$S_{li}^{\max}$ (MVA)	Transformer tap
145	180	0.00050	0.0182	0.000	1000	1.0000
151	170	0.00100	0.0392	0.000	1000	1.0500
153	183	0.00270	0.0639	0.000	1000	1.0730
155	156	0.00080	0.0256	0.000	1000	1.0500
159	117	0.00000	0.0160	0.000	1000	1.0506
160	124	0.00120	0.0396	0.000	1000	0.9750
163	137	0.00130	0.0384	-0.057	1000	0.9800
164	155	0.00090	0.0231	-0.033	1000	0.9560
182	139	0.00030	0.0131	0.000	1000	1.0500
189	210	0.00000	0.2520	0.000	1000	1.0300
193	196	0.00000	0.2370	0.000	1000	1.0300
195	212	0.00080	0.0366	0.000	1000	0.9850
200	248	0.00000	0.2200	0.000	1000	1.0000
201	69	0.00000	0.0980	0.000	1000	1.0300
202	211	0.00000	0.1280	0.000	1000	1.0100
204	2040	0.02000	0.2040	-0.012	1000	1.0500
209	198	0.02600	0.2110	0.000	1000	1.0300
211	212	0.00300	0.0122	0.000	1000	1.0000
218	219	0.00100	0.0354	-0.010	1000	0.9700
223	224	0.00120	0.0195	-0.364	1000	1.0000
229	230	0.00100	0.0332	0.000	1000	1.0200
234	236	0.00050	0.0160	0.000	1500	1.0700
238	239	0.00050	0.0160	0.000	1000	1.0200
196	2040	0.00010	0.0200	0.000	1000	1.0000
119	1190	0.00100	0.0230	0.000	1000	1.0223
120	1200	0.00000	0.0230	0.000	1000	0.9284
7002	2	0.00100	0.0146	0.000	1500	1.0000

continued . . .

Table E.2 Continued: Data of transformers and transmission lines of IEEE 300-bus system

From bus	To bus	R (p.u.)	X (p.u.)	B (p.u.)	$S_{li}^{\max}$ (MVA)	Transformer tap
7003	3	0.00000	0.0105	0.000	2000	1.0000
7061	61	0.00000	0.0238	0.000	1000	1.0000
7062	62	0.00000	0.0321	0.000	1000	0.9500
7166	166	0.00000	0.0154	0.000	1000	1.0000
7024	24	0.00000	0.0289	0.000	1000	1.0000
7001	1	0.00000	0.0195	0.000	1000	1.0000
7130	130	0.00000	0.0193	0.000	2000	1.0000
7011	11	0.00000	0.0192	0.000	1000	1.0000
7023	23	0.00000	0.0230	0.000	1000	1.0000
7049	49	0.00000	0.0124	0.000	1000	1.0000
7139	139	0.00000	0.0167	0.000	1500	1.0000
7012	12	0.00000	0.0312	0.000	1500	1.0000
7017	17	0.00000	0.0165	0.000	1000	0.9420
7039	39	0.00000	0.0316	0.000	1000	0.9650
7057	57	0.00000	0.0535	0.000	1000	0.9500
7044	44	0.00000	0.1818	0.000	1000	0.9420
7055	55	0.00000	0.1961	0.000	1000	0.9420
7071	71	0.00000	0.0690	0.000	1000	0.9565

E.3 Generators

Table E.3: Data of generators of the IEEE 300-bus system

Bus ID	Initial P (MW)	$Q_{\max}$ (MVAr)	$Q_{\min}$ (MVAr)	Initial V_g (p.u.)	$P_{\max}$ (MW)	$P_{\min}$ (MW)	Coefficients a	b	c
8	0	10	-10	1.01530	100.000	30.00	0	40	0.010000
10	0	20	-20	1.02050	100.000	30.00	0	40	0.010000
20	0	20	-20	1.00100	100.000	30.00	0	40	0.010000

continued ...

Table E.3 Continued: Data of generators of the IEEE 300-bus system

Bus ID	Initial P (MW)	$Q_{\max}$ (MVAr)	$Q_{\min}$ (MVAr)	Initial V_g (p.u.)	$P_{\max}$ (MW)	$P_{\min}$ (MW)	Coefficients a	b	c
63	0	25	-25	0.95830	100.000	30.00	0	40	0.010000
76	0	35	12	0.96320	100.000	30.00	0	40	0.010000
84	375	240	-240	1.02500	475.000	142.50	0	20	0.026667
91	155	96	-11	1.05200	255.000	76.50	0	20	0.064516
92	290	153	-153	1.05200	390.000	117.00	0	20	0.034483
98	68	56	-30	1.00000	168.000	50.40	0	20	0.147059
108	117	77	-24	0.99000	217.000	65.10	0	20	0.085470
119	1930	1500	-500	1.04350	2030.000	609.00	0	20	0.005181
124	240	120	-60	1.02330	340.000	102.00	0	20	0.041667
125	0	200	-25	1.01030	100.000	30.00	0	40	0.010000
138	0	350	-125	1.05500	100.000	30.00	0	40	0.010000
141	281	75	-50	1.05100	381.000	114.30	0	20	0.035587
143	696	300	-100	1.04350	796.000	238.80	0	20	0.014368
146	84	35	-15	1.05280	184.000	55.20	0	20	0.119048
147	217	100	-50	1.05280	317.000	95.10	0	20	0.046083
149	103	50	-25	1.07350	203.000	60.90	0	20	0.097087
152	372	175	-50	1.05350	472.000	141.60	0	20	0.026882
153	216	90	-50	1.04350	316.000	94.80	0	20	0.046296
156	0	15	-10	0.96300	100.000	30.00	0	40	0.010000
170	205	90	-40	0.92900	305.000	91.50	0	20	0.048781
171	0	150	-50	0.98290	100.000	30.00	0	40	0.010000
176	228	90	-45	1.05220	328.000	98.40	0	20	0.043860
177	84	35	-15	1.00770	184.000	55.20	0	20	0.119048
185	200	80	-50	1.05220	300.000	90.00	0	20	0.050000
186	1200	400	-100	1.06500	1300.000	390.00	0	20	0.008333
187	1200	400	-100	1.06500	1300.000	390.00	0	20	0.008333
190	475	300	-300	1.05510	575.000	172.50	0	20	0.021053
191	1973	1000	-1000	1.04350	2073.000	621.90	0	20	0.005068

continued . . .

Table E.3 Continued: Data of generators of the IEEE 300-bus system

Bus ID	Initial P (MW)	$Q_{\max}$ (MVAr)	$Q_{\min}$ (MVAr)	Initial V_g (p.u.)	$P_{\max}$ (MW)	$P_{\min}$ (MW)	Coefficients a	b	c
198	424	260	-260	1.01500	524.000	157.20	0	20	0.023585
213	272	150	-150	1.01000	372.000	111.60	0	20	0.036765
220	100	60	-60	1.00800	200.000	60.00	0	20	0.100000
221	450	320	-320	1.00000	550.000	165.00	0	20	0.022222
222	250	300	-300	1.05000	350.000	105.00	0	20	0.040000
227	303	300	-300	1.00000	403.000	120.90	0	20	0.033003
230	345	250	-250	1.04000	445.000	133.50	0	20	0.028986
233	300	500	-500	1.00000	400.000	120.00	0	20	0.033333
236	600	300	-300	1.01650	700.000	210.00	0	20	0.016667
238	250	200	-200	1.01000	350.000	105.00	0	20	0.040000
239	550	400	-400	1.00000	650.000	195.00	0	20	0.018182
241	575	600	-600	1.05000	675.430	202.63	0	20	0.017378
242	170	100	40	0.99300	270.000	81.00	0	20	0.058824
243	84	80	40	1.01000	184.000	55.20	0	20	0.119048
7001	467	210	-210	1.05070	567.000	170.10	0	20	0.021413
7002	623	280	-280	1.05070	723.000	216.90	0	20	0.016051
7003	1210	420	-420	1.03230	1310.000	393.00	0	20	0.008264
7011	234	100	-100	1.01450	334.000	100.20	0	20	0.042735
7012	372	224	-224	1.05070	472.000	141.60	0	20	0.026882
7017	330	350	0	1.05070	430.000	129.00	0	20	0.030303
7023	185	120	0	1.05070	285.000	85.50	0	20	0.054054
7024	410	224	-224	1.02900	510.000	153.00	0	20	0.024390
7039	500	200	-200	1.05000	600.000	180.00	0	20	0.020000
7044	37	42	0	1.01450	137.000	41.10	0	20	0.270270
7049	0	10	0	1.05070	2399.010	0.00	0	40	0.010000
7055	45	25	0	0.99670	145.000	43.50	0	20	0.222222
7057	165	90	-90	1.02120	265.000	79.50	0	20	0.060606
7061	400	150	-150	1.01450	500.000	150.00	0	20	0.025000

continued . . .

Table E.3 Continued: Data of generators of the IEEE 300-bus system

Bus ID	Initial P (MW)	$Q_{\max}$ (MVAr)	$Q_{\min}$ (MVAr)	Initial V_g (p.u.)	$P_{\max}$ (MW)	$P_{\min}$ (MW)	Coefficients		
							a	b	c
7062	400	150	0	1.00170	500.000	150.00	0	20	0.025000
7071	116	87	0	0.98930	216.000	64.80	0	20	0.086207
7130	1292	600	-100	1.05070	1392.000	417.60	0	20	0.007740
7139	700	325	-125	1.05070	800.000	240.00	0	20	0.014286
7166	553	300	-200	1.01450	653.000	195.90	0	20	0.018083
9002	0	2	-2	0.99450	100.000	30.00	0	40	0.010000
9051	0	17	-17	1.00000	100.000	30.00	0	40	0.010000
9053	0	13	-13	1.00000	100.000	30.00	0	40	0.010000
9054	50	38	-38	1.00000	150.000	45.00	0	20	0.200000
9055	8	6	-6	1.00000	108.000	32.40	0	20	1.250000

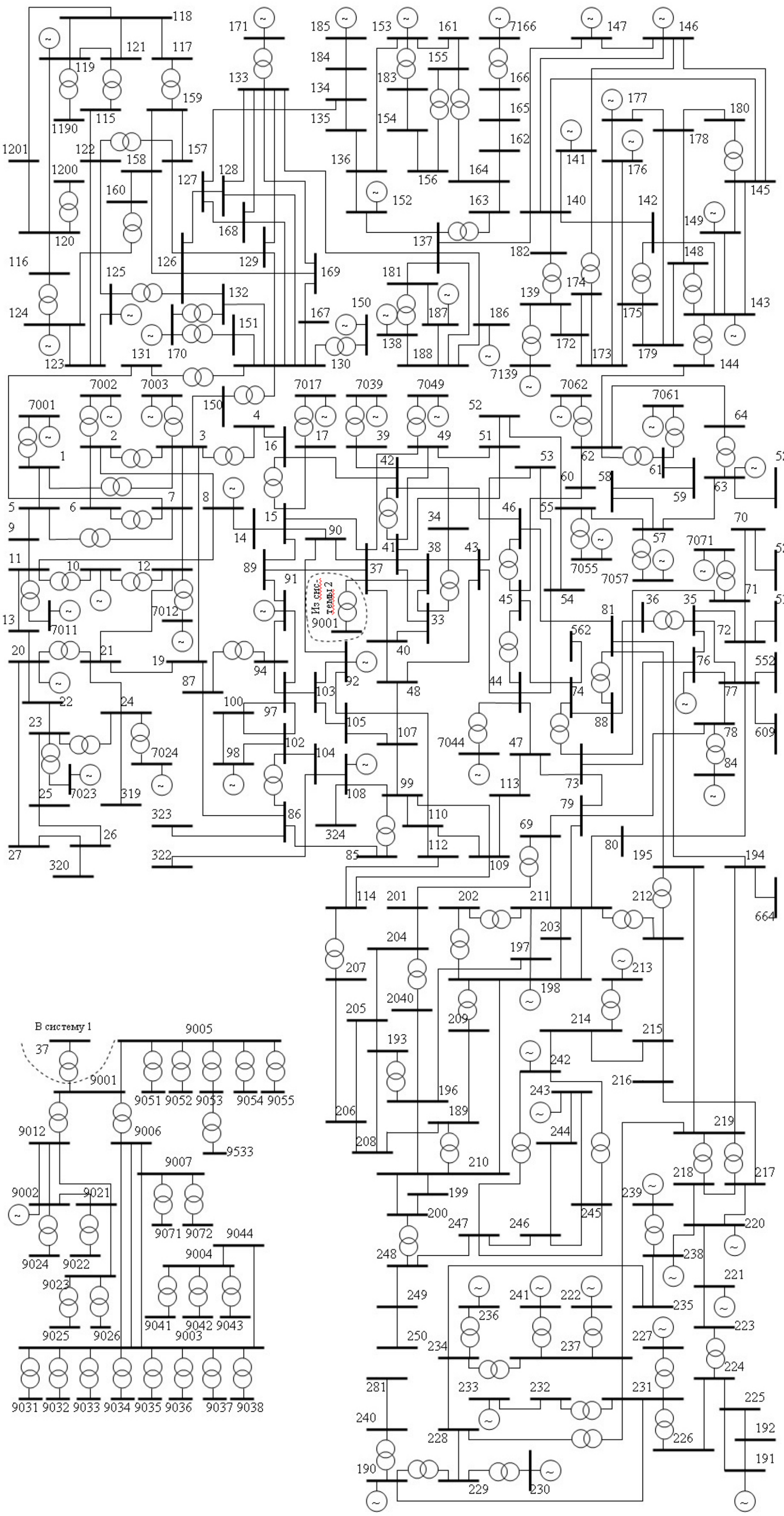

Рис.1. IEEE тестовая схема, состоящая из 300 узлов

FIGURE E.1: Redrawn one-line diagram of IEEE 300-bus system

Appendix F

Matlab code of Self-Learning Cuckoo search algorithm for Example 4.1

```
clc
clear

%Cuckoo parameter
pa       = 0.1; %Discover rate of allien eggs
pl       = 0.6; %Learning factor
beta     = 1.5; % Cuckoo parameter
K1       = 0.05;
K2       = 1;
sigma
   =(gamma(1+beta)*sin(pi*beta/2)/(gamma((1+beta)/2)*beta*2^((beta-1)/2)))^(1/beta);
%% Input Data
Data = [
%Pmin Pmax a b c d f
254      550      785.96      6.63      0.00298   300  0.035
94       375      654.69      12.8      0.00569   200  0.042
];
%Bloss = [0.00003,0.00009,0.00012];
Bloss = [];
Pload = 500;
```

```
Pmin = Data(:,1)';
Pmax = Data(:,2)';
a = Data(:,3)';
b = Data(:,4)';
c = Data(:,5)';
d = Data(:,6)';
f = Data(:,7)';

NP = 3;
Dim = 2;
%% Data processing
pUpper = repmat(Pmax,NP,1);
pLower = repmat(Pmin,NP,1);
aRep = repmat(a,NP,1);
bRep = repmat(b,NP,1);
cRep = repmat(c,NP,1);
dRep = repmat(d,NP,1);
fRep = repmat(f,NP,1);
BlossRep = repmat(Bloss,NP,1);
%% Initial case
Nest = pLower + rand(NP,Dim).*(pUpper - pLower);
% Evaluate Fitness function
%Ploss = sum(BlossRep.*(Nest.^2),2);
Ploss = 0;
K = 1e4;
Penalty = (sum(Nest,2) - Pload - Ploss).^2;
FC  = sum(aRep + bRep.*Nest + cRep.*(Nest.^2) + abs(dRep.*sin(fRep.*(pLower -
    Nest))),2);
FF = FC + K*Penalty;

[Fbest,inv] = min(FF);
sto_FFbest = Fbest;
Nbest = Nest(inv,:);
err = 1e-2;
```

```
iter = 1;
%% Main Process

tic;
while min(Penalty) >= err
%Create Cuckoo eggs
mat_u = randn(NP,Dim)*sigma;
mat_v = randn(NP,Dim);
step=mat_u./abs(mat_v).^(1/beta);
stepsize=K1*step.*(Nest - ones(NP,1)*Nbest);
newNest = Nest + stepsize.*randn(NP,Dim);
%Fix solutions volating limit constraints
newNest = ((newNest>=pLower)&(newNest<=pUpper)).*newNest+...
(newNest<pLower).*(pLower+0.25.*(pUpper-pLower).*rand(NP,Dim))+...
(newNest>pUpper).*(pUpper-0.25.*(pUpper-pLower).*rand(NP,Dim));
%Evaluate Fitness
%Ploss = sum(BlossRep.*(newNest.^2),2);
Ploss = 0;
Penalty = (sum(newNest,2) - Pload - Ploss).^2;
FC  = sum(aRep + bRep.*newNest + cRep.*(newNest.^2) +
    abs(dRep.*sin(fRep.*(pLower - newNest))),2);
newFF = FC + K*Penalty;
%Update current best solution
for iter1 = 1:NP
if newFF(iter1) < FF(iter1)
FF(iter1) = newFF(iter1);
Nest(iter1,:) = newNest(iter1,:);
end
end
iter = iter +1
[FFbest,inv] = min(FF)
Nbest = Nest(inv,:)
sto_FFbest(iter) = FFbest;
% Check stopping criteria
```

```
%Ploss = sum(Bloss.*(Nbest.^2),2);
Ploss = 0;
Penalty = (sum(Nbest,2) - Pload - Ploss).^2;
if Penalty < err
break;
end
%Discovery stage
if rand()< pl
student1 = 1:NP;
student2 = randperm(NP);
while sum(student1 == student2) > 0
student2 = randperm(NP);
end
tmp = FF(student1) < FF(student2);
temp = repmat(tmp,1,Dim);
temp = (-1).^(temp +1);
stepsize = (Nest - Nest(student2,:)).*rand(NP,Dim);
newNest = Nest + temp.*stepsize;
else
mat_K = rand(NP,Dim) > pa;
stepsize=K2*rand.*(Nest(randperm(NP),:)-Nest(randperm(NP),:));
newNest=(Nest+stepsize.*mat_K);
end
%Fix solutions volating limit constraints
newNest = ((newNest>=pLower)&(newNest<=pUpper)).*newNest+...
(newNest<pLower).*(pLower+0.25.*(pUpper-pLower).*rand(NP,Dim))+...
(newNest>pUpper).*(pUpper-0.25.*(pUpper-pLower).*rand(NP,Dim));
%Evaluate Fitness
%Ploss = sum(BlossRep.*(newNest.^2),2);
Ploss = 0;
Penalty = (sum(newNest,2) - Pload - Ploss).^2;
FC  = sum(aRep + bRep.*newNest + cRep.*(newNest.^2) +
    abs(dRep.*sin(fRep.*(pLower - newNest))),2);
newFF = FC + K*Penalty;
```

```
%Update current best solution
for iter1 = 1:NP
if newFF(iter1) < FF(iter1)
FF(iter1) = newFF(iter1);
Nest(iter1,:) = newNest(iter1,:);
end
end
iter = iter +1
[FFbest,inv] = min(FF)
Nbest = Nest(inv,:)
sto_FFbest(iter) = FFbest;
%    Ploss = sum(Bloss.*(Nbest.^2),2);
Ploss = 0;
Penalty = (sum(Nbest,2) - Pload - Ploss).^2;
end
caltime = toc;
A = [FFbest,Nbest,caltime];
fprintf('%f %f %f %f \n',A)
plot(sto_FFbest)
```

Bibliography

[1] Seyedali Mirjalili. Moth-flame optimization algorithm: A novel nature-inspired heuristic paradigm. *Knowledge-Based Systems*, 89:228–249, 2015.

[2] Vinay Kumar Jadoun, Nikhil Gupta, KR Niazi, and Anil Swarnkar. Multi-area economic dispatch with reserve sharing using dynamically controlled particle swarm optimization. *International Journal of Electrical Power & Energy Systems*, 73:743–756, 2015.

[3] Jizhong Zhu. *Optimization of power system operation*, volume 47. John Wiley & Sons, 2015.

[4] George Polya. *How to solve it: A new aspect of mathematical method*. Princeton university press, 2014.

[5] Fred Glover. Future paths for integer programming and links to artificial intelligence. *Computers & operations research*, 13(5):533–549, 1986.

[6] Prakash Shelokar, Abhijit Kulkarni, Valadi K Jayaraman, and Patrick Siarry. Metaheuristics in process engineering: A historical perspective. In *Applications of Metaheuristics in Process Engineering*, pages 1–38. Springer, 2014.

[7] J. Kennedy and R. Eberhart. Particle swarm optimization. In *1995 IEEE international conference on neural networks*, 1998.

[8] Marco Dorigo and Luca Maria Gambardella. Ant colony system: a cooperative learning approach to the traveling salesman problem. *IEEE Transactions on evolutionary computation*, 1(1):53–66, 1997.

[9] Fred Glover, James P Kelly, and Manuel Laguna. Genetic algorithms and tabu search: hybrids for optimization. *Computers & Operations Research*, 22(1):111–134, 1995.

[10] Yi-Tung Kao and Erwie Zahara. A hybrid genetic algorithm and particle swarm optimization for multimodal functions. *Applied Soft Computing*, 8(2):849–857, 2008.

[11] Wen-Jun Zhang and Xiao-Feng Xie. Depso: hybrid particle swarm with differential evolution operator. In *Systems, Man and Cybernetics, 2003. IEEE International Conference on*, volume 4, pages 3816–3821. IEEE, 2003.

[12] Maurice Clerc and James Kennedy. The particle swarm-explosion, stability, and convergence in a multidimensional complex space. *IEEE transactions on Evolutionary Computation*, 6(1):58–73, 2002.

[13] Halgamuge S. K. Ratnaweera, A. and H. C. Watson. Self-organizing hierarchical particle swarm optimizer with time-varying acceleration coefficients. *IEEE Transactions on Evolutionary Computation*, 8(3):240–255, 2004.

[14] Rainer Storn and Kenneth Price. Differential evolution–a simple and efficient heuristic for global optimization over continuous spaces. *Journal of global optimization*, 11 (4):341–359, 1997.

[15] Kang Seok Lee and Zong Woo Geem. A new meta-heuristic algorithm for continuous engineering optimization: harmony search theory and practice. *Computer methods in applied mechanics and engineering*, 194(36):3902–3933, 2005.

[16] M Mahdavi, Mohammad Fesanghary, and E Damangir. An improved harmony search algorithm for solving optimization problems. *Applied mathematics and computation*, 188(2):1567–1579, 2007.

[17] RV Rao, Vimal J Savsani, and DP Vakharia. Teaching–learning-based optimization: an optimization method for continuous non-linear large scale problems. *Information Sciences*, 183(1):1–15, 2012.

[18] Kevin J Gaston, Jonathan Bennie, Thomas W Davies, and John Hopkins. The ecological impacts of nighttime light pollution: a mechanistic appraisal. *Biological reviews*, 88(4):912–927, 2013.

[19] Kenneth D Frank, C Rich, and T Longcore. Effects of artificial night lighting on moths. *Ecological consequences of artificial night lighting*, pages 305–344, 2006.

[20] Xin-She Yang and Suash Deb. Cuckoo search: recent advances and applications. *Neural Computing and Applications*, 24(1):169–174, 2014.

[21] Jane-Jing Liang, Ponnuthurai Nagaratnam Suganthan, and Kalyanmoy Deb. Novel composition test functions for numerical global optimization. In *Swarm Intelligence Symposium, 2005. SIS 2005. Proceedings 2005 IEEE*, pages 68–75. IEEE, 2005.

[22] Alex Van Breedam. Comparing descent heuristics and metaheuristics for the vehicle routing problem. *Computers & Operations Research*, 28(4):289–315, 2001.

[23] Raf Jans and Zeger Degraeve. Meta-heuristics for dynamic lot sizing: A review and comparison of solution approaches. *European Journal of Operational Research*, 177 (3):1855–1875, 2007.

[24] Robert B Payne and Michael D Sorensen. *The cuckoos*, volume 15. Oxford University Press, 2005.

[25] Ilya Pavlyukevich. Lévy flights, non-local search and simulated annealing. *Journal of Computational Physics*, 226(2):1830–1844, 2007.

[26] Andy M Reynolds and Mark A Frye. Free-flight odor tracking in drosophila is consistent with an optimal intermittent scale-free search. *PloS one*, 2(4):e354, 2007.

[27] Xin-She Yang and Suash Deb. Cuckoo search via lévy flights. In *Nature & Biologically Inspired Computing, 2009. NaBIC 2009. World Congress on*, pages 210–214. IEEE, 2009.

[28] Xin-She Yang and Suash Deb. Engineering optimisation by cuckoo search. *International Journal of Mathematical Modelling and Numerical Optimisation*, 1(4):330–343, 2010.

[29] Rosario Nunzio Mantegna. Fast, accurate algorithm for numerical simulation of levy stable stochastic processes. *Physical Review E*, 49(5):4677, 1994.

[30] Ponnuthurai N Suganthan, Nikolaus Hansen, Jing J Liang, Kalyanmoy Deb, Ying-Ping Chen, Anne Auger, and Santosh Tiwari. Problem definitions and evaluation

criteria for the cec 2005 special session on real-parameter optimization. *KanGAL report*, 2005005:2005, 2005.

[31] Q Wang, S Liu, H Wang, and DA Savić. Multi-objective cuckoo search for the optimal design of water distribution systems. In *Civil engineering and urban planning 2012*, pages 402–405. 2012.

[32] Priya Ranjan Pani, Raj Kumar Nagpal, Rakesh Malik, and Nisha Gupta. Design of planar ebg structures using cuckoo search algorithm for power/ground noise suppression. *Progress In Electromagnetics Research M*, 28:145–155, 2013.

[33] Wei Chen Esmonde Lim, G Kanagaraj, and SG Ponnambalam. Cuckoo search algorithm for optimization of sequence in pcb holes drilling process. In *Emerging trends in science, engineering and technology*, pages 207–216. Springer, 2012.

[34] Amir Hossein Gandomi, Xin-She Yang, and Amir Hossein Alavi. Cuckoo search algorithm: a metaheuristic approach to solve structural optimization problems. *Engineering with computers*, 29(1):17–35, 2013.

[35] Ali R Yildiz. Cuckoo search algorithm for the selection of optimal machining parameters in milling operations. *The International Journal of Advanced Manufacturing Technology*, 64(1-4):55–61, 2013.

[36] Majid Khodier. Optimisation of antenna arrays using the cuckoo search algorithm. *IET Microwaves, Antennas & Propagation*, 7(6):458–464, 2013.

[37] Manian Dhivya, Murugesan Sundarambal, and J Oswald Vincent. Energy efficient cluster formation in wireless sensor networks using cuckoo search. In *International Conference on Swarm, Evolutionary, and Memetic Computing*, pages 140–147. Springer, 2011.

[38] Viorica Rozina Chifu, Cristina Bianca Pop, Ioan Salomie, Mihaela Dinsoreanu, Alexandru Nicolae Niculici, and Dumitru Samuel Suia. Bio-inspired methods for selecting the optimal web service composition: Bees or cuckoos intelligence? *International Journal of Business Intelligence and Data Mining*, 6(4):321–344, 2011.

[39] Arulanand Natarajan and Premalatha K Subramanian. An enhanced cuckoo search for optimization of bloom filter in spam filtering. *Global Journal of Computer Science and Technology*, 2012.

[40] Monica Sood and Gurline Kaur. Speaker recognition based on cuckoo search algorithm. *International Journal of Innovative Technology and Exploring Engineering (IJITEE)*, 2(5):311–313, 2013.

[41] Vipinkumar Tiwari. Face recognition based on cuckoo search algorithm. *image*, 7 (8):9, 2012.

[42] Kullawat Chaowanawatee and Apichat Heednacram. Implementation of cuckoo search in rbf neural network for flood forecasting. In *Computational Intelligence, Communication Systems and Networks (CICSyN), 2012 Fourth International Conference on*, pages 22–26. IEEE, 2012.

[43] Abdollah Kavousi-Fard and Farzaneh Kavousi-Fard. A new hybrid correction method for short-term load forecasting based on arima, svr and csa. *Journal of Experimental & Theoretical Artificial Intelligence*, 25(4):559–574, 2013.

[44] Dieu N Vo, Peter Schegner, and Weerakorn Ongsakul. Cuckoo search algorithm for non-convex economic dispatch. *IET Generation, Transmission & Distribution*, 7(6): 645–654, 2013.

[45] Jubaer Ahmed and Zainal Salam. A maximum power point tracking (mppt) for pv system using cuckoo search with partial shading capability. *Applied Energy*, 119: 118–130, 2014.

[46] Shivakumar Rangasamy and Panneerselvam Manickam. Stability analysis of multimachine thermal power systems using the nature-inspired modified cuckoo search algorithm. *Turkish Journal of Electrical Engineering & Computer Sciences*, 22(5): 1099–1115, 2014.

[47] Pinar Civicioglu and Erkan Besdok. A conceptual comparison of the cuckoo-search, particle swarm optimization, differential evolution and artificial bee colony algorithms. *Artificial Intelligence Review*, 39(4):315–346, 2013.

[48] Hongqing Zheng and Yongquan Zhou. A novel cuckoo search optimization algorithm based on gauss distribution. *Journal of Computational Information Systems*, 8(10): 4193–4200, 2012.

[49] Aziz Ouaarab, Belaïd Ahiod, and Xin-She Yang. Discrete cuckoo search algorithm for the travelling salesman problem. *Neural Computing and Applications*, 24(7-8): 1659–1669, 2014.

[50] PS Manoharan, PS Kannan, S Baskar, and M Willjuice Iruthayarajan. Evolutionary algorithm solution and kkt based optimality verification to multi-area economic dispatch. *International Journal of Electrical Power & Energy Systems*, 31(7):365–373, 2009.

[51] Lingfeng Wang and Chanan Singh. Reserve-constrained multiarea environmental/economic dispatch based on particle swarm optimization with local search. *Engineering Applications of Artificial Intelligence*, 22(2):298–307, 2009.

[52] M Basu. Teaching–learning-based optimization algorithm for multi-area economic dispatch. *Energy*, 68:21–28, 2014.

[53] Chao-Lung Chiang. Improved genetic algorithm for power economic dispatch of units with valve-point effects and multiple fuels. *IEEE transactions on power systems*, 20 (4):1690–1699, 2005.

[54] M Basu. Artificial bee colony optimization for multi-area economic dispatch. *International Journal of Electrical Power & Energy Systems*, 49:181–187, 2013.

[55] Nidul Sinha, R Chakrabarti, and PK Chattopadhyay. Evolutionary programming techniques for economic load dispatch. *IEEE Transactions on evolutionary computation*, 7(1):83–94, 2003.

[56] Jong-Bae Park, Yun-Won Jeong, Joong-Rin Shin, and Kwang Y Lee. An improved particle swarm optimization for nonconvex economic dispatch problems. *IEEE Transactions on Power Systems*, 25(1):156–166, 2010.

[57] O Alsac and B Stott. Optimal load flow with steady-state security. *IEEE transactions on power apparatus and systems*, (3):745–751, 1974.

[58] Jason Yuryevich and Kit Po Wong. Evolutionary programming based optimal power flow algorithm. *IEEE Transactions on Power Systems*, 14(4):1245–1250, 1999.

[59] HREH Bouchekara, MA Abido, and M Boucherma. Optimal power flow using teaching-learning-based optimization technique. *Electric Power Systems Research*, 114:49–59, 2014.

[60] Ruey-Hsun Liang, Sheng-Ren Tsai, Yie-Tone Chen, and Wan-Tsun Tseng. Optimal power flow by a fuzzy based hybrid particle swarm optimization approach. *Electric Power Systems Research*, 81(7):1466–1474, 2011.

[61] Ray Daniel Zimmerman, Carlos Edmundo Murillo-Sánchez, and Robert John Thomas. Matpower: Steady-state operations, planning, and analysis tools for power systems research and education. *IEEE Transactions on power systems*, 26(1):12–19, 2011.

[62] KY Lee, YM Park, and JL Ortiz. A united approach to optimal real and reactive power dispatch. *IEEE Transactions on power Apparatus and systems*, (5):1147–1153, 1985.

[63] Samir Sayah and Khaled Zehar. Modified differential evolution algorithm for optimal power flow with non-smooth cost functions. *Energy conversion and Management*, 49 (11):3036–3042, 2008.

[64] W Ongsakul and T Tantimaporn. Optimal power flow by improved evolutionary programming. *Electric Power Components and Systems*, 34(1):79–95, 2006.

[65] I Erlich, K Lee, J Rueda, and S Wildenhues. Competition on application of modern heuristic optimization algorithms for solving optimal power flow problems. In *2014 IEEE Power Engineering Society General Meeting*, 2014.

[66] Serhat Duman, Uğur Güvenç, Yusuf Sönmez, and Nuran Yörükeren. Optimal power flow using gravitational search algorithm. *Energy Conversion and Management*, 59: 86–95, 2012.

[67] M Rezaei Adaryani and A Karami. Artificial bee colony algorithm for solving multi-objective optimal power flow problem. *International Journal of Electrical Power & Energy Systems*, 53:219–230, 2013.

[68] Mojtaba Ghasemi, Sahand Ghavidel, Mohsen Gitizadeh, and Ebrahim Akbari. An improved teaching–learning-based optimization algorithm using lévy mutation strategy for non-smooth optimal power flow. *International Journal of Electrical Power & Energy Systems*, 65:375–384, 2015.

[69] R Rao and Vivek Patel. An elitist teaching-learning-based optimization algorithm for solving complex constrained optimization problems. *International Journal of Industrial Engineering Computations*, 3(4):535–560, 2012.

[70] K Aoki, M Fan, and A Nishikori. Optimal var planning by approximation method for recursive mixed-integer linear programming. *IEEE Transactions on power Systems*, 3(4):1741–1747, 1988.

[71] VH Quintana and M Santos-Nieto. Reactive-power dispatch by successive quadratic programming. *IEEE Transactions on Energy Conversion*, 4(3):425–435, 1989.

[72] VA de Sousa, Edméa Cássia Baptista, and GRM da Costa. Optimal reactive power flow via the modified barrier lagrangian function approach. *Electric Power Systems Research*, 84(1):159–164, 2012.

[73] AA Abou El Ela, MA Abido, and SR Spea. Differential evolution algorithm for optimal reactive power dispatch. *Electric Power Systems Research*, 81(2):458–464, 2011.

[74] AH Khazali and M Kalantar. Optimal reactive power dispatch based on harmony search algorithm. *International Journal of Electrical Power & Energy Systems*, 33 (3):684–692, 2011.

[75] John G Vlachogiannis and Kwang Y Lee. Quantum-inspired evolutionary algorithm for real and reactive power dispatch. *IEEE transactions on power systems*, 23(4): 1627–1636, 2008.

[76] Rudra Pratap Singh, V Mukherjee, and SP Ghoshal. Optimal reactive power dispatch by particle swarm optimization with an aging leader and challengers. *Applied Soft Computing*, 29:298–309, 2015.

[77] Barun Mandal and Provas Kumar Roy. Optimal reactive power dispatch using quasi-oppositional teaching learning based optimization. *International Journal of Electrical Power & Energy Systems*, 53:123–134, 2013.

[78] K Mahadevan and PS Kannan. Comprehensive learning particle swarm optimization for reactive power dispatch. *Applied soft computing*, 10(2):641–652, 2010.

[79] Kürşat Ayan and Ulaş Kılıç. Artificial bee colony algorithm solution for optimal reactive power flow. *Applied soft computing*, 12(5):1477–1482, 2012.

[80] Mojtaba Ghasemi, Sahand Ghavidel, Mohammad Mehdi Ghanbarian, and Amir Habibi. A new hybrid algorithm for optimal reactive power dispatch problem with discrete and continuous control variables. *Applied soft computing*, 22:126–140, 2014.

[81] Y Del Valle, JC Hernandez, GK Venayagamoorthy, and Ronald G Harley. Optimal statcom sizing and placement using particle swarn optimization. In *Transmission & Distribution Conference and Exposition: Latin America, 2006. TDC'06. IEEE/PES*, pages 1–6. IEEE, 2006.

[82] Yann-Chang H. Kun-Yuan H. & Hong-Tzer Y. Chao-Ming, H. A harmony search algorithm for optimal power flow considering flexible ac transmission systems. In *Intelligent Systems Applications to Power Systems, ISAP 2013. International Conference on*, pages 1–6, 2013.

[83] I Pisica, C Bulac, L Toma, and M Eremia. Optimal svc placement in electric power systems using a genetic algorithms based method. In *PowerTech, 2009 IEEE Bucharest*, pages 1–6. IEEE, 2009.

[84] Reza Sirjani, Azah Mohamed, and Hussain Shareef. Optimal placement and sizing of static var compensators in power systems using improved harmony search algorithm. *Przeglad Elektrotechniczny*, 87(7):214–218, 2011.

[85] Reza Sirjani, Azah Mohamed, and Hussain Shareef. Optimal allocation of shunt var compensators in power systems using a novel global harmony search algorithm. *International Journal of Electrical Power & Energy Systems*, 43(1):562–572, 2012.

[86] Zahra Moravej and Amir Akhlaghi. A novel approach based on cuckoo search for dg allocation in distribution network. *International Journal of Electrical Power & Energy Systems*, 44(1):672–679, 2013.

[87] LJ Cai, Istvan Erlich, and Georgios Stamtsis. Optimal choice and allocation of facts devices in deregulated electricity market using genetic algorithms. In *Power Systems Conference and Exposition, 2004. IEEE PES*, pages 201–207. IEEE, 2004.

List of Publications

Accepted journals:

[P.1] Nguyen, K. P., Fujita, G., & Dieu, V. N. (2016). Cuckoo Search Algorithm for Optimal Placement and Sizing of Static VAR Compensator in Large-Scale Power Systems. *Journal of Artificial Intelligence and Soft Computing Research*, 6(2), 59-68.

International conferences:

[P.3] Nguyen, K. P. & Fujita, G. (2017, February). Self-Learning Cuckoo Search Algorithm for Optimal volt-VAR control, *In The 11th South East Asian Technical University Consortium (SEATUC) Symposium* Vietnam.

[P.4] Nguyen, K. P. & Fujita, G. (2016, July), Optimal reactive power dispatch considering various objectives using Moth -Flame optimization, In *The International Conference on Electrical Engineering (ICEE)* Japan.

[P.5] Nguyen, K. P. & Fujita, G. (2016, February). Moth-Flame Optimization for Optimal Reactive Power Dispatch, *In The 10th South East Asian Technical University Consortium (SEATUC) Symposium* Japan.

[P.6] Nguyen, K. P., Dinh, N. D., & Fujita, G. (2015, September). Multi-area economic dispatch using Hybrid Cuckoo search algorithm.In *Power Engineering Conference (UPEC), 2015 50th International Universities* (pp. 1-6). IEEE.

[P.7] Nguyen, K. P., Fujita, G., & Dieu, V. N. (2015, May). Optimal placement and sizing of Static Var Compensator using Cuckoo search algorithm. In *2015 IEEE Congress on Evolutionary Computation (CEC)* (pp. 267-274). IEEE.

[P.8] Nguyen, K. P., Fujita, G., Tuyen, N. D., Dieu, V. N., & Funabashi, T. (2014, December). Optimal placement and sizing of SVC by using various meta-heuristic optimization methods. In *Power Engineering and Renewable Energy (ICPERE), 2014 International Conference on* (pp. 7-12). IEEE.

[P.9] Nguyen, K. P. & Fujita, G. (2016, September), Hybrid Cuckoo Search Algorithm for Optimal Reactive Power Dispatch. In. *Power & Energy Convention Heisei 28 - B section* IEEJ

[P.10] Nguyen, K. P., Vo, D. N., & Fujita, G. (2016). Hybrid Cuckoo Search Algorithm for Optimal Placement and Sizing of Static VAR Compensator. *Handbook of Research on Modern Optimization Algorithms and Applications in Engineering and Economics*, 288